NOVEL MOLECULAR BUILDING BLOCKS BASED ON BODIPY CHROMOPHORE: APPLICATIONS IN METALLOSUPRAMOLECULAR POLYMERS AND ION SENSING

A THESIS SUBMITTED TO
THE GRADUATE SCHOOL OF NATURAL AND APPLIED SCIENCES
OF
MIDDLE EAST TECHNICAL UNIVERSITY

BY

ONUR BÜYÜKÇAKIR

IN PARTIAL FULFILLMENT OF THE REQUIREMENTS
FOR
THE DEGREE OF MASTER OF SCIENCE
IN
CHEMISTRY

SEPTEMBER 2008

Approval of the Thesis:

NOVEL MOLECULAR BUILDING BLOCKS BASED ON BODIPY CHROMOPHORE: APPLICATIONS IN METALLOSUPRAMOLECULAR POLYMERS AND ION SENSING

submitted by **ONUR BÜYÜKÇAKIR** in partial fulfillment of the requirements for the degree of **Master of Science in Chemistry Department, Middle East Technical University** by

Prof. Dr. Canan Özgen _____
Dean, Graduate School of **Natural and Applied Sciences**

Prof. Dr. Ahmet Önal _____
Head of Department, **Chemistry**

Prof. Dr. Engin U. Akkaya _____
Supervisor, **Chemistry Dept., METU**

Examining Committee Members:

Prof. Dr. Ayhan S. Demir _____
Chemistry Dept.,METU

Prof. Dr. Engin U. Akkaya _____
Chemistry Dept., METU

Prof. Dr. Özdemir Doğan _____
Chemistry Dept., METU

Asst.Prof. Dr. Neslihan Şaki _____
Chemistry Dept., Koceli University

Dr. Ö. Altan Bozdemir _____
Researcher

Date: 10.09.2008

I hereby declare that all information in this document has been obtained and presented in accordance with academic rules and ethical conduct. I also declare that, as required by these rules and conduct, I have fully cited and referenced all material and results that are not original to this work.

Name, Last name: Onur Büyükçakır

Signature :

ABSTRACT

NOVEL MOLECULAR BUILDING BLOCKS BASED ON BODIPY CHROMOPHORE: APPLICATIONS IN METALLOSUPRAMOLECULAR POLYMERS AND ION SENSING

Büyükçakır, Onur

M.S., Department of Chemistry

Supervisor: Prof. Dr. Engin U. Akkaya

September 2008, 96 pages

We have designed and synthesized boradiazaindacene (BODIPY) derivatives, appropriately functionalized for metal ion mediated supramolecular polymerization. Thus, ligands for 2- and 2,6-terpyridyl and bipyridyl functionalized BODIPY dyes were synthesized through Sonogashira couplings. These new fluorescent building blocks are responsive to metal ions in a stoichiometry dependent manner. Octahedral coordinating metal ions such as Zn(II), result in polymerization at a stoichiometry which corresponds to two terpyridyl ligands to one Zn(II) ion. However, at increased metal ion concentrations, the dynamic equilibria are re-established in such a way that, monomeric metal complex dominates. The position of equilibria can easily be monitored by ^{1}H NMR and fluorescence spectroscopy. As expected, open shell Fe(II) ions while forming similar complex structures, quench the fluorescence emission of all four functionalized BODIPY ligands.

Keywords: BODIPY, Supramolecular Polymers, Fluorescent probes, Coordination Polymers, Sonogashira Coupling.

ÖZ

BODIPY KROMOFORU ESASLI YENİ MOLKÜLER YAPI BLOKLARI; METALLO SÜPRAMOLEKÜLER POLİMERLERİ VE İYON ALGILANMASINDA UYGULAMALAR

Büyükçakır, Onur

Yüksek Lisans , Kimya Bölümü

Tez Yürütücüsü: Prof. Dr. Engin U. Akkaya

Eylül 2008, 96 sayfa

Bu çalışmada metal iyonlarının yardımıyla supramoleküler polimerizasyona uğrayabilecek şekilde fonksiyonlandırılmış boradiazaindasen (BODIPY) türevleri tasarlanmış ve sentezlenmiştir. Bu nedenle, 2- ve 2,6-terpiridil ve bipiridil fonksiyonalize BODIPY boyar maddeleri için ligandlar Sonogashira reaksiyonlarıyla sentezlenmiştir. Bu yeni floresan yapı blokları stokiyometriye bağımlı bir biçimde metal iyonlarına yanıt verebilir durumdadırlar. Zn(II) gibi oktahedral koordinasyona sahip metal iyonları iki terpiridin ligandına bir Zn(II) iyonu tekabül edecek şekilde bir stokiyometri ile polimerizasyona yol açmaktadırlar. Bununla beraber artan metal iyonu konsantrasyonların da dinamik dengeler, monomerik metal kompleksi baskın tür olacak şekilde yeniden kurulmaktadırlar. Dengelerin pozisyonu ^{1}H NMR ve floresans spektroskopileriyle kolaylıkla izlenebilmektedir. Beklendiği gibi, Fe(II) iyonları da benzer karmaşık yapıları oluşturmalarına rağmen, dört fonksiyonalize Bodipy ligandının da floresans emisyonlarını sönümlendirmişlerdir.

Anahtar kelimeler: BODIPY, süpramoleküler polimer, floresan algılayıcı, Sonogashira reaksiyonu.

To My Parents, Grandmother and Grandfather,

ACKNOWLEDGEMENTS

I would like to express my sincere thanks to my supervisor Prof. Dr. Engin U. Akkaya for his guidance, support, endless imagination, patience and for teaching us how to become a good scientist. I will never forget his support throughout my life.

I want to thank to TÜBİTAK for financial support.

I would like to express my gratitude to the NMR technician Fatoş Doğanel Polat and Seda Karayılan for NMR spectra and for their patience.

I am obliged to each and every member of Supramolecular Chemistry Laboratory, Yusuf Çakmak, Ruslan Guliyev, Tuğba Özdemir, Deniz Yılmaz, Serdar Atılgan, Gökhan Barın, Suriye Özlem, Kadir Kaleli, Erhan Deniz, Bora Bilgiç, Sündüs Erbaş, Safacan Kölemen, Fazlı Sözmen, and Zeynep Ekmekçi for the great atmosphere in the laboratory. They are very precious for me. I wish to express my sincere appreciation to Dr. Ö. Altan Bozdemir and Dr. Ali Coşkun for their support, help and wonderful guidance.

My special thanks to go to my family for their continous support, patience and encouragement and also my uncle Adnan E. Bölükoğlu for his support and encouragement.

TABLE OF CONTENTS

ABSTRACT iv

ÖZ v

ACKNOWLEDGEMENTS vii

TABLE OF CONTENTS viii

LIST OF FIGURES xi

CHAPTER

1.INTRODUCTION 1

1.1 Supramolecular Polymers; Definition, Formation and Types 1

1.1.1 Introduction to Supramolecular Polymers 1

1.1.2 Types of Supramolecular Polymers 3

1.1.2.1 Hydrogen-bonded Supramolecular Polymers 4

1.1.2.2 π- π Stacking Supramolecular Polymers 7

1.1.2.3 Coordination Polymers 11

1.2 Metal Directed Assemblies 20

1.2.1Introduction 20

1.2.2 Grid-Like Metal Ion Directed Architectures 21

1.2.3 Rack and Ladders 23

1.2.4 Helicates 23

1.2.5 Molecular boxes and Macrocycles 25

1.3 BODIPY Dyes 26

1.3.1 Introduction to BODIPY Dyes 26

1.3.2 The Numbering System of BODIPY Dyes 26

1.3.3 Functionalization of BODIPY Dyes 27

1.3.4 Application of BODIPY Dyes 31

1.3.4.1 Chemosensors 31

1.3.4.2 Biological Labelling 33

1.3.4.3 Photodynamic Therapy 33

1.3.4.4 Light harvesting and Energy Transfer Cassettes 34

1.3.4.5 Solar cells 36

2.EXPERIMENTAL 37

2.1 Instrumentation 37

2.2 Syntheses 39

2.2.1 Synthesis of 3,5-Bis(decyloxy)benzyl alcohol (**70**) 39

2.2.2 Synthesis of 3,5-Bis(decyloxy)benzaldehyde (**71**) 40

2.2.3 Synthesis of 4,4-difluoro-8-(3′,5′-bis(decyloxy)phenyl)-1,3,5,7-tetramethyl-4-bora-3a,4a-diaza-*s*-indacene (**72**) 41

2.2.4 Synthesis of 4,4-difluoro-8-(3′,5′-bis(decyloxy)phenyl)-2-iodo-1,3,5,7-tetramethyl-4-bora-3a,4adiaza-*s*-indacene (**73**) 42

2.2.5 Synthesis of 4,4-difluoro-8-(3,5-bisdecyloxy)phenyl-2,6-diiodo-1,3,5,7-tetramethyl-4-bora-3a,4adiaza-*s*-indacene (**74**).....43

2.2.6 Synthesis of 4,4-difluoro-8-(3′,5′-bis(decyloxy)phenyl)-2-(p-(2″,2‴:6‴,2⁗-terpyridin-4″-yl)ethynylphenyl)-1,3,5,7-tetramethyl-4-bora-3a,4a-diaza-*s*-indacene (**75**).....44

2.2.7 Synthesis of 5,5′-Bis(4″,4″-difluoro-8″-(3‴,5‴-bis(decyloxy)phenyl)-1″,3″,5″,7″-tetramethyl-4″-bora-3″a,4″a-diaza-*s*-indacene-2″-ethynyl)-2,2′-bipyridine (**76**).....45

2.2.8 Synthesis of 4,4-difluoro-8-(3′,5′-bis(decyloxy)phenyl)-2,6-bis-(p-(2″,2‴:6‴,2⁗-terpyridin-4″-yl)ethynylphenyl)-1,3,5,7-tetramethyl-4-bora-3a,4a-diaza-*s*-indacene (**77**).....46

2.2.9 Synthesis of 4,4-difluoro-8-(3′,5′-bis(decyloxy)phenyl)-2,6-bis(2″,2‴-bipyridine-5″-ethynyl)-1,3,5,7-tetramethyl-4-bora-3a,4a-diaza-s-indacene (**78**) 47

3.RESULTS AND DISCUSSION.....49

4.CONCLUSION.....63

REFERENCES.....64

APPENDIX.....71

LIST OF FIGURES

Figure 1. Schematic representation of main-chain, side-chain, branched and cross-linked supramolecular polymers.....2

Figure 2. Classes of supramolecular polymers according intermolecular interaction type.....3

Figure 3. The first generation of hydroden-bounded supramolecular polymer 5

Figure 4. Rigid rod supramolecular polymer 5

Figure 5. The liquid crystalline examples of supramolecular polymers based on hydrogen bonding 6

Figure 6. Hydrogen-bonded supramolecular polymer bearing ureidopyromidone group 7

Figure 7. Different aggregates formation as a function of concentration 8

Figure 8. First examples of discotic liquid crystalline polymers.....9

Figure 9. Helical and rigid-rod structured discotic polymers.....10

Figure 10. Schematic representation of metallosupramolecular polymers 12

Figure 11. Formation of coordination polymers from bifunctional ammonium compounds and bifunctional crown ether derivatives 14

Figure 12. Coordination polymer formation from pentacoordinating zinc-porphyrin units.....14

Figure 13. The first metallosupramolecular polymer 15

Figure 14. Ruthenium(II) directed ireversible and/or chiral polymers.....16

Figure 15. The first examples of molecular building blocks in oligomeric and polymeric frameworks bearing ditopic terpyridine units 17

Figure 16. Terpyridine based metallosupramolecular polymers showing photoactive and mechanoresponsive gels characteristic 17

Figure 17. Electroluminescent polymers derived from terpyridine based moieties ..18

Figure 18. Fluorescent supramolecular polymers based on terpyridine unit. 19

Figure 19. Flourescent coordination polymers bearing carbozole dyes with ditopic terpyridine units. 20

Figure 20. Schematic representation of grid-like stuctures.....21

Figure 21. Assembly of a bipyridine based grid.....22

Figure 22. Building blocks for grid type entities.....22

Figure 23. Schematic representation of rack and ladder with examples.....23

Figure 24. Assemblies of bipyridine derivatives to construct helicates.....24

Figure 25. Molecular boxes and macrocycles 25

Figure 26. Numbering systems of BODIPY core and dipyrromethene 26

Figure 28. Water soluble BODIPY Derivative.....27

Figure 27. The functionalization points of BODIPY core 27

Figure 29. Diiodo and Bibromo functionalized BODIPY dyes 28

Figure 30. Nucleophilic substitution reactions at haloginated BODIPY cores.....28

Figure 31. Condensation reactions from 3,5-positions of Bodipy cores.....29

Figure 32. Functionalization at Boron center of BODIPY core 30

Figure 33. Palladium-assisted coupling reactions at BODIPY skeleton.....31

Figure 34. BODIPY Based Chemosensors 32

Figure 35. BODIPY Dye derivatives for PDT 34

Figure 36. Dendritic light harvesting system bearing BODIPY core 35

Figure 37. BODIPY dyes in energy transfer cassettes.....35

Figure 38. Solar cell material including BODIPY chromophore 36

Figure 39. Synthesis of Compound **70**.....39

Figure 40. Synthesis of Compound **71**.....40

Figure 41. Synthesis of Compound **72**.....41

Figure 42. Synthesis of Compound **73**.....42

Figure 43. Synthesis of Compound **74**.....43

Figure 44. Synthesis of Compound **75**.....45

Figure 45. Synthesis of Compound **76**.....46

Figure 46. Synthesis of Compound **77**.....47

Figure 47. Synthesis of Compound **78**.....48

Figure 48. Total reaction scheme.....50

Figure 49. ^{1}H NMR spectra obtained by the titration of **75** in 60:40 $CDCl_3$: DMSO-d_6 (13 mM) with $Zn(OTf)_2$. Zn^{2+}: **75** ratio varies from bottom to top as: 0:1, 0.25:1, 0.5:1, 0.75:1, 1:1.....51

Figure 50. Formation of dimeric and open formed structures by the addition of $Zn(OTf)_2$.....53

Figure 51. ^{1}H NMR spectra obtained by the titration of **77** in 60:40 $CDCl_3$: DMSO-d_6 (13 mM) with $Zn(OTf)_2$. Zn^{2+} : **77** ratio varies from bottom to top as : 0:1, 0.25:1, 0.5:1, 0.75:1, 1:1, 2:1, 3:1.....54

Figure 52. Formation of polymeric and open formed structures by the addition of $Zn(OTf)_2$.....55

Figure 53. UV-vis spectra obtained by the titration of **75** in 80:20 $CHCl_3$: MeOH ($5x10^{-6}$ M) with $Zn(OTf)_2$. The inset shows the absorption coefficient at 325 nm as a function of Zn^{2+}/**75** ratio.....57

Figure 54. Fluorescence spectra obtained by the titration of **75** in 80:20 $CHCl_3$: MeOH ($5x10^{-6}$ M) with $Zn(OTf)_2$.....57

Figure 55. UV-vis spectra obtained by the titration of **77** in 80:20 $CHCl_3$: MeOH ($5x10^{-6}$ M) with $Zn(OTf)_2$. The inset shows the absorption coefficient at 325 nm as a function of Zn^{2+}/**77** ratio.....58

Figure 56. Fluorescence spectra obtained by the titration of **77** in 80:20 $CHCl_3$: MeOH ($5x10^{-6}$ M) with $Zn(OTf)_2$.....59

Figure 57. UV-vis spectra obtained by the titration of **76** in 80:20 $CHCl_3$:MeOH ($5x10^{-6}$ M) with $Zn(NO_3)_2$.....60

Figure 58. Fluorescence spectra obtained by the titration of **76** in 80:20 $CHCl_3$: MeOH ($5x10^{-6}$ M) with $Zn(NO_3)_2$. 60

Figure 59. UV-vis spectra obtained by the titration of **78** in 80:20 $CHCl_3$:MeOH ($5x10^{-6}$ M) with $Zn(NO_3)_2$.....61

Figure 60. Fluorescence spectra obtained by the titration of **78** in 80:20 $CHCl_3$: MeOH ($5x10^{-6}$ M) with $Zn(NO_3)_2$. 62

Figure 61. ^1H NMR spectrum (400 MHz, $CDCl_3$) of (**70**).....71

Figure 62. ^{13}C NMR spectrum (100 MHz, $CDCl_3$) of (**70**).....72

Figure 63. ^1H NMR spectrum (400 MHz, $CDCl_3$) of (**71**).....73

Figure 64. ^{13}C NMR spectrum (100 MHz, $CDCl_3$) of (**71**).....74

Figure 65. ^1H NMR spectrum (400 MHz, $CDCl_3$) of (**72**).....75

Figure 66. ^{13}C NMR spectrum (100 MHz, $CDCl_3$) of (**72**).....76

Figure 67. ^{1}H NMR spectrum (400 MHz, $CDCl_3$) of (**73**).....77

Figure 68. ^{13}C NMR spectrum (100 MHz, $CDCl_3$) of (**73**).....78

Figure 69. ^{1}H NMR spectrum (400 MHz, $CDCl_3$) of (**74**).....79

Figure 70. ^{13}C NMR spectrum (100 MHz, $CDCl_3$) of (**74**).....80

Figure 71. ^{1}H NMR spectrum (400 MHz, $CDCl_3$) of (**75**).....81

Figure 72. ^{13}C NMR spectrum (100 MHz, $CDCl_3$) of (**75**).....82

Figure 73. ^{1}H NMR spectrum (400 MHz, $CDCl_3$) of (**76**).....83

Figure 74. ^{13}C NMR spectrum (100 MHz, $CDCl_3$) of (**76**).....84

Figure 75. ^{1}H NMR spectrum (400 MHz, $CDCl_3$) of (**77**).....85

Figure 76. ^{13}C NMR spectrum (100 MHz, $CDCl_3$) of (**77**).....86

Figure 77. ^{1}H NMR spectrum (400 MHz, $CDCl_3$) of (**78**).....87

Figure 78. ^{13}C NMR spectrum (100 MHz, $CDCl_3$) of (**78**).....88

Figure 79. Mass Spectrum of (**72**).....89

Figure 80. Mass Spectrum of (**73**).....90

Figure 81. Mass Spectrum of (**74**).....91

Figure 82. Mass Spectrum of (**75**).....92

Figure 83. Mass Spectrum of (**76**).....93

Figure 84. Mass Spectrum of (**77**).....94

Figure 85. Mass Spectrum of (**78**).....95

Figure 86. UV-Vis spectra obtained by the titration of **77** with $Fe(ClO_4)_2$. 96

Figure 87. Fluorescence spectra obtained by the titration of **77** with $Fe(ClO_4)_2$ 96

LIST OF ABBREVIATIONS

BODIPY: Boradizaindacene

THF: Tetrahydrofuran

PCC: Pyridinium chlorochoromate

DMSO: Dimethyl sulfoxide

TFA: Trifluoroacetic acid

DDQ: Dichloro Dicyano Quinone

TLC: Thin Layer Chromatography

CHAPTER 1

INTRODUCTION

1.1 Supramolecular Polymers; Definition, Formation and Types

1.1.1 Introduction to Supramolecular Polymers

Application of secondary interactions in a proper way to organize the molecules through self-assembly from nano size to polymolecular entities makes "supramolecular chemistry beyond the molecule".[1,2] In recent years, supramolecular polymer chemistry emerges as a new concept and adds a new perspective not only to supramolecular chemistry but also to polymer chemistry. By means of their remarkable and unique characteristics, supramolecular polymers have steadily increased their popularity in a short time period and these smart polymers which respond to external parameters such as temperature, solvent composition or a chemical species attract considerable attention. A subset of this group of polymers known as "Supramolecular Polymers" differs from other polymers in that the monomers are brought via self-assembly.[3] The process of self-assembly is in principle reversible under certain conditions, it is possible to revert the polymerization process back to the monomers. This dynamic nature, results in a smart function, which allows the use of polymeric material when needed, and when they are no longer needed, they could easily be converted to their constituent monomers.

The reversibility of supramolecular polymers stem from the highly directional non-covalent interactions. Therefore, the polymerization process is carried out

under thermodynamic conditions which mean that the length of chains directly related with the strength of secondary interactions (non-covalent interactions), temperature and the concentration of monomers. In other words, the degree of polymerization, regulation of structure, life time of chains and their conformation can be regulated by changing the strength and type of non-covalent interactions, temperature, pH, and monomer concentration. The adjustability of architectural and dynamic properties makes supramolecular polymers superior over the other conventional polymers.

According to the number and disposition of the interaction subunits supramolecular polymers can be divided into minor groups; main-chain, side-chain, branched and cross-linked polymers. The striking characteristic of main-chain supramolecular polymers is the monomeric units of polymers having two identical or different recognition/interaction (ligand) groups which construct the main chain of polymer by means of secondary interactions (Figure 1). Main-chain polymers can also be subdivided into two groups; homo-polymers bearing exactly two identical interaction groups and random copolymers with different interaction groups. Attachment of recognition groups to the complementary groups which are on main chain of conventional covalent polymers forms the side-chain supramolecular polymers (Figure 1).

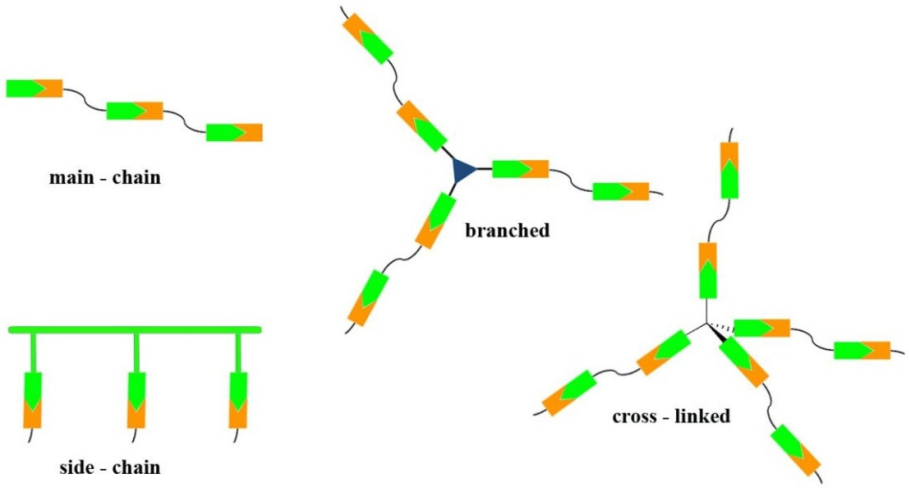

Figure 1. Schematic representation of main-chain, side-chain, branched and cross-linked supramolecular polymers

On the other hand, if the monomer units of supramolecular polymers bear more than two recognition groups, these types of materials are called branched or cross- linked supramolecular polymers. In fact, there is a critical nuance between branched and cross-linked polymers; two dimensional associations of more than two recognition groups leads to the formation of branched type supramolecular polymers, whereas three dimensional associations of recognition groups forms the cross-linked type supramolecular polymers (networks and physical gels) (Figure 1).

1.1.2 Types of Supramolecular Polymers

Based on their intermolecular interaction type, there are three main classes of supramolecular polymers which are hydrogen-bonded polymers, π-π stacking polymers and coordination polymers (Figure 2).[4-6]

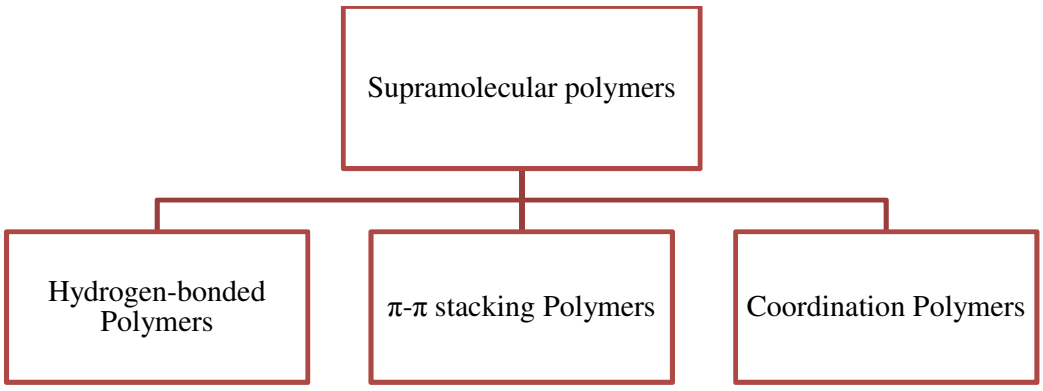

Figure 2. Classes of supramolecular polymers according intermolecular interaction type

1.1.2.1 Hydrogen-bonded Supramolecular Polymers

Lots of literature examples for supramolecular polymeric systems based on hydrogen-bonding have been reported since the first hydrogen-bounded supramolecular polymer was published by Lehn and co-workers in 1990.[7]

Hydrogen bond is the strongest non-covalent interaction. Although the strength of bond is closely related with the nature of the acceptor and donor parts, temperature, pressure, bond angle and external parameters (especially solvent) can also affect the strength of the bond. However, by designing monomers bearing suitable functional units for multiple hydrogen bonding, it is possible to construct supramolecular polymers that can maintain their structural integrity in polar solvents whose molecules may compete with the monomer units of polymers for hydrogen bonding. This is a good evidence for the hydrogen bonding suitability to construct the supramolecular polymers. In spite of this high strength characteristic of hydrogen bonds, their reversible characteristics are preserved. Moreover, hydrogen bonds form only one direction which minimizes the undesired interactions to unwanted directions.

The high strength bonding characteristic, directionality and reversibility make hydrogen bonds appropriate for construction of supramolecular polymers. By means of multiple-hydrogen-bonds or hydrogen-bonds enforced by additional forces like liquid crystallinity make possible reach the moderate degree of polymerization. Therefore, there are several supramolecular polymers that have been reported based on hydrogen bonding.[4,5,8-11]

The first generation of supramolecular polymers **3** were synthesized by Lehn and et al. in 1990 by using the tartaric acid derivatives containing the 2,6-diaminopyridine **1** and uracil units **2** (Figure 3).[7] Moreover, Kato and Frechet introduced supramolecular polymer containing polyacrylic acid derivative and trans-stilbazole ester.[12] These first examples of supramolecular polymers showed liquid crystallinity, also.

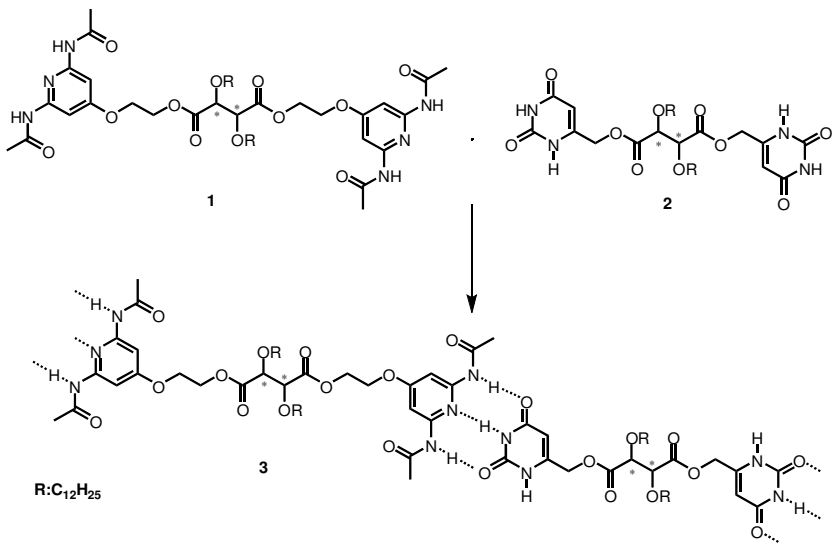

Figure 3. The first generation of hydroden-bounded supramolecular polymer

Lehn and co-workers expanded the scope one step further by synthesizing rigid rod polymer **4** (Figure 4).[13] The hydrogen bonded groups were connected with the core 9,10-dialkoxyanthracene groups by imides group. In fact, the 9,10 dialkoxyanthracene groups provides the rigidity in a suitable manner.

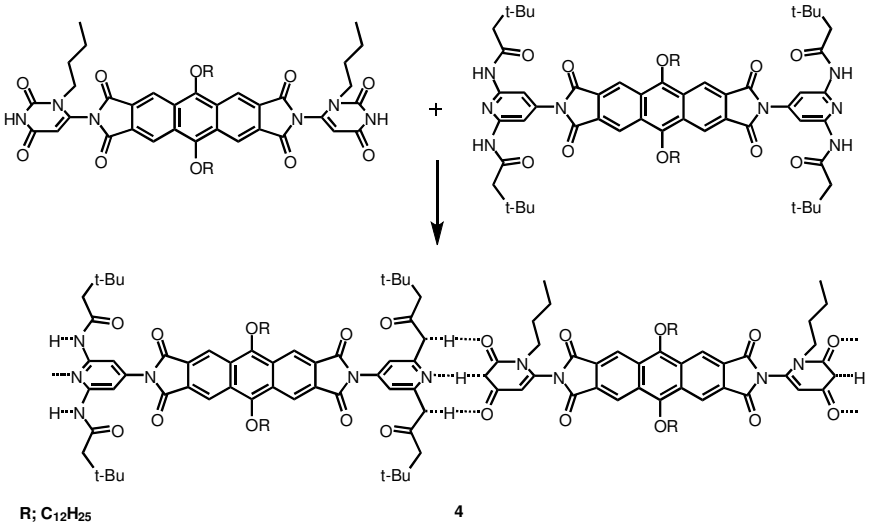

Figure 4. Rigid rod supramolecular polymer

Griffin and co-workers were also reported the liquid crystalline examples of supramolecular polymers based on hydrogen bonding.[14] The connection of tetra functional bipyridine units **5** with benzoic acid units **6** via hydrogen bonding resulted in the formation of ladder-like polymers **7** or networks **8** (Figure 5). The individual units do not show any liquid crystallinity whereas the rigid mesogens arise as a result of the formation of the hydrogen bond.

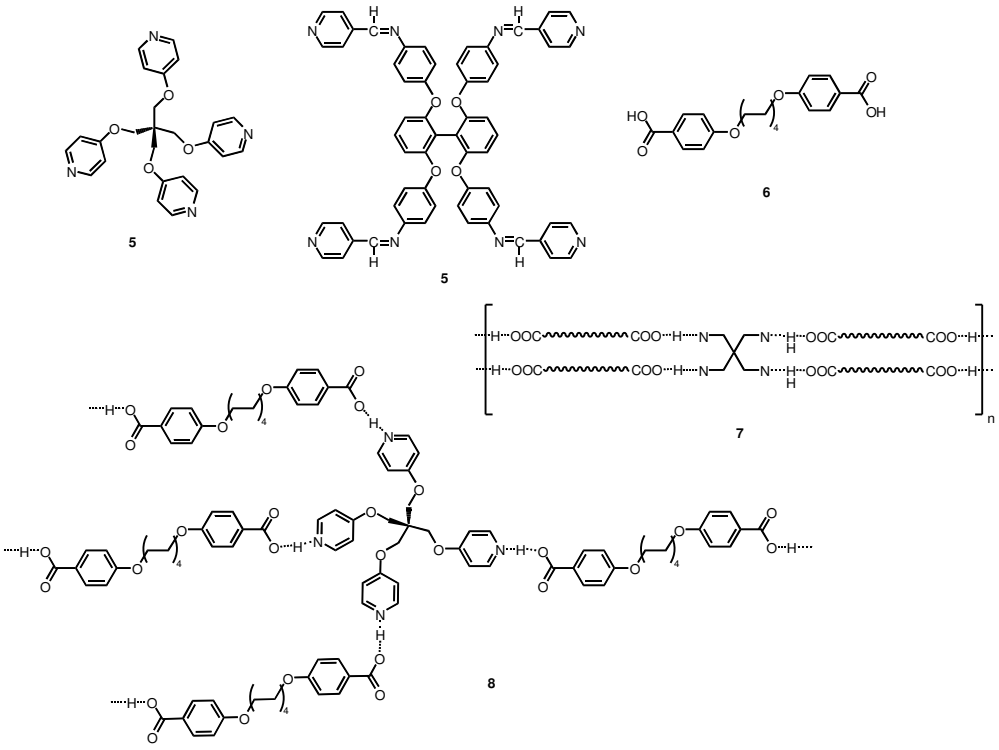

Figure 5. The liquid crystalline examples of supramolecular polymers based on hydrogen bonding

It is an undeniable fact that the development of ureidopyromidones bearing four hydrogen bonded self-complementary units by Meijer and Sijbesma is the pioneer and important step for the supramolecular polymer chemistry (Figure 6).[10,15] This type of supramolecular polymers bearing ureidopyromidone groups **9** has excellent degree of polymerization and has similar macroscopic characteristics as

the most covalent polymers. These properties of ureidopyromidone based ligands make possible construct linear type[10] or network[11] type supramolecular polymers.

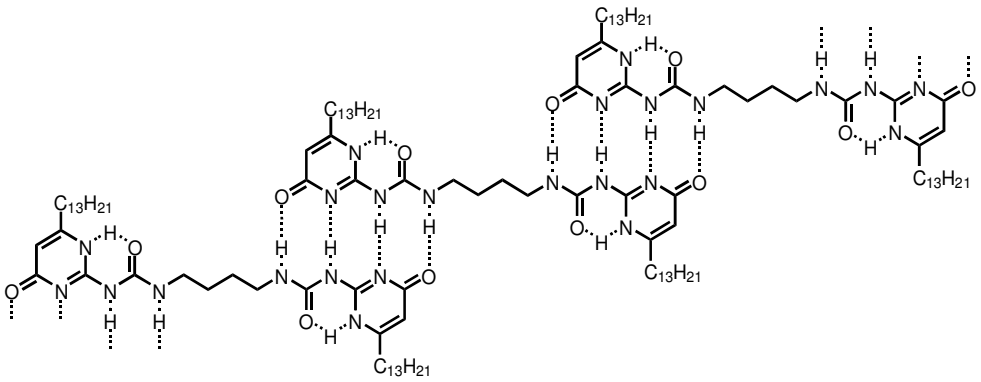

9

Figure 6. Hydrogen-bonded supramolecular polymer bearing ureidopyromidone group

1.1.2.2 π- π Stacking Supramolecular Polymers

The other type of supramolecular polymers is π- π stacking polymers. In these of type polymers, the polymerization is formed by π- π stacking or arene-arene interaction. They are highly ordered polymers and polymerization process occurs usually in solution. Discotic (disc-shaped) liquid crystalline polymers are well-known and typical examples. Discotic liquid crystalline polymers have a bipartite structure which consists of a disc-shaped core and a number of flexible side chains at the edge. Core units usually contain a planar aromatic system. On the other hand, the side chains consist of flexible long alkyl chains. These structural properties of discotic materials make possible to construct supramolecular polymers in solution.

In fact, various types of liquid crystals have been reported in literature.[5] However, discotic liquid crystals are unique examples of liquid crystal having linear architecture. The other type of liquid crystals has ordering interactions of the same order of magnitude in at least two dimensions. This variety of interactions for most liquid crystals leads to yield gels at high concentrations because of uncontrolled growth of the aggregates, whereas in low concentrations these interactions are too weak to form polymeric architectures.[16] However, the inner disc stacking interaction is stronger than inter columnar interactions which powered by side alkyl chains having van der Waals interaction. This strong interaction of the aromatic core enables the aggregation of monomers via arene-arene interaction or π-π stacking even in low concentration. The inter columnar interactions become prominent as monomer concentration increases and these side interaction leads to the formation of gel like material and liquid crystalline phase in the bulk (Figure 7).

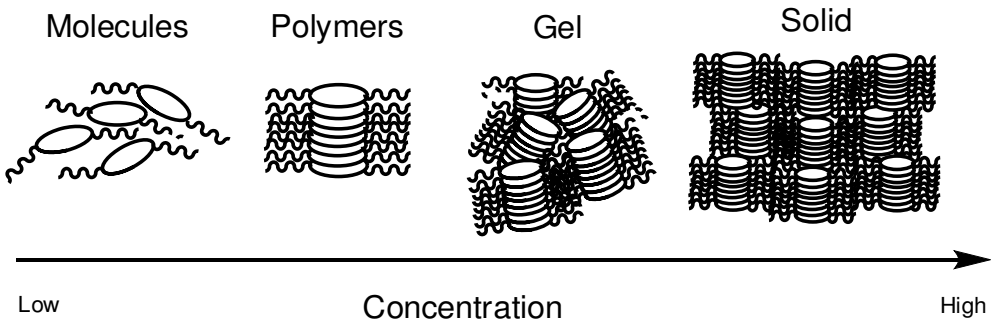

Figure 7. Different aggregates formation as a function of concentration

There are many examples of discotic liquid crystalline materials reported in the literature.[5,8] The first reported discotic liquid crystalline examples are **10 a-e** (Figure 8).[17,18] Although thriphenylenes core is small, polymers are generated in deuterated hexadecane. Furthermore, phthalocyanine based discotic liquid crystals have also been reported **11 a-c** (Figure 8).[19,20]

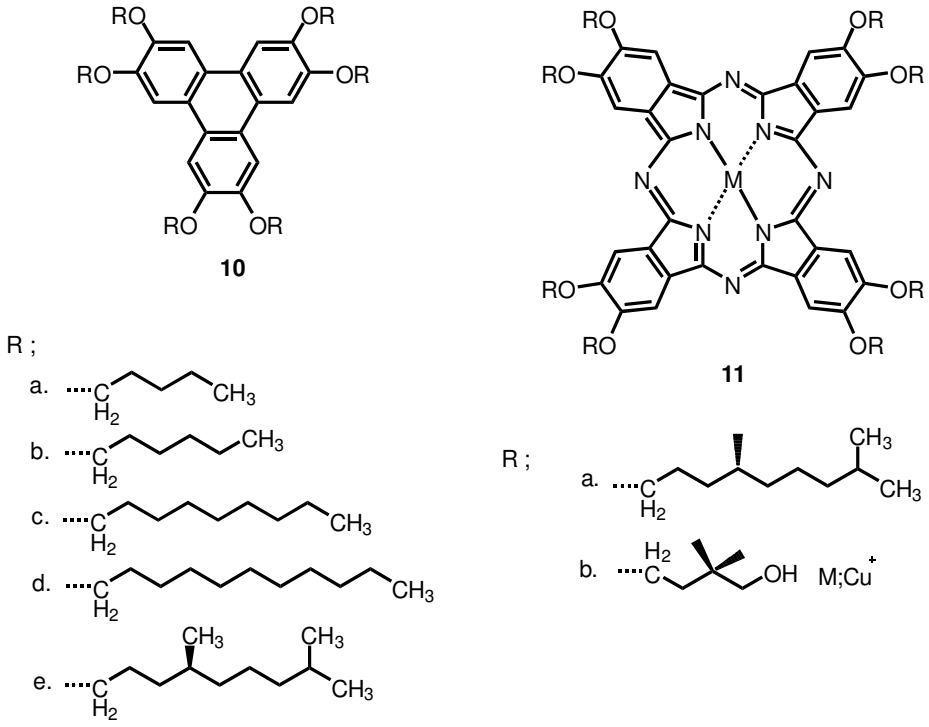

Figure 8. First examples of discotic liquid crystalline polymers

Attachment of crown-ethers onto the phthalocyanine core provides helical structured discotic materials **12 a-b** (Figure 9).[21,22] **13** has a perfect discotic molecule which form long polymers with a rigid-rod structure and large dissociation constant leads to large degree of polymerization in highly dilute solutions (Figure 9).[23]

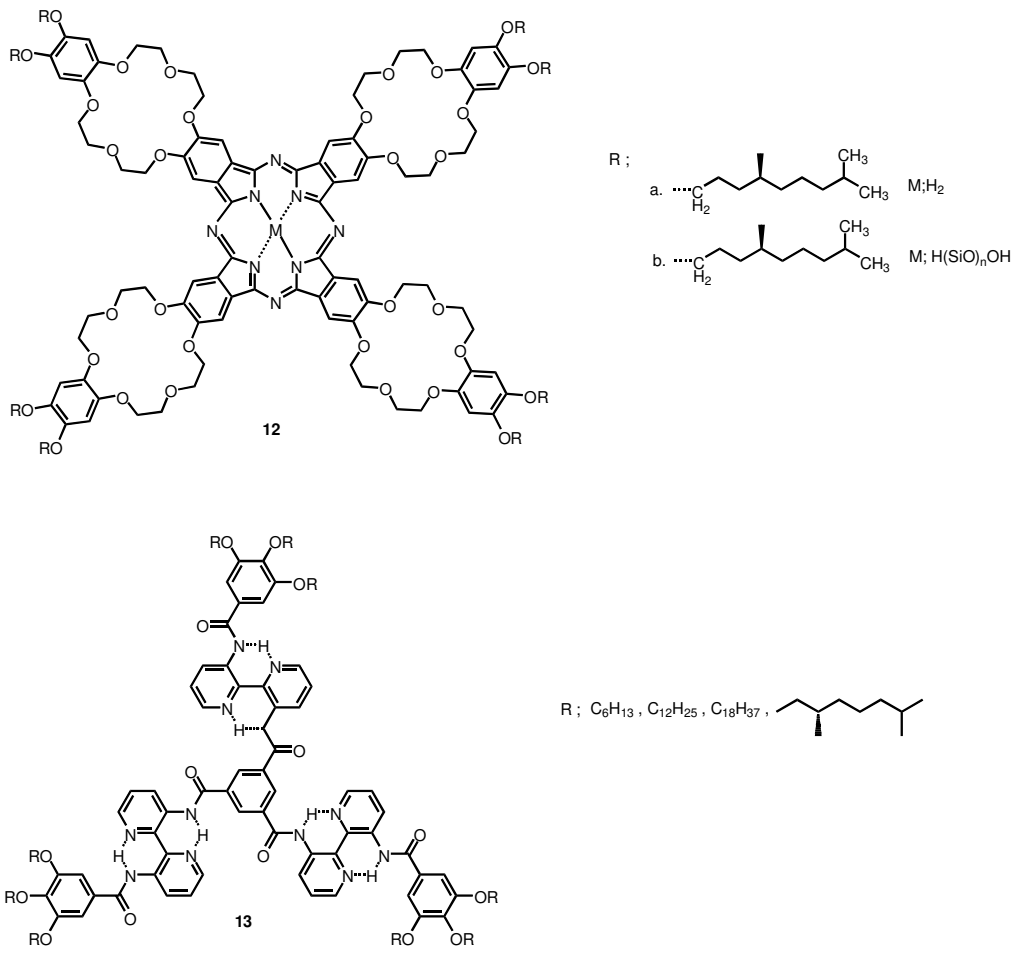

Figure 9. Helical and rigid-rod structured discotic polymers

Actually, supramolecular polymers from discotic liquid crystalline materials have poor mechanical properties. However, discotic liquid crystalline molecules are perfect choice to construct rigid-rod and helical architectures in solution because of their strong and selective interaction between disks. Furthermore, their high electronic mobility enables them be used as plastic transistors and photovoltaics.

1.1.2.3 Coordination Polymers

Conventional polymers can be simply defined as high molecular weight molecules formed via the repetition of monomeric units linked with covalent bonds. On the other hand, coordination polymers[5,7,24,25] are defined as infinite systems expanded with attachment of organic ligands and metal ions as main elementary units by means of coordination bonds.

However, the coordination polymer concept is figured out differently from inorganic and supramolecular chemist. One dimensional (1D), two dimensional (2D) and three dimensional (3D) coordination networks are named as coordination polymers in inorganic chemistry. This type of coordination polymers are sometimes named as metal-organic frameworks or organic coordination networks in literature, also.

Although coordination polymer is a more limited concept for supramolecular chemistry, an extensive range of supramolecular complexes has been reported that prepared by using metal coordination. In other words, using metal-ligand attachments by coordinative bond make possible the synthesis of an extensive range of materials from simple dimers to complex architectures i.e. linear polymers and dendrimers.

By taking into consideration supramolecular approach, coordination polymer can be simply defined as construction of polymeric arrays from alternating attachment of organic ligand molecules and metal ions via self-assembly (Figure 10).

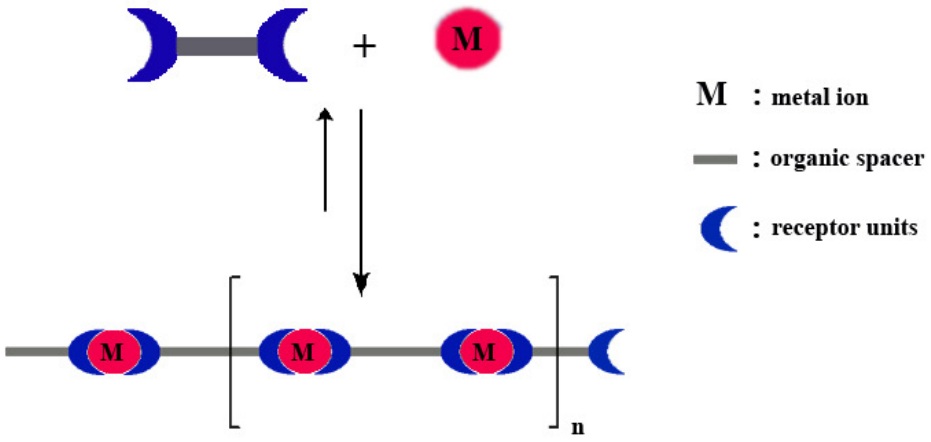

Figure 10. Schematic representation of metallosupramolecular polymers

Reversibility stemming from self-assembly is the main distinction parameter between conventional covalent polymer and coordination polymer. Actually, reversibility, high directionality and strength characteristic of metal-ligand coordination provide a perfect method to construct metallosupramolecular polymers (supramolecular coordination polymer).

The chain length of polymer mainly depends on the binding constant of ligand to metal ion. Temperature and solvent are the other parameters which affect the chain length indirectly by changing the binding constant. The relationship between degree of polymerization (DP), binding constant (K) and monomer (ligand) concentration (M) is ;[6]

$$DP \sim (K[M])^{1/2}$$

By increasing the binding constant and monomer concentration, it is possible to achieve high degree of polymerization. It is a critical point that this relationship is only valid for reversible processes. However, there is a contradiction between binding constant and reversibility because high binding constants generally cause to low reversibility. However, there are some examples providing high reversibility with high binding constant in literature.[26]

It is a well-known fact that this challenge between reversibility and binding constant can be passed over by choosing appropriate metal-ligand system. For choosing suitable system, themodynamic and kinetic properties of metal complexes must be analyzed in details. Thermodynamic properties determine whether the complexes are stable or not. On the other hand, inertness or lability of metal complexes depends upon kinetic properties which is analyzed by ligand exchange experiments and denoted as half-life of the metal complex. Thermodynamic stability and kinetic lability is necessary to synthesize reversible metallosupramolecular polymer with high degree of polymerization.

It is undeniable fact that high degree of polymerization cannot be provided with monomer concentration increase because generally increment of monomer concentration is limited by several factors such as solubility. Therefore, the binding constant plays crucial role for satisfy high degree of polymerization. For hydrogen bonded supramolecular polymers, binding constant can be increased by using multi hydrogen bonded self-complementary units. In same parallelism, high binding constant can be accomplished by using ligands bearing multiple interacting binding sites such as chelating ligands.

Incorporation of bifunctional molecules **14** and **15** was introduced by Gibson and co-workers (Figure 11).[27] The bifunctional crown ethers **14** interact with the bifunctional ammonium compounds **15** and cause chain extended aggregates which leads to a drastic increase in viscosity. Moreover, concentrated mixture of **14** and **15** provides flexible films and fibers which are the result of entanglement of linear aggregates.

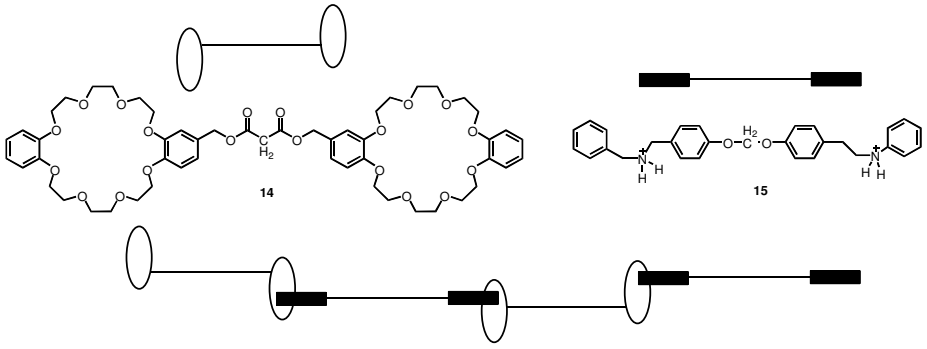

Figure 11. Formation of coordination polymers from bifunctional ammonium compounds and bifunctional crown ether derivatives

Kobuke and co-workers were reported a giant supramolecular porphyrin array by self-coordination.[28] Pentacoordinating zinc-porphyrin units form the skeleton system of coordination polymer. These zinc-porphyrin units show favorable fluorescence properties. As shown in Figure 12 , **16** is the monomer which consists of bearing two porphyrinic units attached each other with covalent bonds and each porphyrin unit bears one imidazole ligand which provides the necessary ditopic self-complementary building blocks for the formation of polymeric arrays **17**.

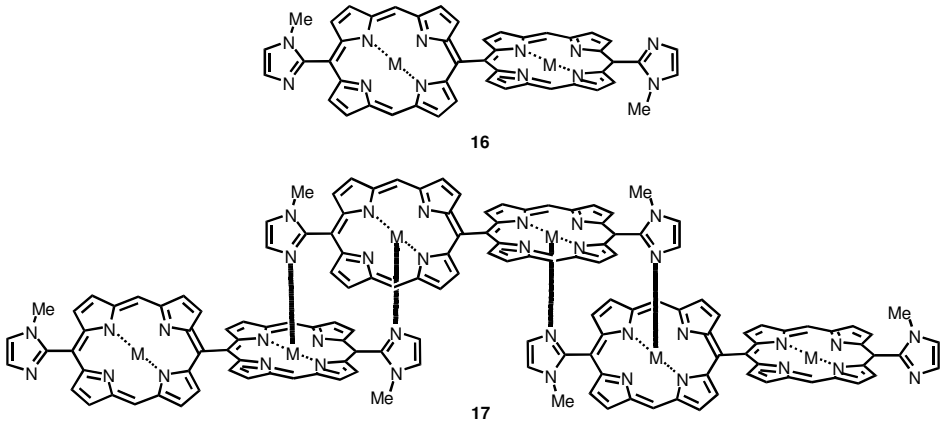

Figure 12. Coordination polymer formation from pentacoordinating zinc-porphyrin units

Although a number of chelating ligands can be used as a monomer, a rich variety of metallosupramolecular polymers based on monomeric units including aromatic nitrogen ligands have been reported so far. Aromatic N-donor ligands can be put in ascending order according to their binding constant value; pyridine, bipyridine, phenatroline and terpyridine and different metallosupramolecular entities have been designed and synthesized by taking into consideration these binding constant affinities.

Rehahn and et.al. introduced the first metallosupramolecular polymer **19** from ditopic building block **18** bearing two phenanthroline ligand units (Figure 13).[29] These phenanthroline units enable not only thermodynamically stable but also kinetically labile coordination complexes. The polymerization process starts with the addition of silver (I) and copper (I) metal ions in the medium of non-coordinating solvent since competitive solvent molecules decreases the coordination polymer length, effectively.

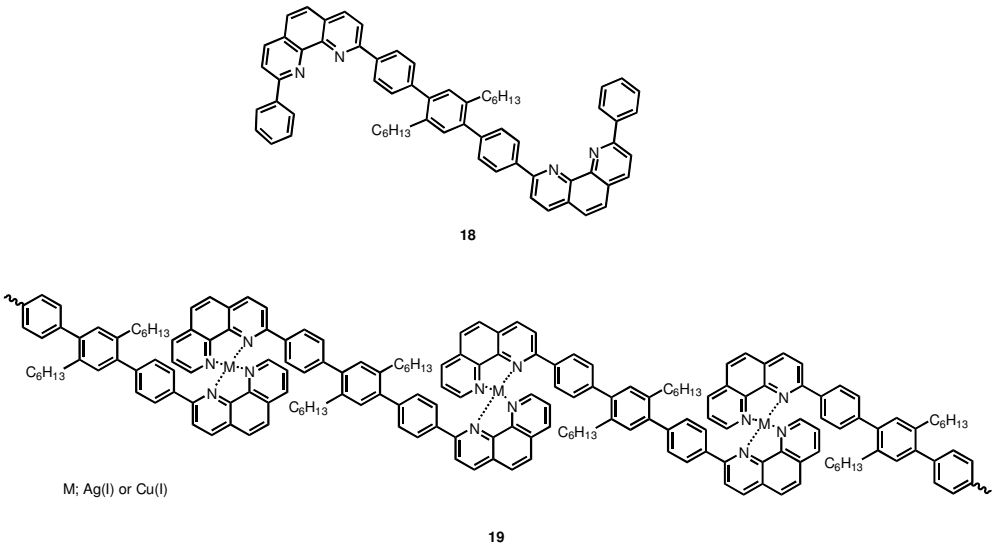

Figure 13. The first metallosupramolecular polymer

Although copper(I) and silver(I) serve a reversible coordination polymer, ruthenium metal ions provide irreversible but stable complexes. Rehahn and coworkers were introduced the synthesis of polymer **24**.[30] This polymer was constructed from tetrapyridophenazine **20** and 2,2'-bipyridine $Ru(bpy)Cl_3$ **21** units(Figure 14). Tetrapyridophenazine units formed the bridge of polymer.

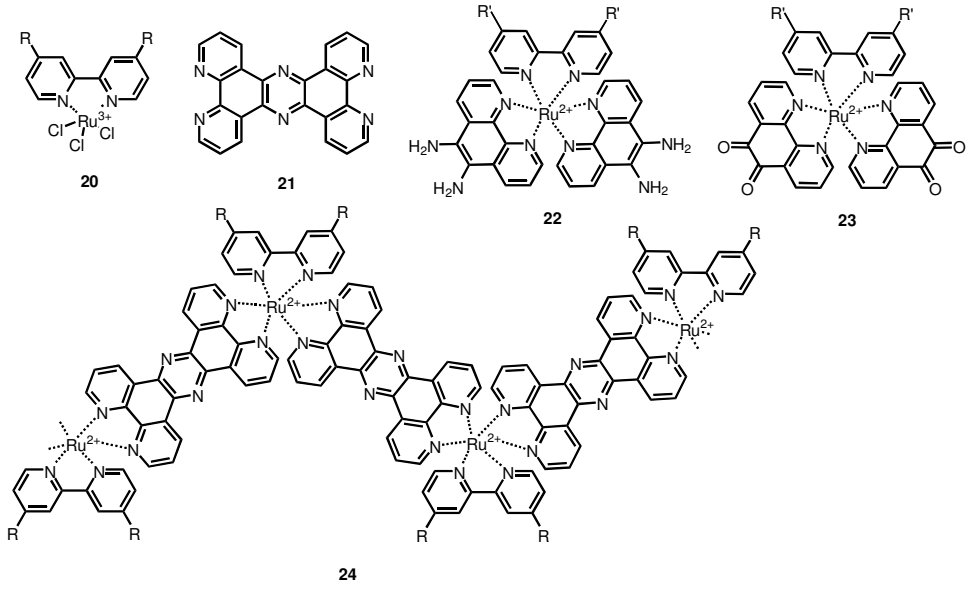

Figure 14. Ruthenium(II) directed ireversible and/or chiral polymers

On the other hand, the variable steric hindrances by substituents R at the bipyridine units effect the chain conformation and enable the synthesis of chiral polymers. Complexation of **20** and **21** yields a racemic mixture of complexes. On the other hand, the group of MacDonnell published the polymer having defined chirality starting from enantiomerically pure complexes **22** and **23** (Figure 14).[31]

As mentioned above, the ligand is especially important to satisfy optimal binding constant and 2,2′;6′,6″ – terpyridine units have appropriate properties to meet the needs for the construction of metallosupramolecular systems. Constable and Cargill Thompson were introduced the concept of usage of ditopic terpyridine units **25-27** as a molecular building blocks in oligomeric and polymeric entities

(Figure 15).[32-34] A great number of literature examples of coordination polymers bearing terpyridine units have been reported so far.[35-37]

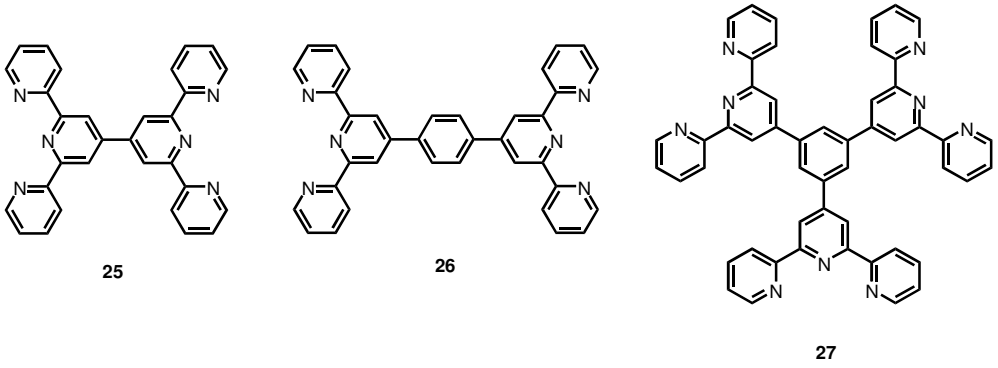

Figure 15. The first examples of molecular building blocks in oligomeric and polymeric frameworks bearing ditopic terpyridine units

On the other hand, metallosupramolecular polymers bearing fluorescent units in their structure are a novel generation of coordination polymers and only a few examples have been reported to date. In recent years, Beck and Rowan reported coordination polymers bearing terpyridine units.[38] Moreover, these polymers show photoactive and mechanoresponsive gels characteristic (Figure 16). Combination of lanthanoid and transition metal ions with monomer unit **28** enables the formation of gel like material.

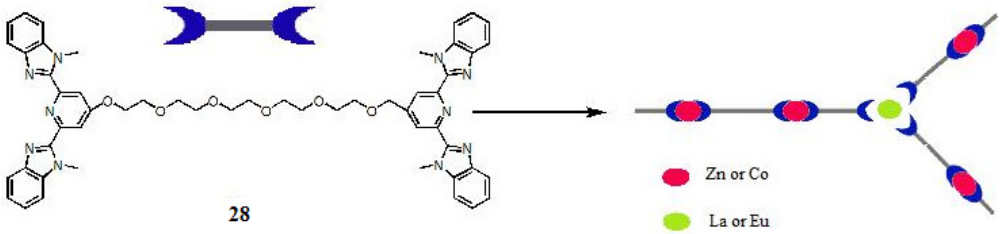

Figure 16. Terpyridine based metallosupramolecular polymers showing photoactive and mechanoresponsive gels characteristic

In 2003, Chi-Ming Che and co-workers were reported electroluminescent polymers derived from terpyridine based moieties via self-assembly.[39] The attachment of terpyridyl zinc(II) moieties to different main-chain structures **29 a-i** (Figure 17) provides exhibition of different emission wavelengths ranging from violet to yellow colors with highly photoluminescent quantum yields. These polymers can be applicable as high efficient polymeric light-emitting diode (PLED) devices.

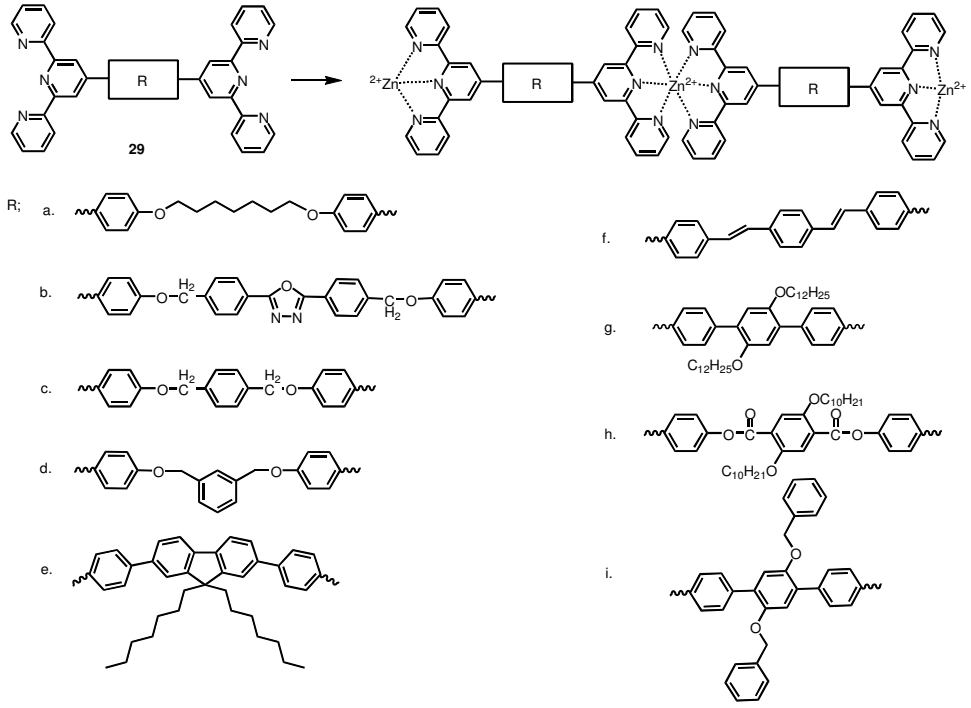

Figure 17. Electroluminescent polymers derived from terpyridine based moieties

Würthner and co-workers were reported fluorescent supramolecular polymers based on terpyridine unit. Incorporation of perylene bisimide dyes to terpyridine units make way for construction of metal directed fluorescent supramolecular polymers which shows outstanding properties.[40] Polymerization is processed with coordination of zinc ions to functional units. Würthner and et.al were reported not only mono terpyridine functionalized perlene bisimide dye **30** leading to

dimerization **31** but also di terpyridine equipped monomers **32**, which construct polymeric array **33** (Figure 16). The properties and characteristics of these materials were analyzed and reported in detail, also.[41]

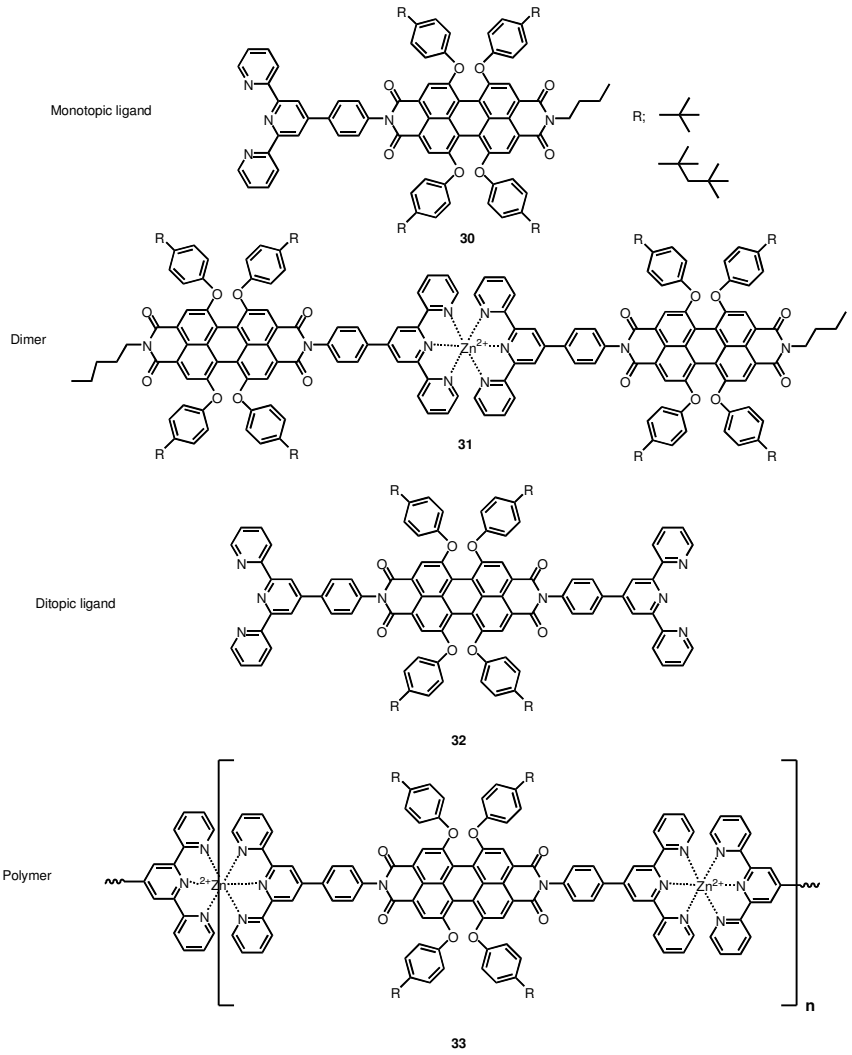

Figure 18. Fluorescent supramolecular polymers based on terpyridine unit.

Hong-cheu Lin and workers were also reported metallo-homopolymers and metallo-alt-copolymer bearing terpyridyl zinc(II) moieties.[42] The **34a** and **34b**

was synthesized by the attachment of 2,2′;6′,6″ – terpyridine units to carbozole unit via metal directed coupling reaction (Figure 19).

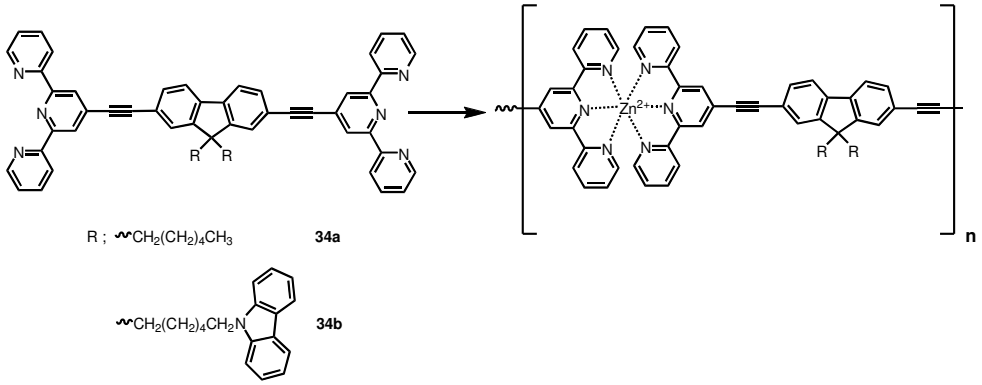

Figure 19. Flourescent coordination polymers bearing carbozole dyes with ditopic terpyridine units.

1.2 Metal Directed Assemblies

1.2.1 Introduction

Self-assembly make accessible to construct new molecular architectures. In other words, incorporation of several units to building blocks enable them to build up more complex structures from small molecules via self-assembly.[3] The non-covalent interactions such as charge transfer, hydrogen bonding and metal coordination can be used as a driven force for formation of complex entities.

Metallosupramolecular chemistry serves appropriate templates to produce complex architectures by using the interaction between organic ligands and metal ions. Thermodynamic stability and variable lability of metal-ligand bonds play a crucial role for directing molecular assembly. Furthermore, selective characteristic of metal ions to specific coordination sites of organic ligands allows controlling the geometry of the molecular assembly. Of course, design of organic ligand and metal ion selection is a must to drive self-assembly in desired direction spontaneously. These properties of metal directed self-assemblies lead

construction of a number of different architectures like catenanes, catenands, helicates, molecular macrocycles, boxes, racks, ladders and grids.

1.2.2 Grid-Like Metal Ion Directed Architectures

A rich variety of examples of grid like structures have been reported.[43] As mentioned above, geometry of grid like architectures based on the directing coordination interactions which stem from the structure of organic based ligands and metal ions' coordination geometry. Actually, ligand planes have to be arranged perpendicularly onto metal ions. 2-D arrangement of metal ions results with square [mxm] and rectangular [mxn] grids(Figure 20).

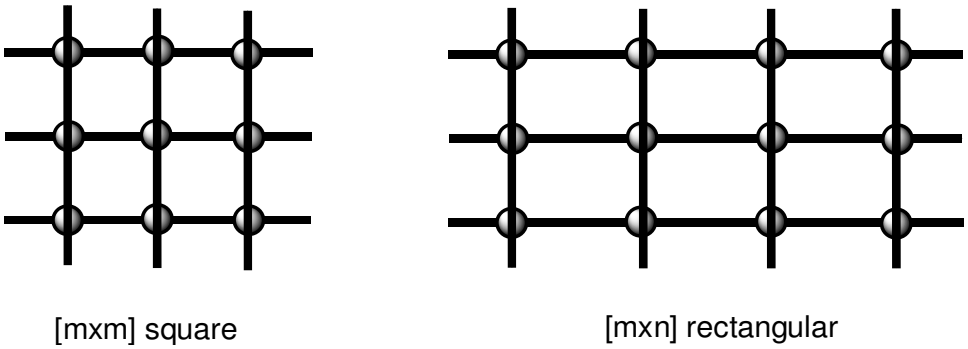

Figure 20. Schematic representation of grid-like stuctures

Lehn and co-workers were reported the 3x3 molecular grid **36** constructed using six units of ligand **35**.[44] As seen in Figure 21, six units of ligand were coordinated to nine silver(I) ions. These arrays of metals may be used in information storage. The metal ions can be matched up as a bit of information. The photochemical and redox properties of such structures can be used as information storage parameter such as one oxidation state of metal ion correspond to "on" and another to "off".

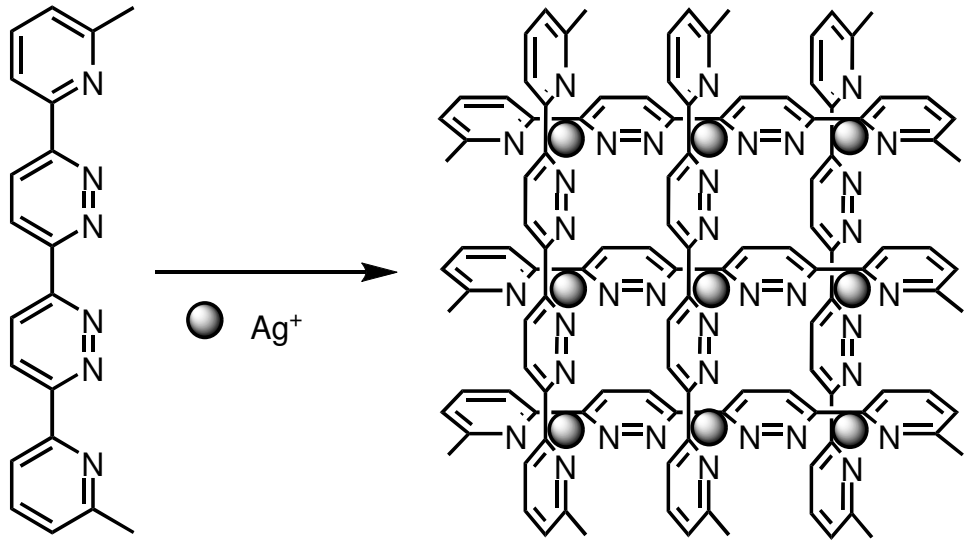

Figure 21. Assembly of a bipyridine based grid

As mentioned, to design grid like entities appropriate ligand should be synthesized by taking coordination geometry of metal ions into consideration. Many research groups expend great performance to synthesize a rich variety of ligands (Figure 22).[43]

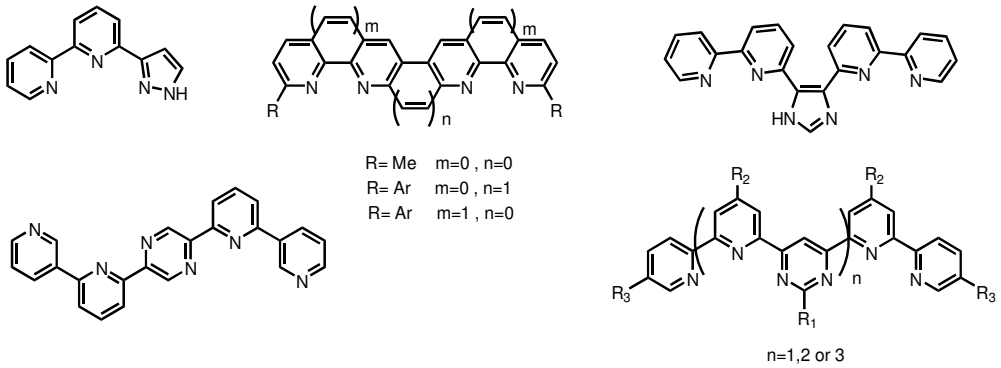

Figure 22. Building blocks for grid type entities

1.2.3 Rack and Ladders

Rack and ladder like architectures have been introduced in literature as schematically shown in Figure 23. When mixture of tris-bipyridine ligand **37**, 1,10-phenanthroline crown ether **38** and copper (I) ions result with a rack strucrure **39**.[45] On the other hand, when tris-bipyridine ligand **37** is mixed with a bipyridine strand **40**, it leads to ladder type entities **41**. [46]

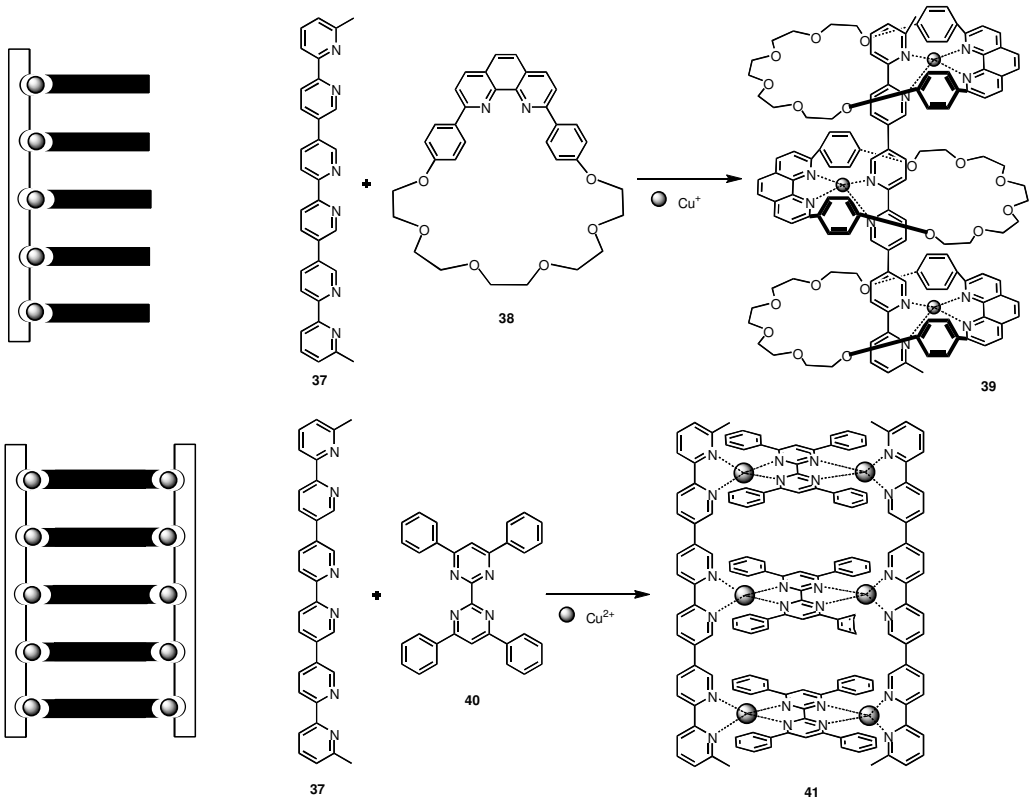

Figure 23. Schematic representation of rack and ladder with examples

1.2.4 Helicates

Although double and triple helicates include lots of challenge, they are the first innovation template examples of DNA. As it's known that biological systems

serve many examples for self-assembling processes and one of them is DNA produced by incorporation two complementary units to form helical entities. With the same analogy, it is possible to synthesize artificial helical structures by using ligands containing multiple binding sites and metal ions that are in appropriate coordination geometry.

Jean-Marie Lehn and co-workers constructed double helices **43** by using poly-bipyridine ligand **42** which were connected to each other with ether linkages.[47] As it is seen in Figure- that the ligand are connected each other with copper (I) ions which enable four coordination sites with tetrahedral geometry. These incorporation leads to form helical architecture.

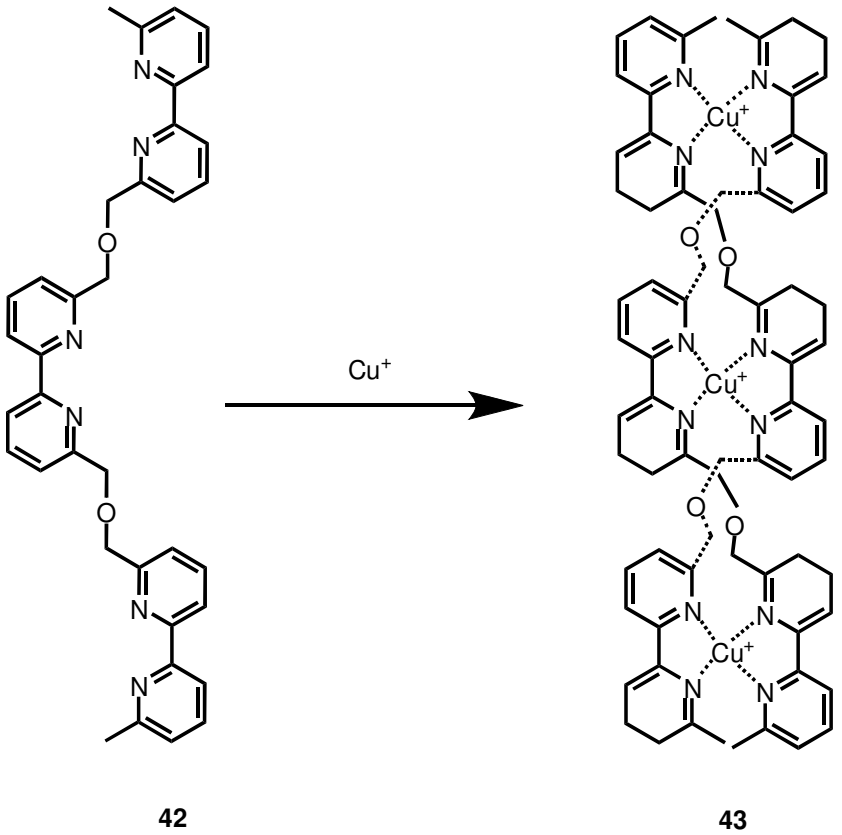

Figure 24. Assemblies of bipyridine derivatives to construct helicates

1.2.5 Molecular boxes and Macrocycles

Molecular boxes and macrocycles showing interesting luminescent and redox-active properties have also been introduced. **44** is an example for macrocycle bearing a ligand consisting of two terpyridine unit and ruthenium (II) ions. Six coordination geometry of ruthenium (II) ion enables the attachment of two terpyridine units in a proper way (Figure 25). [48] Generally, this type of architectures is called metal-based dendrimers.

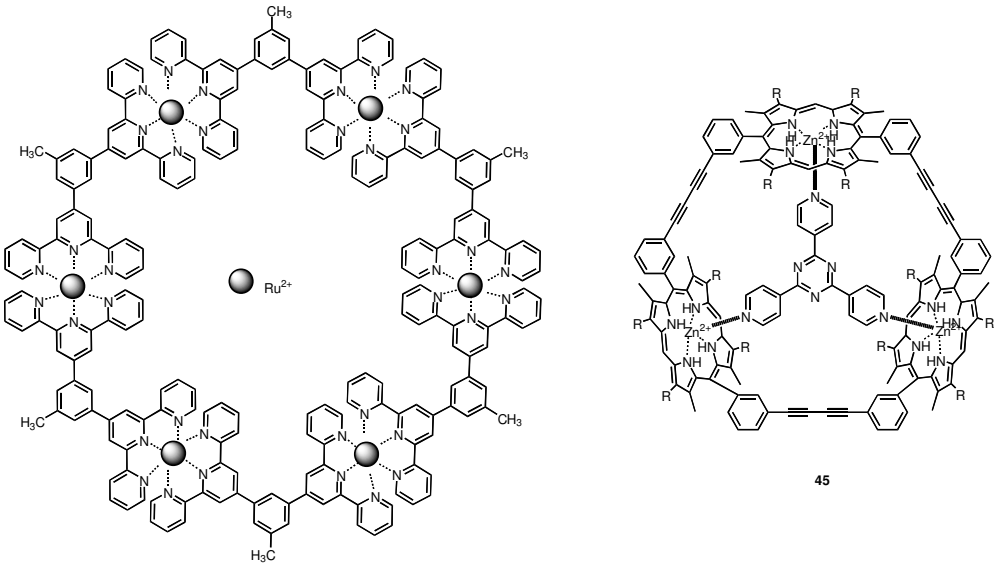

Figure 25. Molecular boxes and macrocycles

45 is an another example of macrocycle showing trimeric forms. **45** was synthesized by means of metal-directed coupling reaction of dialkyne metalloporphyrin units. The addition of 1,3,5-tris (4-pyridiyl)triazine results with the formation of **45** ; cage like macrocycle (Figure 25).[49]

1.3 BODIPY Dyes

1.3.1 Introduction to BODIPY Dyes

In recent years, there are lots of fluorescent organic compounds reported in the literature. Although these dyes are known, 4,4-difluoro-4-bora-3a,4a-diaza-s-indacene (BODIPY) dyes has steadily become famous and increased its popularity over the past two decades. Since the first BODIPY dyes have been reported by Treibs and Kreuzer[50] in 1968, several different BODIPY dyes have been synthesized and used for many different applications [51,52] It is a well known fact that high fluorescent quantum yield, narrower emission bandwidths, the thermal and photostability, great solubility and ease of functionalization from various positions make BODIPY fluorophore superior over commonly used dyes. These excellent characteristics of BODIPY dyes increase its potential using in different applications. BODIPY dyes have been used as chemosensors[53-60], laser dyes[61], biological labeling reagents[62], energy transfer reagents[63,64], light harvester[65], photo dynamic therapy reagents[66], and for solar cell applications[67].

1.3.2 The Numbering System of BODIPY Dyes

Although the numbering system of BODIPY core and dipyrromethene is different, the terms alpha, beta and meso positions are used for same positions (Figure 26).

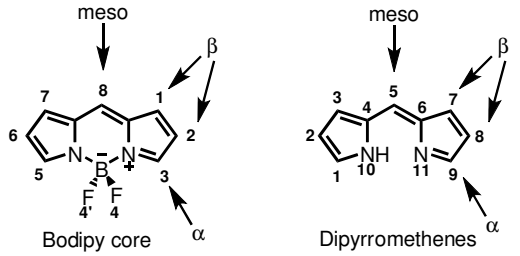

Figure 26. Numbering systems of BODIPY core and dipyrromethene

1.3.3 Functionalization of BODIPY Dyes

It is a well known fact that the most important characteristic of BODIPY core is the ease and variety of functionalization. The BODIPY core gives several different reactions from different positions (Figure 27).

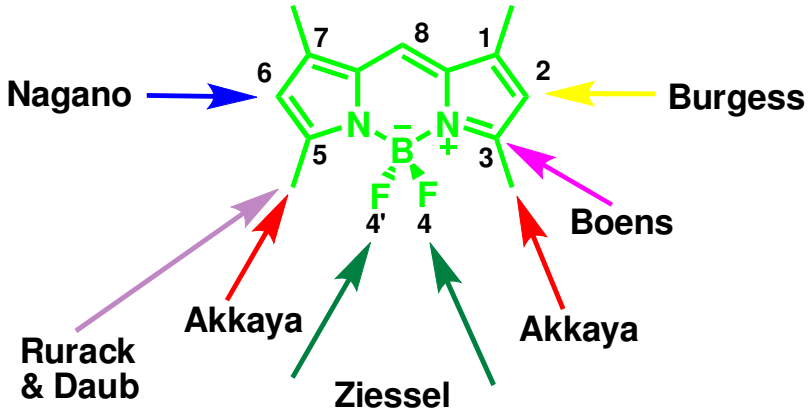

Figure 27. The functionalization points of BODIPY core

The 2,6-positions of BODIPY core give electrophilic substitution reaction if it is treated with chlorosulphonic acid.[68] The main advantage of this functionalization is that it provides a new BODIPY core **46** which is soluble in water (Figure 28).

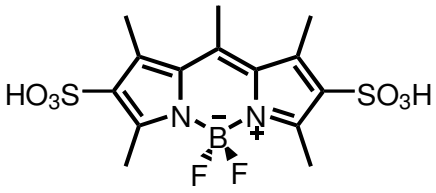

46

Figure 28. Water soluble BODIPY Derivative

Moreover, the treatment of the bodipy core with other electrophiles such as iodine **47a** or bromine **47b** opens further synthetic modification ways. Diiodo substituted BODIPY derivatives was easily synthesized by Nagano (Figure 29).[69]

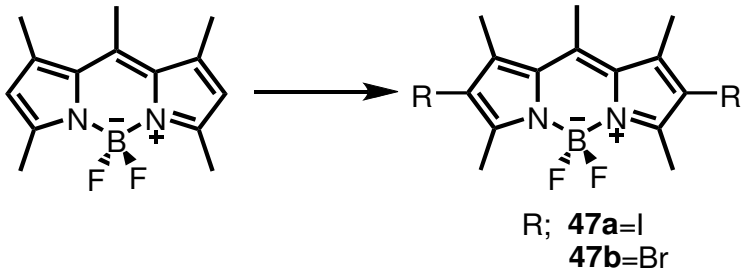

Figure 29. Diiodo and Bibromo functionalized Bodipy dyes

The 3,5-positions, which involves good leaving groups such as chlorine atoms, of the BODIPY core undergo nucleophilic substitution reactions with amino, alkoxy or thioalkoxide groups. The attachment of these electron donating groups to the 3- and 5- positions cause to considerable change in absorption and emission wavelength (red shift) at the BODIPY core (Figure 30).[70,71]

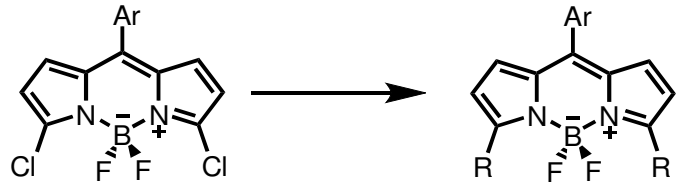

Figure 30. Nucleophilic substitution reactions at haloginated BODIPY cores

The 3- and 5- positioned methyl groups of BODIPY core give Knoevenagel reactions by means of their moderate acidic character. These condensation

reactions between methyl groups of BODIPY cores with different aromatic aldehydes make possible synthesize different styryl substituted BODIPY core derivatives. Moreover, this styryl substitution yields BODIPY cores which have long absorption and emission wavelength. Mono **48** or di **49**, **50** and **51** styryl substituted BODIPY cores can be easily synthesized by using this method (Figure 31).[72,73]

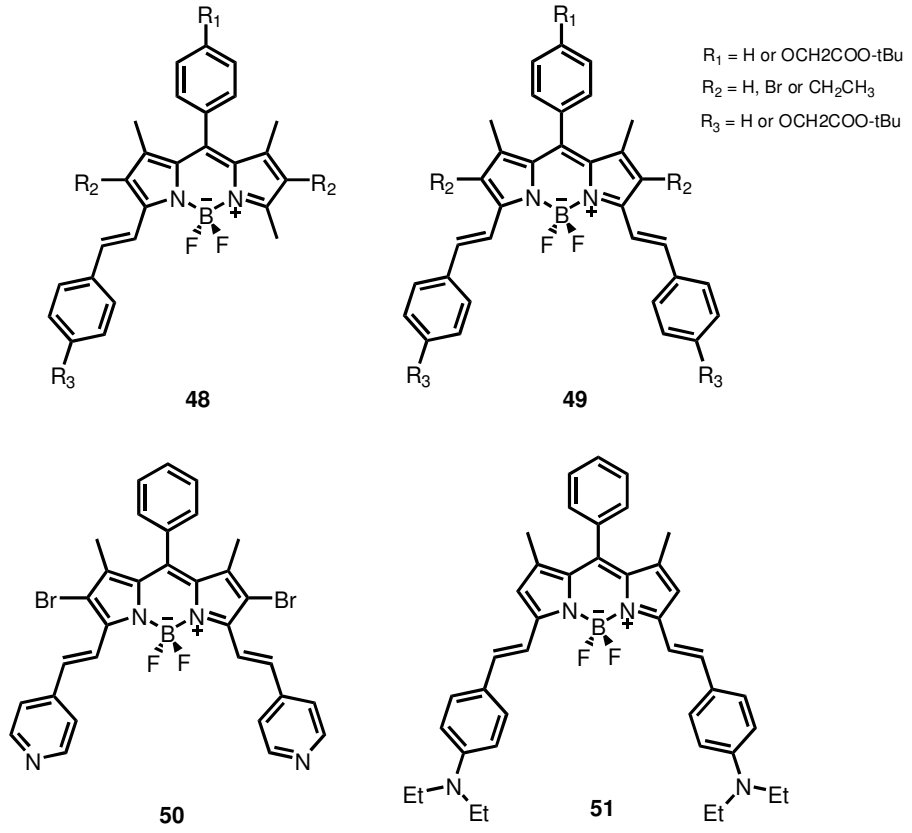

Figure 31. Condensation reactions from 3,5-positions of Bodipy cores

Other functionalization method of BODIPY core is the displacement of fluoride atoms located at boron center of BODIPY core. Limited literature examples have been reported for this type of functionalization. However, Ziessel and co-workers

have replaced floride units of boron center of BODIPY core with ethynyl[74] **52**, ethynylaryl[75] **53** and aryl[76] **54** groups (Figure 32). This type of functionalization does not cause to significant change in the absorption and emission wavelength at Bodipy core.

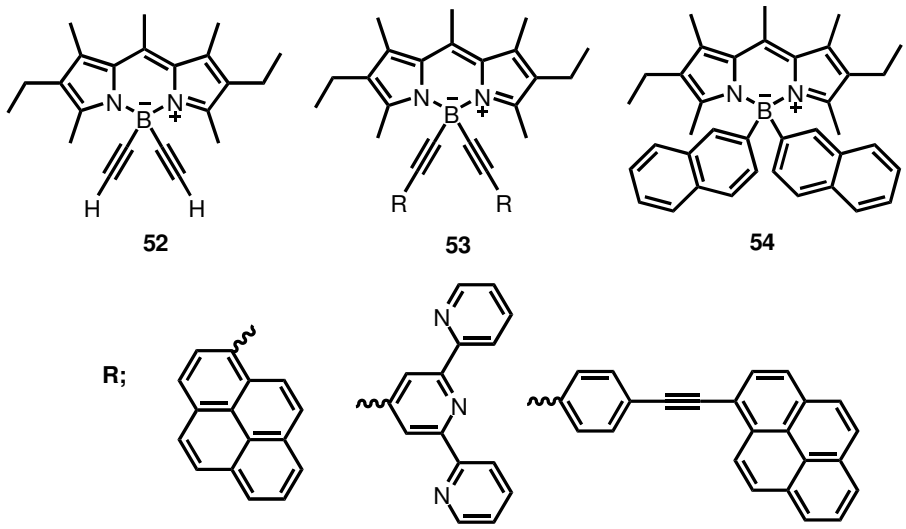

Figure 32. Functionalization at Boron center of BODIPY core

Sonogashira, Stille, Heck, and Suzuki type coupling reactions have been used to functionalize the different positions of BODIPY core. Coupling reactions are not only applicable to directly BODIPY core but also to aryl groups which connected to BODIPY skeleton. Burgess and co-workers have reported some BODIPY derivatives which were prepared from halogenated BODIPY core derivatives via palladium-mediated cross coupling reactions.[77] **55** is an example for Suzuki type coupling; on the other hand, **56** and **57** are examples for Sonogashira reaction which were directly applied on BODIPY skeleton and indirectly, respectively (Figure 33).

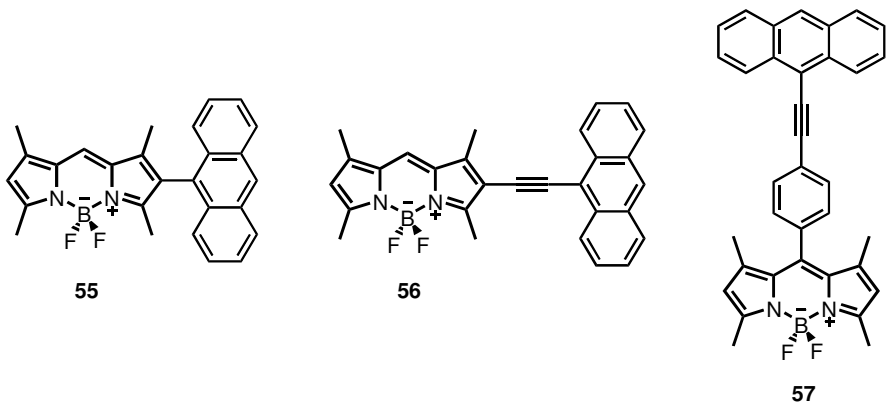

Figure 33. Palladium-assisted coupling reactions at Bodipy skeleton

The absorption and emission wavelength of compounds **55** and **56** are different form unsubstituted BODIPY dye. In fact, red shift is observed, clearly.

1.3.4 Application of BODIPY Dyes

As mentioned above, high fluorescent quantum yield, narrower emission bandwidths, the thermal and photostability, great solubility and ease of functionalization from various positions make BODIPY dyes appreciable to use in different applications such as chemosensors, biological labeling, photodynamic therapy, light harvesting system, energy transfer systems and solar cells.

1.3.4.1 Chemosensors

Design and synthesis of fluorescent sensors have attracted great interest in supramolecular chemistry. The working principle of chemosensors is that trapping of an analyte by pre-designed site leads to change in fluorescent properties of the sensor. Binding of analyte can generally cause an increase or decrease in fluorescence. A rich variety of fluorophore is incorporated to lots of different ligands bearing recognition sites selective to a specific analyte.

However, these types of chemosensors fall outside the scope of this thesis. In fact, there will be given some examples of chemosensors based on BODIPY dyes. Daub and Rurack[78] were reported the first examples of BODIPY based chemosensors in 1997 and then countless examples of BODIPY based fluorescent molecular sensors have been reported.[51,52]

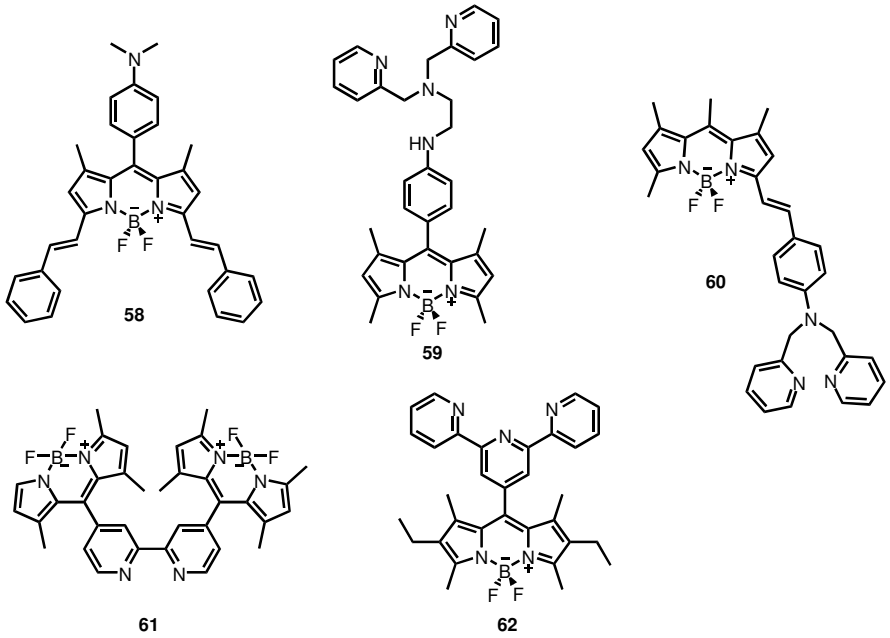

Figure 34. BODIPY Based Chemosensors

Some examples are given for sensors bearing BODIPY core units as a flourophore in Figure 34. Molecule **58** is a near-IR emitter pH indicators or chemical sensor for protons present in organic media.[79] The strong electron donor characteristic of dimethylamino group leads to decrease in florescence since the intramolecular charge transfer from dimethylamino nitrogen atoms to the excited singlet state of the BODIPY dyes occur. However, protonation of dimethylamino group blocks the intramolecular charge transfer and so the fluorescence of BODIPY core is observed.

59[80] and **60**[81] have anilino groups as recognition sites. Incorporation of flexible arms to aniline groups enables these chemosensors to recognize certain transition metals. **59** detects zinc(II) cation while **60** detects cadmium(II) cation. In similar aspect, 4 senses mercury(II) salts by means of crown ether based recognition sites positioned at meso center of BODIPY core. On the other hand, **61**[82] and **62**[83] have recognition groups bipyridine and terpyridine, respectively.

1.3.4.2 Biological Labelling

Excellent photo physical properties make BODIPY dyes superior over other common dyes which are used as Biological Labeling reagents. In fact, its high fluorescence quantum yields, large absorption coefficient, large range of colors, good photo stability and solubility in common solvents make BODIPY dye an excellent Biological Labeling reagent. The first usage of BODIPY dyes as a labeling reagent was practiced in proton and from first time to today, lots of literature examples have been reported for application of BODIPY dyes which have been used as Biological Labeling reagents.[62]

1.3.4.3 Photodynamic Therapy

The other application of BODIPY dyes is the photodynamic therapy. Photodynamic therapy is an alternative cancer treatment by using the combination of photodynamic reagent and visible or near visible light (650-800 nm wavelengths which cannot be absorbed by body tissue). The process starts with the localization of Photodynamic therapy reagents in cancer cells and continues with exposure of light. Afterwards, the photodynamic therapy reagent is excited with light which is between 650-800 nm to generate reactive singlet oxygen ($^1O_2$) which leads to fatal damage in cancer cell. Many common organic dyes have been used as photodynamic therapy reagent such as porphyrins,

texaphyrins, phthalocyanines, squaraines, chalcogenopyrylium dyes, and perylenediimides.

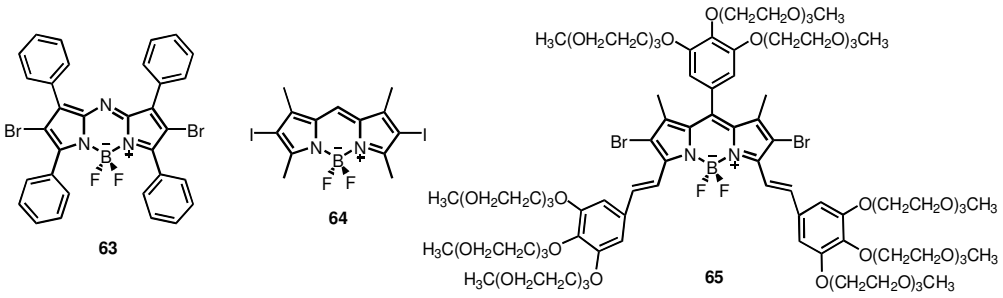

Figure 35. BODIPY Dye derivatives for PDT

And in recent years, BODIPY dyes have also been used as photodynamic therapy reagent. O'shea and co-workers[84] were reported some azaboradiazaindacenes dyes **63** as photodynamic therapy reagents. Nagano[85], Akkaya and co-workers[66] were also introduced some BODIPY derivatives **64**, **65** which are appropriate for Photodynamic therapy, respectively (Figure 35).

1.3.4.4 Light harvesting and Energy Transfer Cassettes

The discovery of new fluorescent molecules has added new concepts such as light harvesting system. Transferring the excitation energy to an energy acceptor located at the core is the key feature of working principle of light harvesting system. Akkaya and co-workers[86] were reported dendritic light harvesting system **66** which involves four BODIPY based donor parts and one perylene bisimide group as an acceptor part at the core (Figure 36). The extinction coefficient of BODIPY at 526 nm and perylene bisimide 582 nm is 240 000 and 45 000 M^{-1} cm^{-1}, respectively. The four BODIPY units as acceptor leads to this high extinction coefficient value. At 526 nm is not observed any fluorescence emission from BODIPY core and this indicates efficient energy transfer efficiency.

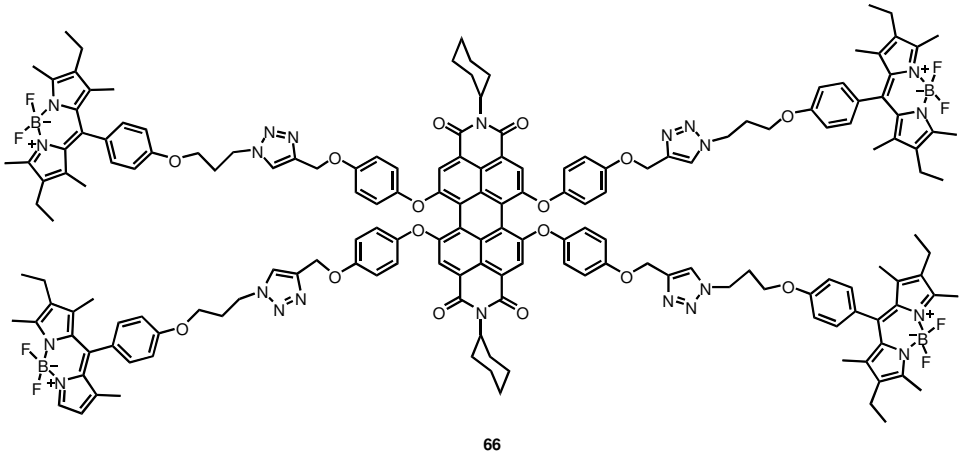

66

Figure 36. Dendritic light harvesting system bearing BODIPY core

The other application of BODIPY dye is the energy transfer cassettes. Two types of modeling are available for energy transfer which are through-space and through bond. **67**[87] and **68**[88] are two examples for through space and through bond types energy transfer cassettes, respectively (Figure 37).

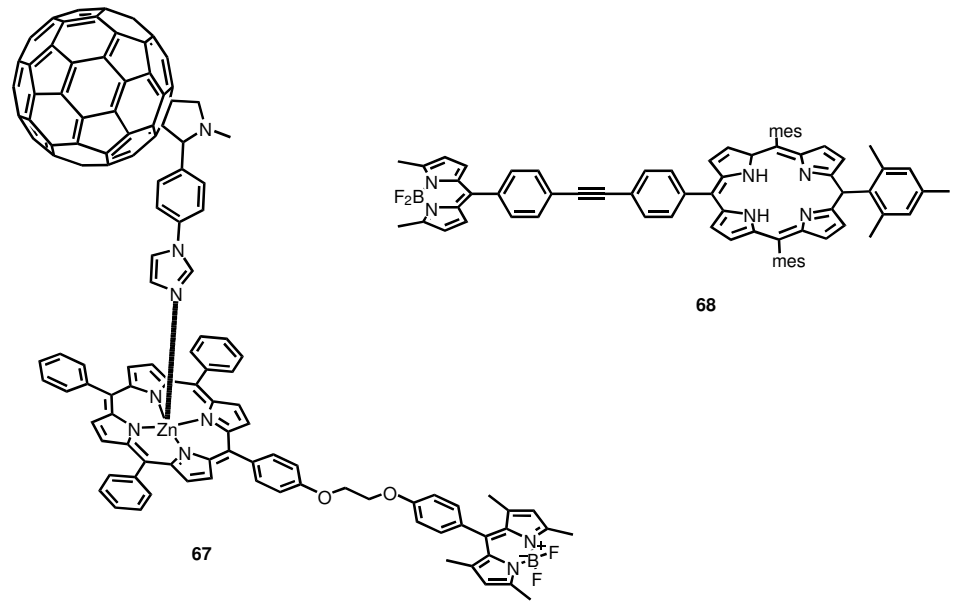

67

68

Figure 37. BODIPY dyes in energy transfer cassettes

1.3.4.5 Solar cells

Dye-sensitized solar cells (DSSc) are seen as highly promising alternatives for more expensive solar cell technologies. Lots of dyes are used by incorporating with appreciate groups which have ability to increase the solar cell efficiency. **69** is a good example for solar cell application of BODIPY dye (Figure 38).[67]

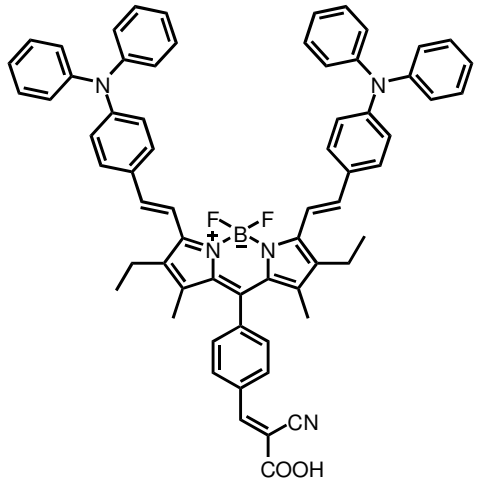

69

Figure 38. Solar cell material including BODIPY chromophore

CHAPTER 2

EXPERIMENTAL

2.1 Instrumentation

General: ^{1}H NMR and ^{13}C NMR spectra were recorded on Bruker DPX-400 (operating at 400 MHz for ^{1}H NMR and 100 MHz for ^{13}C NMR) in $CDCl_3$ and DMSO-d_6 solvents with tetramethylsilane as internal standard. All spectra were recorded at 25^{o}C and coupling constants (*J values*) are given in Hz. Chemical shifts are given in parts per million (ppm). Absorption spectra were performed by using a Varian Carry-100 spectrophotometer. Fluorescence measurements were conducted on a Varian Eclipse spectrofluometer. Mass spectra were recorded at the Ohio State University Mass Spectrometry and Proteomics Facility, Ohio, U.S.A. Reactions were monitored by thin layer chromatography using Merck TLC Silica gel 60 F_{254} and Merck Aluminium Oxide 60 F_{254}. Silica gel column chromatography was performed over Merck Silica gel 60 (particle size: 0.040-0.063 mm, 230-400 mesh ASTM). Aluminium oxide column chromatography was performed using Merck Aluminium Oxide 90 active neutral. 4'-(4-ethynylphenyl)-2,2';6'2"-terpyridine, 5,5'-diethynyl-2,2'-bipyridine, 5-ethynyl-2,2'-bipyridine were synthesized according to literature.[89] Anhydrous tetrahydrofuran was obtained by refluxing over sodium/benzophenone prior to use. All other reagents and solvents were purchased from Aldrich and used without further purification.

UV-vis and Fluorescence Titration Experiments: UV-vis and Fluorescence titrations were conducted at 25^{o}C as constant host titrations. To a solution of **75** and **77** (0.005 mM in 80:20 $CHCl_3$/MeOH) were added aliquots of $Zn(OTf)_2$ (0.005 mM in 80:20 $CHCl_3$/MeOH) and to a solution of **76** and **78** were added

aliquots of $Zn(NO_3)_2$ (0.005 mM in 80:20 $CHCl_3$/MeOH) and solvent mixture (80:20 $CHCl_3$/MeOH) to obtain desired metal to ligand ratio. After each addition, UV-vis and Fluorescence spectra were recorded.

^{1}H NMR Titration Experiments: To a solution of **75** (13 mM in 60:40 $CDCl_3$/ DMSO-d_6) or **77** (13 mM in 60:40 $CDCl_3$/DMSO-d_6) were added aliquots of $Zn(OTf)_2$ (13 mM in 60:40 $CDCl_3$/DMSO-d_6) and solvent mixture (60:40 $CDCl_3$/ DMSO-d_6) to obtain desired metal to ligand ratio and after each addition, ^{1}H NMR spectra were recorded at 25^{o}C.

2.2 Syntheses

2.2.1 Synthesis of 3,5-Bis(decyloxy)benzyl alcohol (70)

A mixture of 3,5-dihydroxybenzyl alcohol (42.81 mmol, 6.00 g), 1-bromodecane (107.03 mmol, 23.7 g), K_2CO_3 (171.24 mmol, 23.7 g), and 18-crown-6 (4.281 mmol, 1.13 g) in dry acetone were reflaxed under nitrogen atmosphere for 24 h. Solvent was evaporated under reduced pressure and water was added to the residue. Reaction product extracted into chloroform (3x100 mL) and after organic phase dried over anhydrous Na_2SO_4. After the evaporation of the solvent, silica gel column chromatography using 2:1 $CHCl_3$: Hexanes as the eluant afforded desired product (17.1 g, 95%).

^{1}H NMR (400 MHz, CDCl3) δ 6.38 (2H, s ArH), 6.25 (1H, s, ArH), 4.45 (2H,s, CH_2OH), 3.30 (4H, t, J = 6.6 Hz, OCH_2), 2.36 (1H, s, OH), 1.65 (4H, m, CH_2), 1.1-1.4 (28H, m, CH_2), 0.8 (6H, t, J= 6.5 Hz, CH_3).

^{13}C NMR (100 MHz, $CDCl_3$) δ 160.5, 143.2, 105.0, 100.5, 68.1, 65.4, 33.9, 32.9, 31.9, 31.9, 29.6, 29.6, 29.5, 29.5, 29.4, 29.3, 29.3, 29.3, 28.8, 28.2, 26.1, 24.8, 22.7, 14.1.

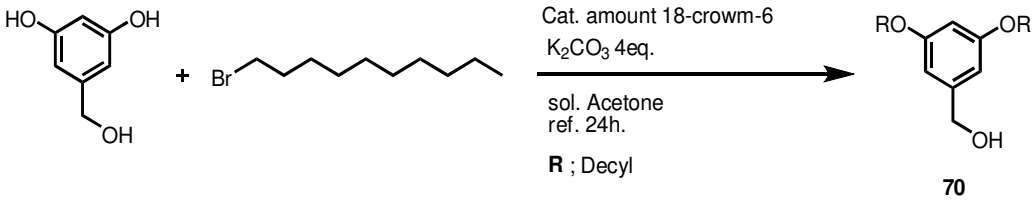

Figure 39. Synthesis of Compound **70**

2.2.2 Synthesis of 3,5-Bis(decyloxy)benzaldehyde (71)

In a 500 mL round-bottomed flask containing 250 mL CH_2Cl_2 were added **70** (21.40 mmol, 9.00 g) and PCC (53.49 mmol, 11.53 g), and the reaction mixture was stirred for 3 h at room temperature. Reaction mixture was then washed with water and organic phase was evaporated at reduced pressure. Silica gel column chromatography using $CHCl_3$ as the eluant afforded a waxy solid (8.1g, 90%).

^{1}H NMR (400 MHz, CDCl3) δ_H 9.80 (1H s), 6.93 (2H, s, ArH), 6.60 (1H, s, ArH), 3.92 (4H, t, J = 6.49 Hz, OCH_2), 1.70 (4H, m, CH_2), 1.38 (4H, m, CH_2), 1.20 (24H, m, CH_2), 0.80 (6H, t, J = 6.59 Hz, CH_3).

^{13}C NMR (100 MHz, $CDCl_3$) δ_C 192.0, 160.8, 138.4, 108.1, 107.1, 68.5, 31.9, 29.6, 29.5, 29.3, 29.1, 26.0, 22.7, 14.1.

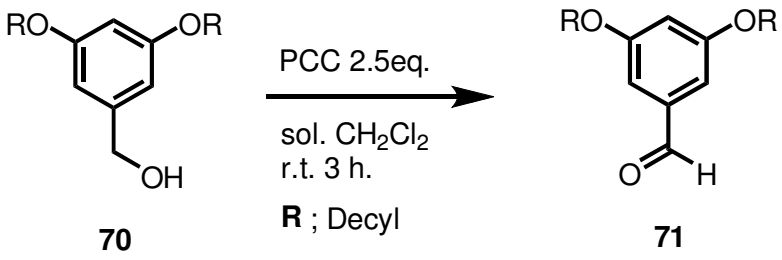

Figure 40. Synthesis of Compound **71**

2.2.3 Synthesis of 4,4-difluoro-8-(3′,5′-bis(decyloxy)phenyl)-1,3,5,7-tetramethyl-4-bora-3a,4a-diaza-*s*-indacene (72)

To a 1L round-bottomed flask containing 400 mL argon-degassed CH_2Cl_2 were added 2,4-dimethyl pyrrole (15.8 mmol, 1.50 g) and **71** (7.17 mmol, 3 g). One drop of TFA was added and the solution was stirred under N_2 at room temperature for 1d. After addition of a solution of DDQ (7.17 mmol, 1.628 g) in 100 mL of CH_2Cl_2 to the reaction mixture, stirring was continued for 30 min. 6 mL of Et_3N and 3 mL of $BF_3.OEt_2$ were successively added and after 30 min, the reaction mixture was washed three times with water and dried over anhydrous Na_2SO_4. The solvent was evaporated and the residue was purified by silica gel column chromatography using 2:1 $CHCl_3$: Hexanes as the eluant. Red waxy solid (1.381 g, 30%).

^{1}H NMR (400 MHz, CDCl3) δ_H 6.45 (1H, s, ArH), 6.35 (2H, s, ArH), 5.90 (2H, s, H2, H6), 3.85 (4H, t, *J* = 6.56 Hz, OCH_2), 2.47 (6H, s, CH_3), 1.70 (4H, m, CH_2), 1.49 (6H, s, CH_3), 1.35 (4H, m, CH_2), 1.20 (24H, m, CH_2), 0.80 (6H, t, *J* = 6.53 Hz, CH_3).

^{13}C NMR (100 MHz, CDCl3) δ_C 161.2, 155.4, 143.2, 136.4, 131.2, 121.0, 106.4, 102.3, 68.4, 31.9, 29.6, 29.5, 29.3, 29.2, 26.0, 22.7, 14.6, 14.2, 14.0.

MS (TOF- ESI): m/z: Calcd: 658.4572 $[M+Na]^+$, Found: 658.4542 $[M+Na]^+$.

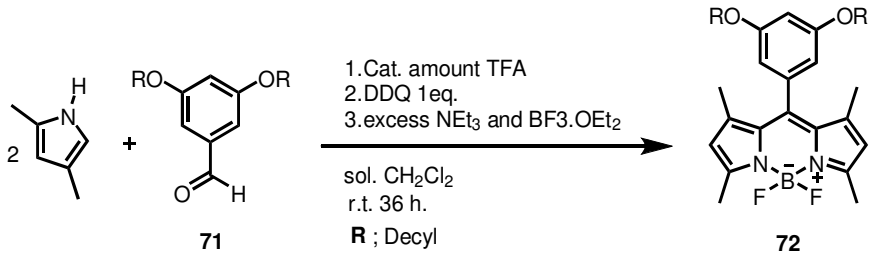

Figure 41. Synthesis of Compound **72**

2.2.4 Synthesis of 4,4-difluoro-8-(3′,5′-bis(decyloxy)phenyl)-2-iodo-1,3,5,7-tetramethyl-4-bora-3a,4adiaza-*s*-indacene (73)

72 (1.91 mmol, 1.21 g) and Iodine (1.52 mmol, 0.387 g) were added to a 500 mL round-bottomed flask and to this solution was added Iodic acid (1.52 mmol, 0.268 g) dissolved in 2 mL of water. The reaction mixture was stirred at 60°C and was monitered by TLC 1:1 $CHCl_3$: Hexanes. When TLC indicated that all the starting material had been consumed, saturated $Na_2S_2O_3$ solution in water was added and the product was extracted into $CHCl_3$. The solvent was evaporated and the residue was purified by silica gel column chromatography using 1:1 $CHCl_3$: Hexanes as the eluant. Red waxy solid (0.98 g, 67%).

^{1}H NMR (400 MHz, CDCl3) δ_H 6.48 (1H, s, ArH), 6.32 (2H, d, J = 1.90 Hz, ArH), 5.97 (1H, s, H2), 3.85 (4H, t, J = 6.60 Hz, OCH_2), 2.55 (3H, s, CH_3), 2.49 (3H, s, CH_3), 1.68 (4H, m, CH_2), 1.49 (6H, s, CH_3), 1.35 (4H, m, CH_2), 1.20 (24H, m, CH_2), 0.8 (6H, t, J = 6.60, CH_3).

^{13}C NMR (100 MHz, CDCl3) δ_C 161.3, 157.7, 154.4, 145.1, 143.2, 141.5, 136.2, 131.6, 130.7, 122.1, 106.2, 102.5, 84.1, 68.4, 38.2, 33.8, 32.9, 31.9, 31.3, 29.7, 29.6, 29.5, 29.4, 29.3, 29.2, 28.8, 28.2, 26.1, 26.0, 25.8, 22.7, 16.5, 15ç7, 14.7, 14.5, 14.1.

MS (TOF- ESI): m/z: Calcd: 784.3538. $[M+Na]^+$, Found: 784.3513 $[M+Na]^+$.

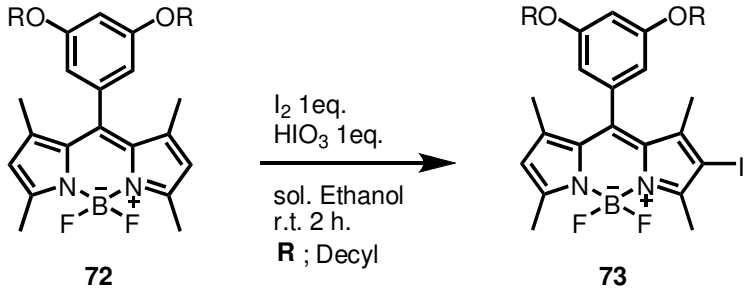

72 73

Figure 42. Synthesis of Compound **73**

2.2.5 Synthesis of 4,4-difluoro-8-(3,5-bisdecyloxy)phenyl-2,6-diiodo-1,3,5,7-tetramethyl-4-bora-3a,4adiaza-*s*-indacene (74)

72 (2.47 mmol, 1.57 g) and Iodine (6.18 mmol, 1.57 g) were added to a 500 mL round-bottomed flask and to this solution was added Iodic acid (4.93 mmol, 0.87 g) dissolved in 2 mL of water. The reaction mixture was stirred at 60°C and was monitored by TLC 1:1 $CHCl_3$: Hexanes. When all the starting material had been consumed, saturated $Na_2S_2O_3$ solution in water was added and the product was extracted into $CHCl_3$. The solvent was evaporated and the residue was purified by silica gel column chromatography using 1:1 $CHCl_3$: Hexanes as the eluant. Red waxy solid (2.09 g, 95%).

^{1}H NMR (400 MHz, CDCl3) δ_H 6.49 (1H, s, ArH), 6.28 (2H, s, ArH), 3.85 (4H, t, *J* = 6.45 Hz, OC*H*$_2$), 2.55 (6H, s, C*H*$_3$), 1.69 (4H, m, C*H*$_2$), 1.49 (6H, s, C*H*$_3$), 1.35 (4H, m, C*H*$_2$), 1.20 (24H, m, C*H*$_2$), 0.80 (6H, t, *J* = 6.32 Hz, C*H*$_3$).

^{13}C NMR (100 MHz, CDCl3) δ_C 161.4, 156.7, 145.4, 141.4, 136.1, 131.0, 106.1, 102.7, 85.5, 68.5, 31.9, 29.6, 29.5, 29.4, 29.3, 29.1, 26.0, 22.7, 16.9, 16.0, 14.1.

MS (TOF- ESI): m/z: MS (TOF- ESI): m/z: Calcd: 910,2505 $[M+Na]^+$, Found: 910.2495 $[M+Na]^+$.

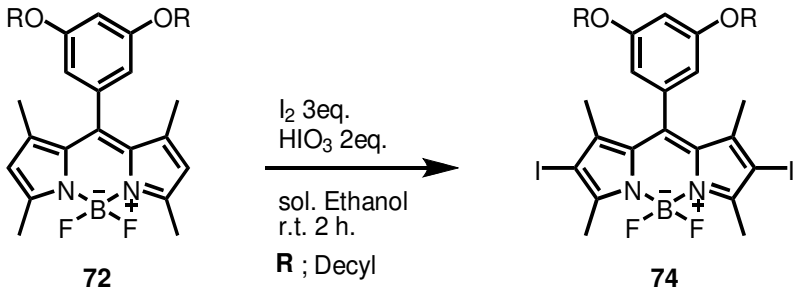

72 **74**

Figure 43. Synthesis of Compound **74**

2.2.6 Synthesis of 4,4-difluoro-8-(3′,5′-bis(decyloxy)phenyl)-2-(p-(2″,2‴:6‴,2⁗-terpyridin-4″-yl)ethynylphenyl)-1,3,5,7-tetramethyl-4-bora-3a,4a-diaza-*s*-indacene (75)

In a 50 mL Schlenk tube were added **73** (0.30 mmol, 0.23 g), 4'-(4-ethynylphenyl)-2,2';6'2"-terpyridine (0.60 mmol, 0.20 g), $(PPh_3)_2PdCl_2$ (0.018 mmol, 12.64 mg), CuI (0.03 mmol, 5.71 mg). 10 mL of freshly distilled THF and 5 mL of diisopropyl amine were added and resulting suspension was excessively deaerated by bubbling with Argon at 50^{o}C for 40 min. The reaction mixture was stirred at room temperature for 1d. After removal of the solvents at reduced pressure the residue was washed with water (100 mL) and extracted into $CHCl_3$. The organic layer was evaporated and column chromatographic separation of the residue on neutral Alumina using 1:1 $CHCl_3$: Hexanes as the eluant yielded the desired product as a purple solid. (0.203 g, 70%).

^{1}H NMR (400 MHz, CDCl3) δ_H 8.67 (2H, s, H3‴, H5‴), 8.65 (2H, d, *J* = 5.78 Hz, H6″, H6⁗), 8.58 (2H, d, *J* = 7.94 Hz, H3″, H3⁗), 7.82 (4H, m, H4″, H4⁗, ArH), 7.51 (2H, d, *J* = 8.23 Hz, ArH) 7.30 (2H, m, H5″, H5⁗), 6.48 (1H, s, H4′), 6.37 (2H, d, *J* = 1.93 Hz, H2′, H6′), 5.97 (1H, s, H6), 3.87 (4H, t, *J* = 6.57 Hz, OCH_2), 2.66 (3H, s, CH_3), 2.52 (3H, s, CH_3), 1.69 (4H, m, CH_2), 1.65 (3H, s, CH_3), 1.52 (3H, s, CH_3), 1.38 (4H, m, CH_2), 1.20 (24H, m, CH_2), 0.80 (6H, t, *J* = 6.63 Hz, CH_3).

^{13}C NMR (100 MHz, CDCl3) δ_C 161.3, 156.1, 156.0, 149.4, 149.1, 137.7, 137.0, 136.1, 131.7, 127.2, 124.5, 123.9, 121.4, 118.6, 106.2, 102.4, 95.6, 83.8, 68.5, 31.9, 29.6, 29.5, 29.4, 29.3, 29.2, 26.0, 22.7, 14.8, 14.1.

MS (TOF- ESI): m/z: Calcd: 989.5661 $[M+Na]^+$, Found: 989.5676 $[M+Na]^+$.

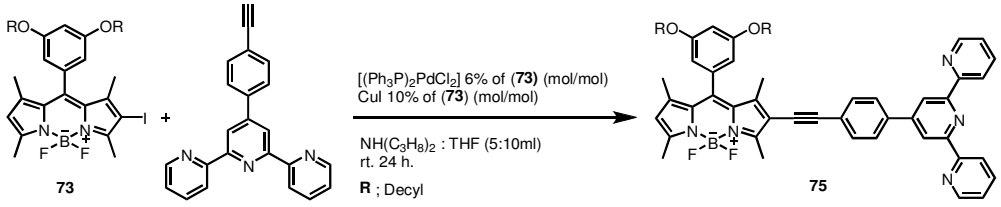

Figure 44. Synthesis of Compound **75**

2.2.7 Synthesis of 5,5′-Bis(4″,4″-difluoro-8″-(3‴,5‴-bis(decyloxy)phenyl)-1″,3″,5″,7″-tetramethyl-4″-bora-3″a,4″a-diaza-*s*-indacene-2″-ethynyl)-2,2′-bipyridine (76)

In a 50 mL Schlenk tube were added **73** (0.265 mmol, 0.202 g), 5,5'-diethynyl-2,2'-bipyridine (0.0256 mmol, 18 mg), $(PPh_3)_2PdCl_2$ (0.032 mmol, 22.3 mg), CuI (0.0265 mmol, 5.05 mg). 10 mL of freshly distilled THF and 5 mL of diisopropyl amine were added and resulting suspension was excessively deaerated by bubbling with Argon at 50°C for 40min. After degassing the reaction mixture was stirred at 50°C for 1d. After removal of the solvents at reduced pressure the residue was washed with water (100 mL) and extracted into $CHCl_3$. The organic layer was evaporated and separation by column chromatography on silica gel using $CHCl_3$ as the eluant yielded the desired product as a purple solid (0.215 g, 55%).

^{1}H NMR (400 MHz, CDCl3) δ_H 8.65 (2H, d, $J_{H6\text{-}H4}$ = 1.44 Hz, H6, H6′), 8.28 (2H, d, $J_{H3\text{-}H4}$ = 8.28 Hz, H3, H3′), 7.73 (2H, dd, $J_{H4\text{-}H3}$ = 8.28, $J_{H4\text{-}H6}$ = 1.04 Hz, H4, H4′), 6.47 (2H, t, J = 2.20 Hz, H4‴), 6.32 (4H, d, J = 2.20 Hz H2‴, H6‴), 5.98 (2H, s, H2″), 3.82 (8H, t, J = 6.62 Hz, OCH_2), 2.63 (6H, s, CH_3), 2.50 (6H, s, CH_3), 1.69 (8H, m, CH_2), 1.60 (6H, s, CH_3), 1.52 (6H, s, CH_3), 1.36 (8H, m, CH_2), 1.20 (48H, m, CH_2), 0.78 (12H, t, J = 5.28 Hz, CH_3).

^{13}C NMR (100 MHz, CDCl3) δ_C 161.3, 158.0, 156.2, 153.9, 151.2, 145.5, 142.2, 138.7, 136.0, 132.6, 129.9, 122.2, 120.5, 114.1, 106.2, 102.5, 93.1, 87.1, 68.5, 31.9, 29.7, 29.5, 29.3, 29.2, 29.1, 26.0, 22.7, 14.8, 13.5.

MS (MALDI-TOF): m/z: Calcd: 1472.965 $[M+Na]^+$, Found: 1473.120 $[M+Na]^+$.

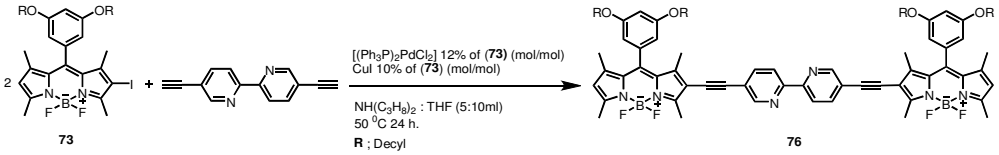

Figure 45. Synthesis of Compound **76**

2.2.8 Synthesis of 4,4-difluoro-8-(3′,5′-bis(decyloxy)phenyl)-2,6-bis-(p-(2″,2‴:6‴,2⁗-terpyridin-4″-yl)ethynylphenyl)-1,3,5,7-tetramethyl-4-bora-3a,4a-diaza-*s*-indacene (77)

In a 50 mL Schlenk tube were added **74** (0.338 mmol, 0.30 g), 4'-(4-ethynylphenyl)-2,2';6'2"-terpyridine (1.182 mmol, 0.394 g), $(PPh_3)_2PdCl_2$ (0.0203 mmol, 14.23 mg), CuI (0.034 mmol, 6.44 mg). 10 mL of freshly distilled THF and 5 mL of diisopropyl amine were added and resulting suspension was excessively deaerated by bubbling with Argon at 50^{o}C for 40min. After degassing, the reaction mixture was stirred at room temperature for 1d. Solvenst were removed at reduced pressure and the residue was washed with water (100 mL) and extracted into $CHCl_3$. The organic layer was removed and separation by column chromatography on neutral Alumina using 1:1 $CHCl_3$: Hexanes as the eluant yielded the desired product as a blue solid. (0.382 g, 87%).

^{1}H NMR (400 MHz, CDCl3) δ_H 8.68 (4H, s, H3‴, H5‴), 8.64 (4H, d, J = 6.55 Hz, H6″, H6⁗), 8.61 (4H, d, J = 7.94 Hz, H3″, H3⁗), 7.83 (4H, m, H4″, H4⁗),

7.82 (4H, d, *J* = 8.03 Hz ArH), 7.52 (4H, d, *J* = 8.15 Hz, ArH), 7.31 (4H, m, H5″, H5‴′), 6.52 (1H, br s, H4′), 6.39 (2H, d, *J* = 1.78 Hz, H1′, H6′), 3.88 (4H, t, *J* = 6.52 Hz, OCH_2), 2.68 (6H, s, CH_3), 1.71 (4H, m, CH_2), 1.69 (6H, s, CH_3), 1.38 (4H, m, CH_2), 1.20 (24H, m, CH_2), 0.80 (6H, t, *J* = 5.26 Hz, CH_3).

^{13}C NMR (100 MHz, CDCl3) δ_C 161.4, 156.2, 155.9, 149.3, 149.1, 141.0, 137.7, 136.9, 132.1, 132.0, 131.9, 131.6, 131.1, 128,6, 128.4, 127.2, 124.2, 123.9, 121.4, 118.6, 106.2, 96.4, 83.0, 68.5, 31.9, 29.6, 29.4, 29.3, 29.2, 26.0, 22.7, 14.1. 13.9.

MS (MALDI-TOF): m/z: Calcd: 1298.686 $[M+Na]^+$, Found: 1298.830 $[M+Na]^+$.

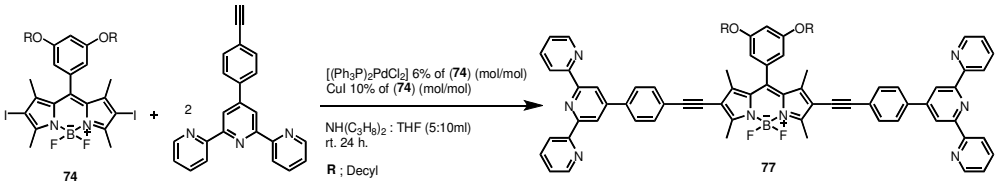

Figure 46. Synthesis of Compound **77**

2.2.9 Synthesis of 4,4-difluoro-8-(3′,5′-bis(decyloxy)phenyl)-2,6-bis(2″,2‴-bipyridine-5″-ethynyl)-1,3,5,7-tetramethyl-4-bora-3a,4a-diaza-s-indacene (78)

In a 50 mL Schlenk tube were added **74** (0.161 mmol, 143 mg), 5-ethynyl-2,2'-bipyridine (0.972 mmol, 175 mg), $(PPh_3)_2PdCl_2$ (0.096 mmol, 6.74 mg), CuI (0.016 mmol, 3 mg). 10 mL of freshly distilled THF and 5 mL of diisopropyl amine were added and resulting suspension was excessively deaerated by bubbling with Argon at 50^{o}C for 40min. After degassing, reaction mixture was stirred at 40^{o}C for 1d. After removal of the solvents at reduced pressure the residue was washed with water (100 mL) and extracted into $CHCl_3$. The solvent

was removed and separation by column chromatography on silica gel using 1 % Methanol : $CHCl_3$ as the eluant yielded the desired product as a blue solid. (0.128 g, 80%).

^{1}H NMR (400 MHz, CDCl3) δ_H 8.68 (2H, s, H6″), 8.61 (2H, d, *J* = 4.52 Hz, H6‴), 8.35 (4H, m, H3″, H3‴), 7.73 (4H, m, H4″, H4‴), 7.25 (2H, m, H5″, H5‴), 6.51 (1H, s, H4′), 6.38 (2H, d, *J* = 1.63 Hz H2′, H6′), 3.88 (4H, t, *J* = 6.54 Hz, OCH_2), 2.68 (6H, s, CH_3), 1.71 (4H, m, CH_2), 1.67 (6H, s, CH_3), 1.35 (4H, m, CH_2), 1.20 (24H, m, CH_2), 0.79 (6H, t, *J* = 6.19 Hz, CH_3).

^{13}C NMR (100 MHz, CDCl3) δ_C 161.4, 159.2, 155.9, 153.0, 151.3, 149.3, 145.3, 143.1, 140.6, 138.9, 135.9, 131.5, 124.2, 121.4, 120.4, 116.2, 106.0, 102.7, 93.5, 86.0, 68.5, 31.9, 29.5, 29.4, 29.3, 29.1, 26.0, 22.7, 14.1, 13.8, 13.4.

MS (MALDI-TOF): m/z: Calcd: 992.570 $[M+Na]^+$, Found: 992.741 $[M+Na]^+$.

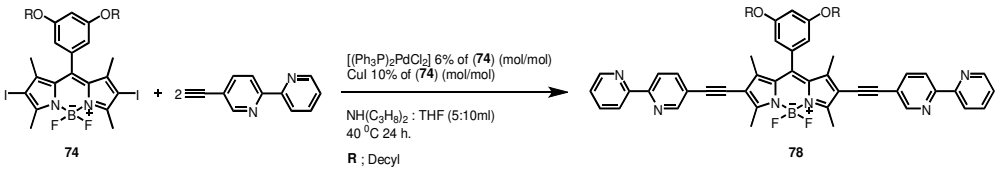

Figure 47. Synthesis of Compound **78**

CHAPTER 3

RESULTS AND DISCUSSION

Synthesis of terpyridine and bipyridine appended mono and ditopic BODIPY derivatives involve the Sonogashira reactions between mono and diiodo BODIPY derivatives and ethynylterpyridine and ethnylbipyridine. To ensure high reaction yields, solubility of reacting components is very important. In order to improve solubility in organic solvents, our synthetic approach required the initial synthesis of a BODIPY derivative with 3,5-bis(decyloxy)phenyl groups on the *meso* positions of the dyes. To that end, we started our synthesis with 3,5-bis(decyloxy)benzaldehyde **71** which can be obtained *via* a two step conversion from commercially available 3,5-dihydroxybenzyl alcohol. Standard procedures yielded bright green emitting BODIPY dye **72** in 30 % yields. Different molar ratios of I_2/HIO_3 to BODIPY **72**, resulted monoiodinated **73**, or diiodinated **74** BODIPY derivatives. Ligands were tethered to the fluorophore unit by Sonogashira couplings using either 4-ethynylphenyl-terpyridyl or bis-ethynylbipyridyl, both of which were described in literature as a result of previous studies in the Ziessel group.[89] The reactions proceeded smoothly, yielding target compounds **75**, **76**, **77** and **78**. Maximal absorption peaks showed larger red shifts in the cases of 2,6-bis substituted products (580 nm). Compound **77** was designed as the monomeric building block for a fluorescent supramolecular coordination polymer. Compound **75** is a reference compound, expected to assist us in identifying spectral changes on polymer formation. Bipyridyl derivatives **76** and **78** are different kind of building blocks which might be useful in the construction of grid-like structures and metal ion coordination mediated energy transfer and light harvesting systems. Compound **78** is particularly relevant in ions sensing applications based on earlier literature data where chromophores were tethered by bipyridyl linkages (Figure 48).

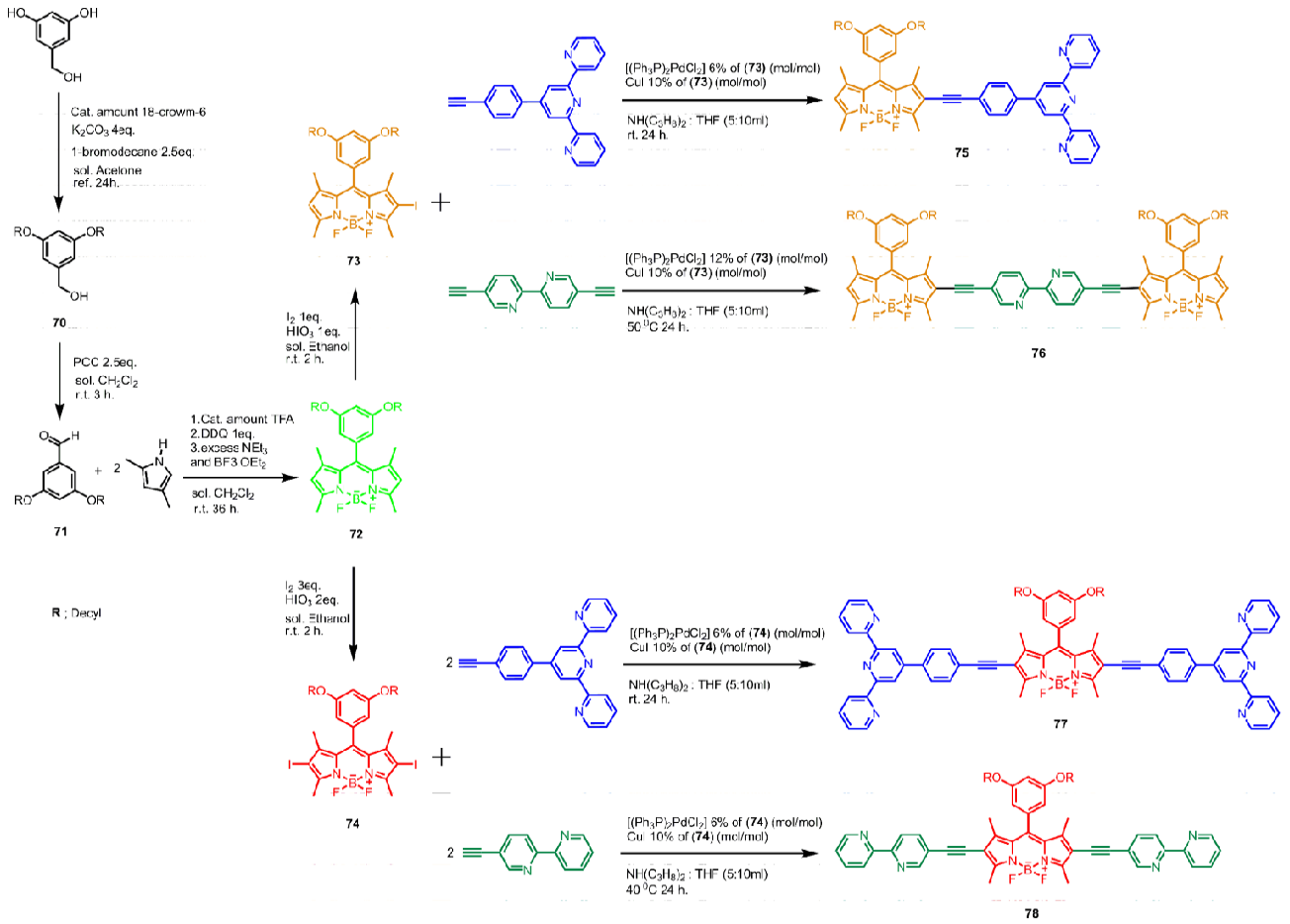

Figure 48. Total reaction scheme

NMR study of the complexation and coordination polymer formation:

Metal ion complexation generates characteristic signal changes in the ^{1}H NMR spectra (Figure 49). Firstly, the case of monoterpyridyl-BODIPY compound **75** is highly instructive. As expected, while the NMR peaks corresponding to BODIPY core is not shifted noticeably, terpyridyl peaks shift to low field on Zn(II) complex formation.

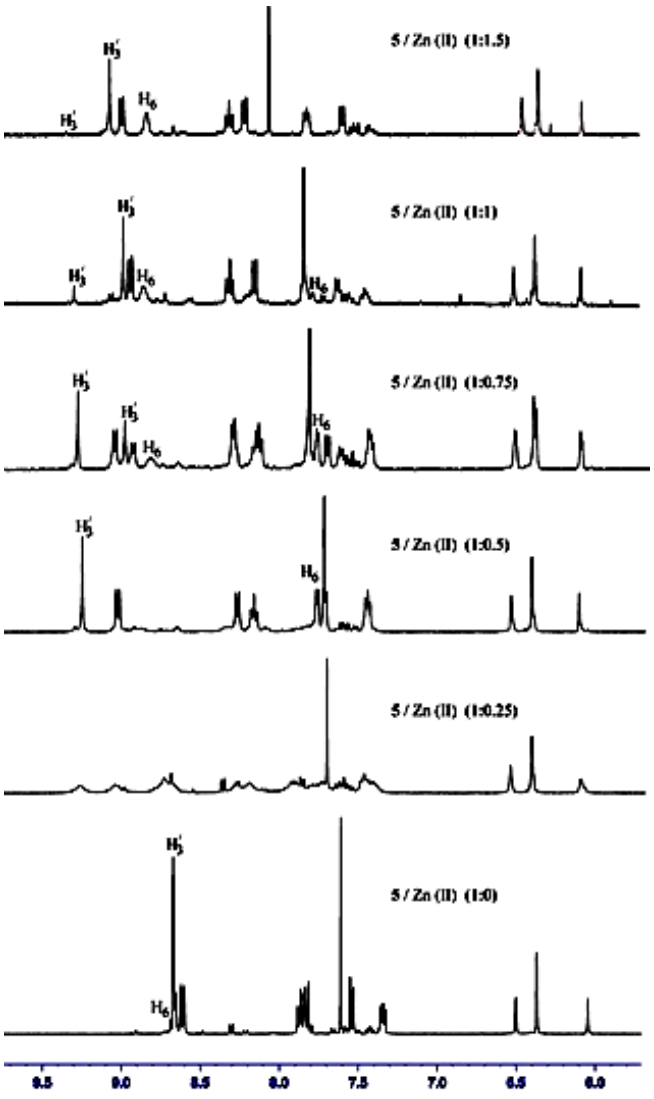

Figure 49. ^{1}H NMR spectra obtained by the titration of **75** in 60:40 $CDCl_3$: DMSO-d_6 (13 mM) with $Zn(OTf)_2$. Zn^{2+}: **75** ratio varies from bottom to top as: 0:1, 0.25:1, 0.5:1, 0.75:1, 1:1.

Addition of 0.25 equivalent of Zn(II) to **75**, results in some broadening together with a downfield shift. When Zn(II) is increased to 0.5 equivalents, the molar ratio is just right for the 2:1 (**75**$_2$-Zn(II)) complex. The most downfield sharp peak has been identified as the H3' singlet. In the 2:1 complex, it moves to 9.3 ppm.

Most characteristic change is that of the H6′ peaks. Complex formation induces a significant upfield shift, because those H nuclei will be brought into the shielding zone of the lateral pyridine rings of the other terpyridyl unit. As a result, in the metal free ligand **75**, H6′ nuclei resonate at 8.7 ppm, but 2:1 complex formation at 0.5 equivalent Zn(II) addition moves that peak to 7.7 ppm. As previously demonstrated, further addition of Zn(II) decreases the equilibrium concentration of the dimeric 2:1 complex, in favor of the "open form" (Figure 50). As a result, the sharp downfield H3′ singlet descreases in intensity as more and more Zn(II) were added.

At 1:1.5 equivalent Zn(II), the peak at 9.3 practically disappears, whereas a new singlet peak at 9.1 becomes prominent. That particular peak corresponds to the open 1:1 Zn(II) compex **75-** Zn(II). In this complex, other coordination sites of Zn(II) should be occupied with DMSO or triflate ions.

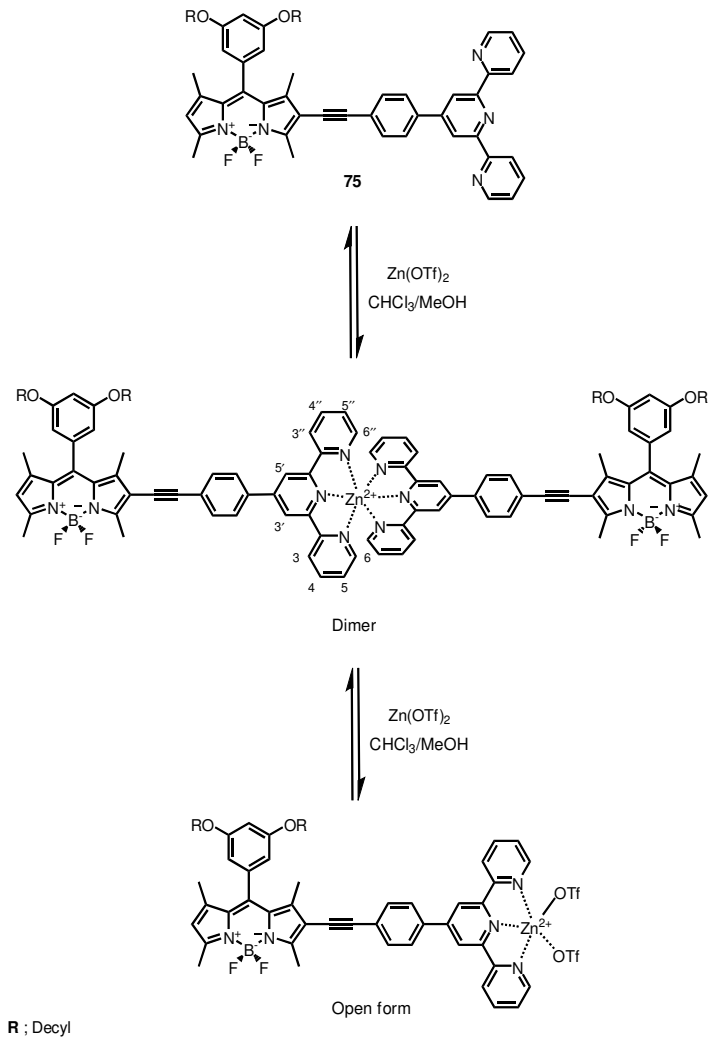

Figure 50. Formation of dimeric and open formed structures by the addition of $Zn(OTf)_2$

Bis-terpyridyl compound **77** on the other hand, displays very clear signs of polymerization on Zn(II) addition (Figure 51).Starting at 0.25 equivalent Zn(II) addition, peaks become very broad. The addition of one equivalent Zn(II) should generate largest polymer chain lengths, and that is clearly reflected in the broadness of signals.Of course, pyridine ring protons of the terpyridyl group shifted downfield.

Most interestingly, further addition beyond the 1:0.5 equivalent ligand **77** to Zn(II) ratio, makes aromatic H's to appear gradually sharper. At 1:1 equivalents ratio or at higher proportions of Zn(II), NMR spectra displays a clear predominance of 1:1 "open form" complex, with very distinctively sharper monomeric aromatic hydrogen signals (Figure 52).

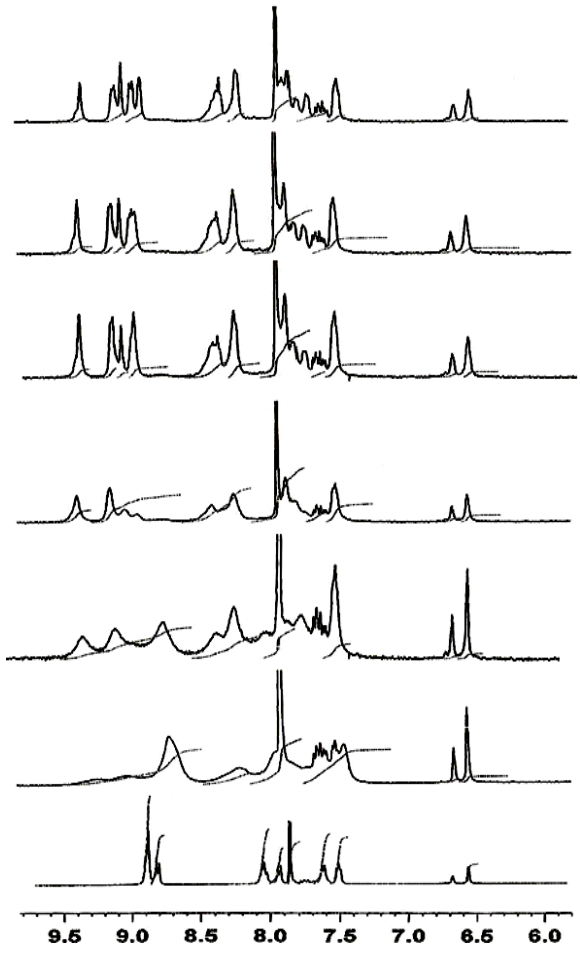

Figure 51. ^{1}H NMR spectra obtained by the titration of **77** in 60:40 $CDCl_3$: DMSO-d_6 (13 mM) with $Zn(OTf)_2$. Zn^{2+} : **77** ratio varies from bottom to top as : 0:1, 0.25:1, 0.5:1, 0.75:1, 1:1, 2:1, 3:1.

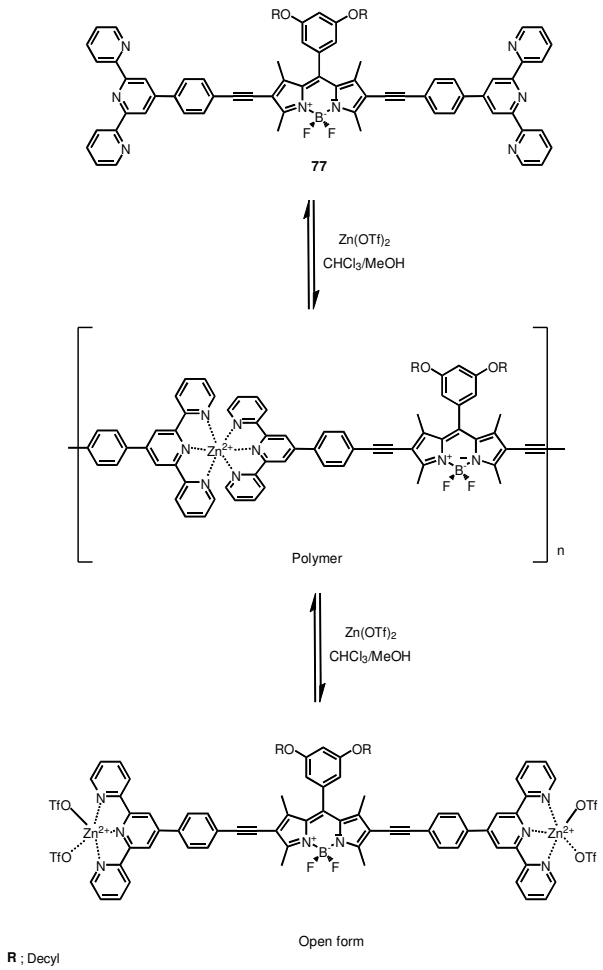

Figure 52. Formation of polymeric and open formed structures by the addition of $Zn(OTf)_2$

Absorbance and steady state fluorescence spectroscopical investigation of the complexation and coordination polymer formation:

In the building blocks synthesized in this study, terpyridyl-phenyl and bipyridyl groups have been attached to the fluorophore core *via* ethynyl-spacers, there is some conjugation and thus electronic communication between the ligand moieties and the BODIPY cores. As a result, we observe spectral changes in not only peaks which correspond to π-π* transition in the oligopyridine moieties, but in BODIPY S_0-S_1 transitions as well.

For example, in the reference compound **75**, the increase in the absorption at the 325 nm peak and the 400 nm shoulder is due to terpyridyl ligand-Zn(II) coordinative interaction. As the inset in Figure 53 shows clearly, above 0.5 equivalents of Zn(II) the change in the absorption levels off very quickly, indicating a strong affinity between the ligand and the Zn(II) in this particular solvent system (80:20 $CHCl_3$:MeOH).

In addition, there is small increase at the BODIPY absorption peak at 546 nm, as the added amount of Zn(II) is increased (extinction coefficient π-π* changes from 92,000 $cm^{-1}M^{-1}$ to 102,000 $cm^{-1}M^{-1}$). Zn(II) titration of the monotopic ligand **5**, shows a gradual increase in the emission intensity (Figure 54), at saturation the intensity of the BODIPY emission is nearly doubled. There is a concomitant small blue shift in the emission intensity in the peak, from 572 nm to 564 nm.

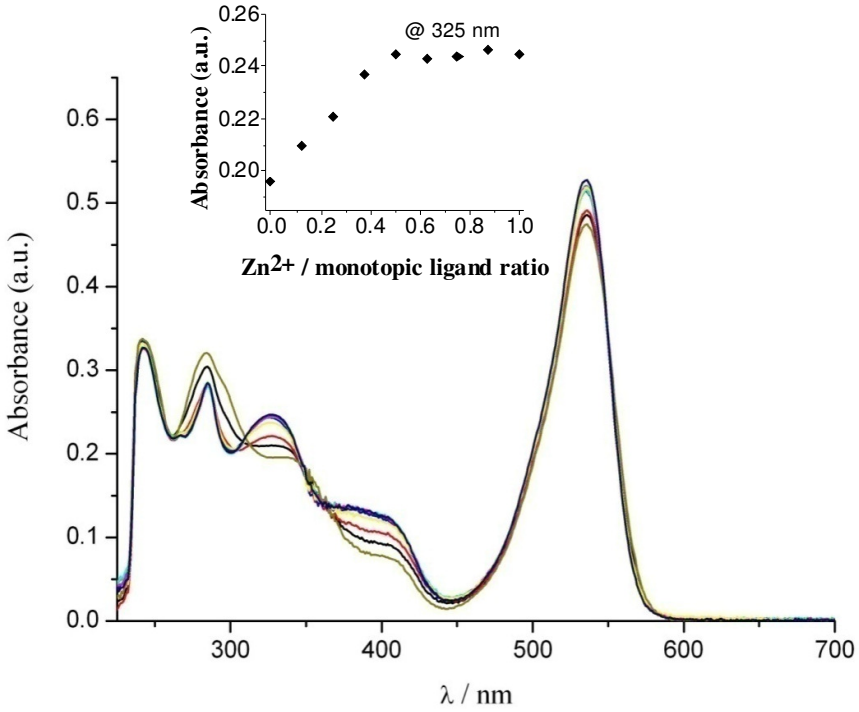

Figure 53. UV-vis spectra obtained by the titration of **75** in 80:20 $CHCl_3$: MeOH ($5x10^{-6}$ M) with $Zn(OTf)_2$. The inset shows the absorption coefficient at 325 nm as a function of Zn^{2+}/**75** ratio.

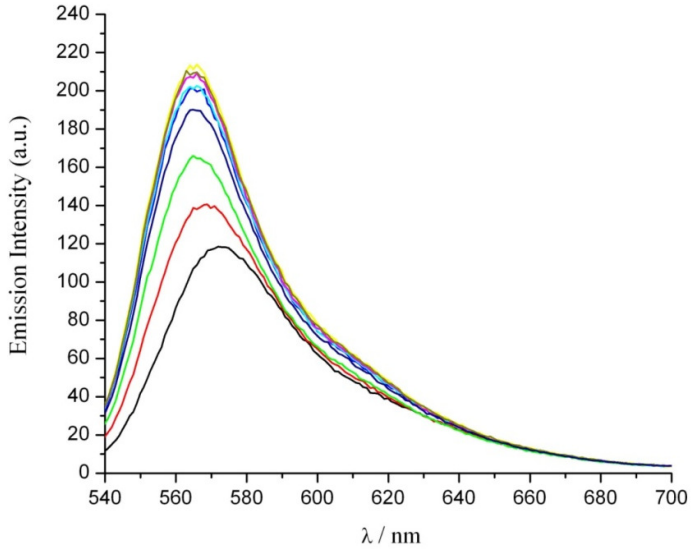

Figure 54. Fluorescence spectra obtained by the titration of **75** in 80:20 $CHCl_3$: MeOH ($5x10^{-6}$ M) with $Zn(OTf)_2$

Zn(II) titration of the ditopic bis-terpyridyl BODIPY ligand **77** shows similar changes. There are again increases in the absorption peaks at 325, 400 (shoulder) and 578 nm (BODIPY S_0-S_1 transition) (Figure 55).

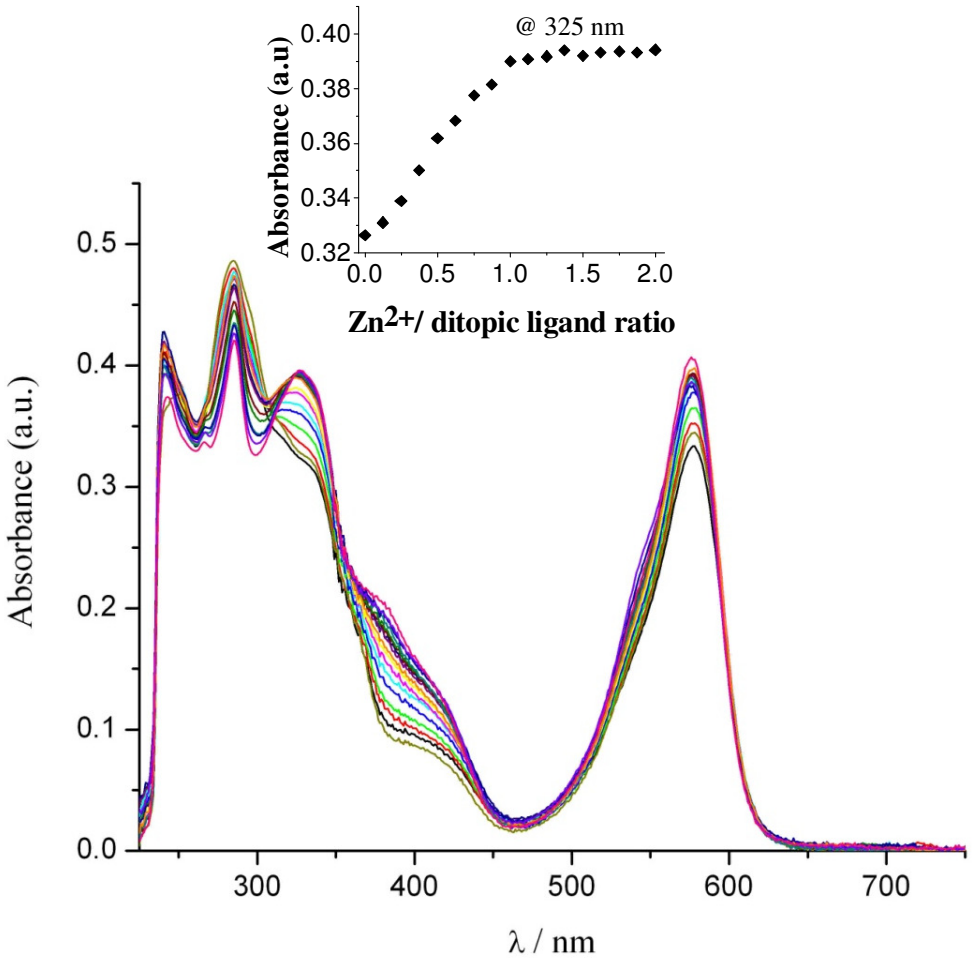

Figure 55. UV-vis spectra obtained by the titration of **77** in 80:20 $CHCl_3$: MeOH ($5x10^{-6}$ M) with $Zn(OTf)_2$. The inset shows the absorption coefficient at 325 nm as a function of Zn^{2+}/**77** ratio

.

In the fluorescence spectrum, (Figure 56) there is minor increase (+30%) in the intensity with just a few nanometers of blue shift in the peak position (from 608 to 603 nm). As expected, the absorption changes at 325 nm (inset, Figure 56) level off only after one equivalent of Zn(II) ions were added (1:1).

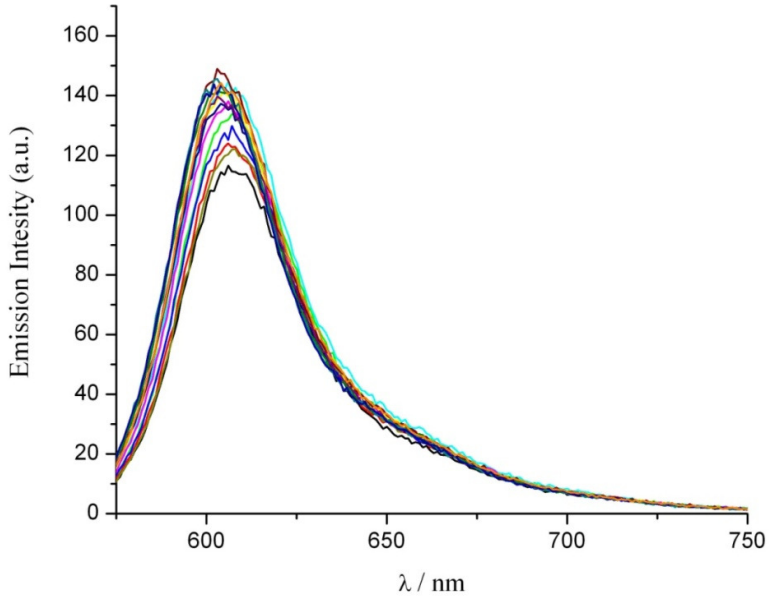

Figure 56. Fluorescence spectra obtained by the titration of **77** in 80:20 $CHCl_3$: MeOH ($5x10^{-6}$ M) with $Zn(OTf)_2$.

Bipyridyl-Zn(II) interaction is weaker, and coordination stoichiometry and spatial arrangement of the BODIPY chromophores should be different compared to the terpyridine derivatives. On saturation with Zn(II), the absorption spectra of the compound **76** (Figure 57) display minor changes (decrease) at 380 nm and 548 nm (increase), in the emission peak intensity (Figure 58) increases (+44%) and the peak shifts blue (from 567 to 558 nm).

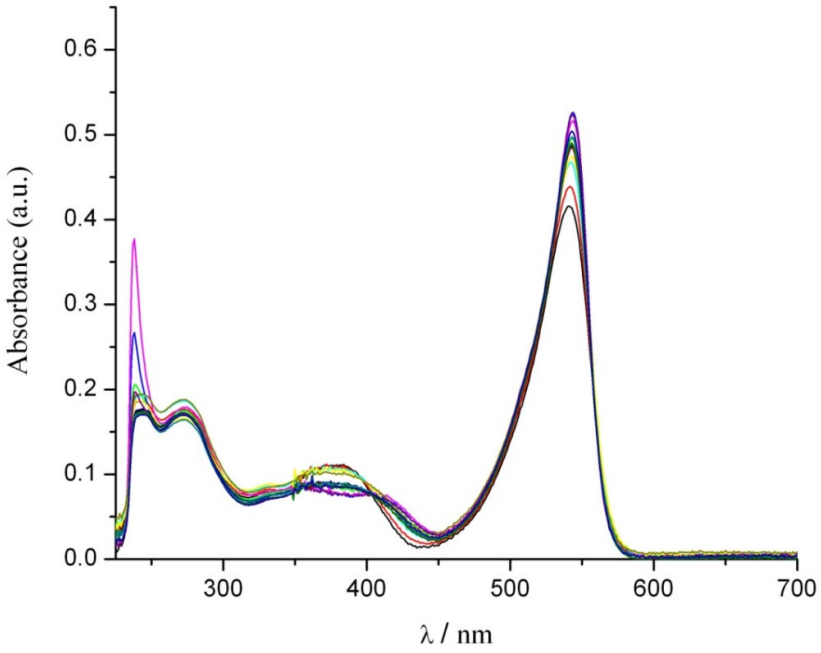

Figure 57. UV-vis spectra obtained by the titration of **76** in 80:20 $CHCl_3$:MeOH ($5x10^{-6}$ M) with $Zn(NO_3)_2$.

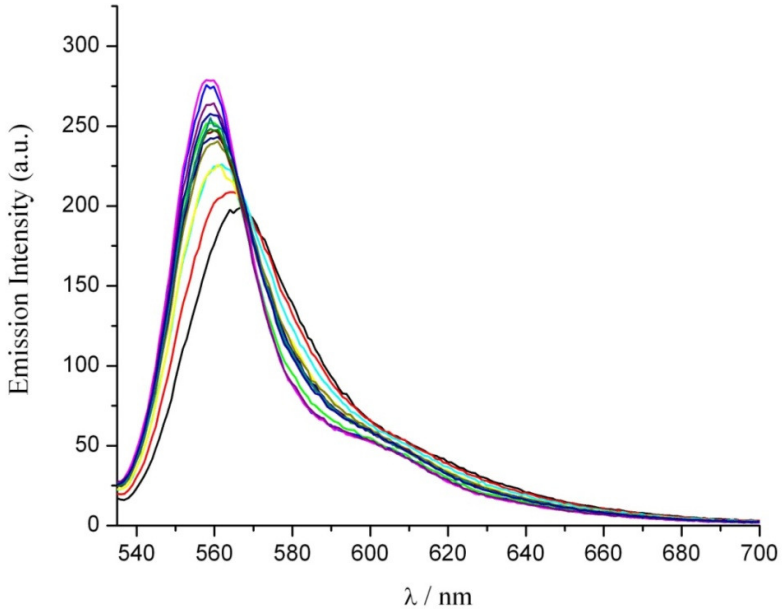

Figure 58. Fluorescence spectra obtained by the titration of **76** in 80:20 $CHCl_3$: MeOH ($5x10^{-6}$ M) with $Zn(NO_3)_2$.

Bis-bipyridyl-BODIPY **78**, on the other hand, shows a somewhat complicated response in absorption spectra during titration (Figure 59). While the peak at 400 nm behaves normally (an increase with an expected saturation behaviour, the BODIPY peak shows an increase, growth of a shoulder at 530 nm and then disapperance of the shoulder with a concomitant final increase at 562 nm. We speculate that the growth of a shoulder is suggestive of interchromophoric stacking with lower Zn(II) to ligand ratios, where two BODIPYs might be brought close together in an octahedral arrangement. Increasing Zn(II) concentration of course, would favor an open form resembling that of the terpyridyl derivatives.

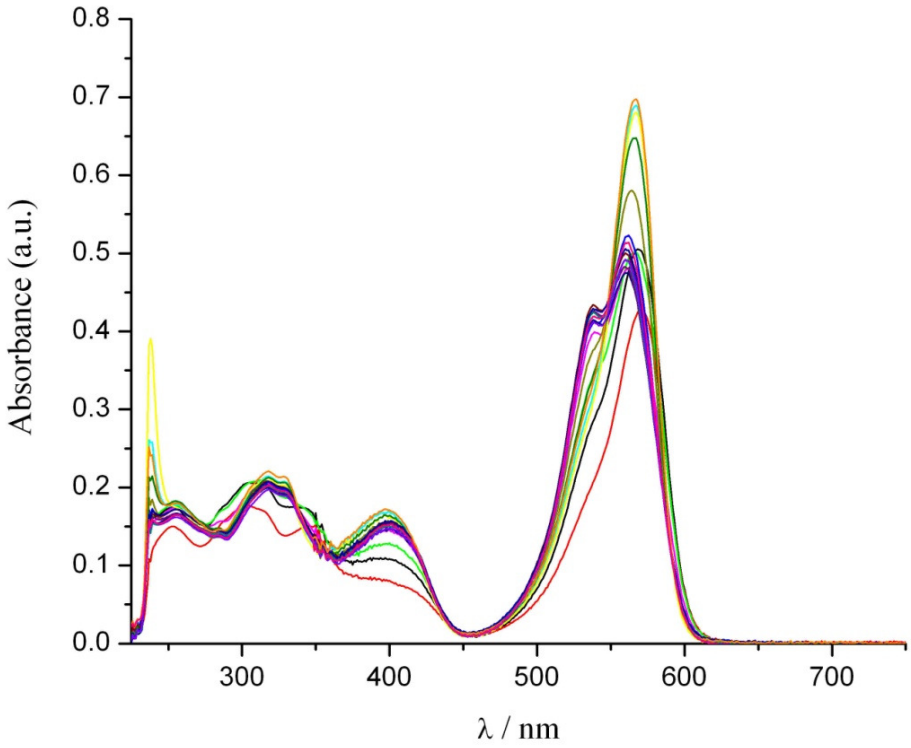

Figure 59. UV-vis spectra obtained by the titration of **78** in 80:20 $CHCl_3$:MeOH ($5x10^{-6}$ M) with $Zn(NO_3)_2$.

Emission spectra (Figure 60) is supportive of this speculation, at lower Zn(II) concentrations, binding causes more spectral blue shift rather than intensity change, but at larger proportions of Zn(II), BODIPY groups are removed from each other with the formation of "open form" structures, decreasing the effects of self-quenching of the BODIPY fluorophores.

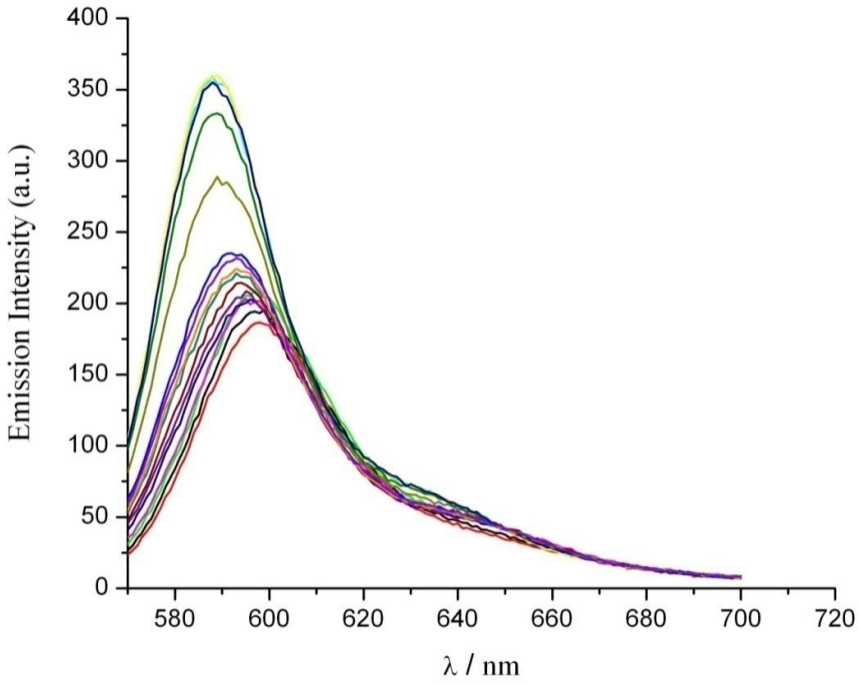

Figure 60. Fluorescence spectra obtained by the titration of **78** in 80:20 $CHCl_3$: MeOH ($5x10^{-6}$ M) with $Zn(NO_3)_2$.

CHAPTER 4

CONCLUSION

The uses of Sonogashira couplings, four functional building blocks carrying BODIPY fluorophores were synthesized. Terpyridyl and bipyridyl ligand have been repeatedly shown to be very useful in the construction of supramolecular structures. Terpyridyl, is a strong enough ligand for Zn(II) ions, and the addition of zinc triflate, forms fluorescent coordination polymer. This polymerization process can easily be followed by the observation of fluorescence characteristics. Ditopic bis-terpyridyl BODIPY ligand **77** shows clear evidence of polymerization when 0.5 equivalent of Zn(II) ions were added. The addition of additional Zn(II) changes the dynamic equilibrium concentration of the polymer and the nmr peaks become more sharp, as more Zn(II) ions were added; an indication of monomeric complex (open form). Bipyrdiyl derivatives, with their lower affinities can be useful as fluorescent chemosensors as well, considering the fact that intracellular Zn(II) concentrations can vary 10 orders of magnitude. A fluorescent coordination polymer on the other hand may find utility novel electrochromic devices or in other device applications where reversible changes between states of different physical properties is an asset.

REFERENCES

1. Lehn J.-M., *Angew Chem Int Ed.*, **1988**, *27*, 89–112.

2. Lehn J.-M., *Science*, **2002**, *295*, 2400–2403.

3. Lehn J.-M., *Supramolecular Chemistry*, **1995,** VCH,Weinheim,.

4. P. S. Corbin, S. C. Zimmerman, in: *Supramolecular Polymers,* A.Cifferi, Ed., Marcel Decker, New York**, 2000**, 147.

5. Brunsveld L, Folmer., B. J. B., Meijer E. W., Sibejsma R. P., *Chem. Rev*., **2001**, *101*, 4071.

6. Cifferi A., *Macromol. Rapid Comm.*, **2002**, *23*, 511.

7. Fouquey C., Lehn J.-M., and Levelut A.-M., *Adv. Mater.,* **1990**, *2*, p. 254.

8. Brunsveld L., Folmer B. J. B., Meijer E. W., *MRSBull*., **2000**, *25*, 49.

9. Sherrington D. C., Taskinen K. A., *Chem. Soc. Rev.*, **2001,** *30*, 83.

10. Sibejsma R. P., Beijer F. H., Brunsveld L., Folmer B. J. B., Hirschberg J. H. K. K., Lange R. F. M., Lowe J. K. L., Meijer E. W., *Science*, **1997**, *278*, 1601.

11. Lange R. F. M Van Gurp., M., Meijer E. W., *J. Polym. Sci: Polym. Chem.*, **1999**, *37*, 3657.

12. Kato T., Fréchet J. M. J., *Macromolecules*, **1989**, *22*, 3818.

13. Kotera M., Lehn J.-M., Vigneron J.-P., *Tetrahedron*, **1995**, *51*,1953-72.

14. St Pourcain C.B. and Griffin A.C., *Macromolecules,* **1995**, *28*, p. 4116.

15. Sijbesma R. P., Beijer F. H., Brusweld L., Meijer E. W., *Supramolecular polymer*, Patent number WO9814504,**1998.**

16. Terech P. and Weiss R.G., *Chem. Rev.*, **1997**, *97*, p. 3133.

17. Billard J., Dubois J. C., Tinh N. H., Zann A., *Nouv. J. Chim.*, **1978**, *2*, 535-540.

18. Destrade C., Mondon M. C., Malthete J., *J. Phys.*, **1979**, *3*, 17-21.

19. Schutte W. J., Sluyters-Rehbach M., Sluyters J. H., *J. Phys. Chem.*, **1993**, *97*, 6069-6073.

20. Kimura M., Muto T., Takimoto H., Wada K., Ohta K., Hanabusa K., Shirai H., Kobayashi N., *Langmuir*, **2000**, *16*, 2078-2082.

21. Sielcken O. E., van Tilborg M. M., Roks M. F. M., Hendriks R., Drenth W., Nolte, R. J. M., *J. Am. Chem. Soc.* **1987**, *109*, 4261-4265.

22. Kobayashi N., Lever A. B. P., *J. Am. Chem. Soc.* **1987**, *109*, 7433-7441.

23. Palmans A. R. A., Vekemans J. A. J. M., Fischer H., Hikmet R. A. M., Meijer E. W., *Chem. Eur. J.* **1997**, *3*, 300-307.

24. Dobrawa R., Würthner F., *Journal of Polymer Science: Part A: Polymer Chemistry*, **2005**, *43*, 4981-4995.

25. Lehn J.-M., *Polym. Int.*, **2002**, *51*, 825-839.

26. Yount W. C., Juwarker H., Craig S. L. *J. Am. Chem. Soc.* **2003**, *125*, 15302-15303.

27. Yamaguchi N., Hamilton L. M., Gibson H. W., *Angew. Chem., Int. Ed.* **1998**, *37*, 3275-3279.

28. Ogawa K., Kobuke Y., *Angew. Chem. Int. Ed.* **2000**, *39*, 4070-4073.

29. Velten U., Lahn B., Rehahn M., *Macromol. Chem. Phys.* **1997**, *198*, 2789-2816.

30. Knapp R., Schott A., Rehahn M., *Macromolecules*, **1996**, *29*, 478-480.

31. Chen, J., MacDonnell F. M., *Chem. Commun.* **1999**, 2529-2530.

32. Constable E. C., *Macromol. Symp.*, **1995**, *98*, 503-524.

33. Constable, E. C., Cargill Thompson A. M. W., *J. Chem. Soc., Dalton Trans.,* **2002***, 6743.*

34. Constable E. C., Thompson Cargill, A. M. W.; Tocher, D. A., *Macromol. Symp.* **1994**, *77*, 219-228.

35. Michelsen U., Hunter C. A., *Angew. Chem., Int. Ed.* **2000**, *39*, 764-767.

36. El-Ghayoury A., Schenning A. P. H. J., Meijer E. W., *J. Polym. Sci. A: Polym. Chem.*, **2002**, *40*, 4020-4023.

37. Yu S.-C., Kwok C.-C., Chan W. K., Che C.-M., *Adv. Mater.* **2003***, 15*, 1643-1647.

38. Beck J. B., Rowan S. J., *J. Am. Chem. Soc.* **2003**, *46*, 13922-13923.

39. Yu, S.-C., Kwok C.-C., Chan W.-K., Che C.-M., *Adv. Mater.* **2003**, *15*, 1643-1647.

40. Dobrawa R., Wurthner F., *Chem. Commun.* **2002**, 1878-1879.

41. Dobrawa R., Lysetska M., Ballester P., Gru¨ne M., Wurthner F., *Macromolecules,* **2005**, *38*, 1315.

42. Chen Y.-Y., Tao Y.-T., and Lin H.-C., *Macromolecules,* **2006**, *39,* 8559-8566.

43. Mario Ruben M., Javier Rojo J., Romero-Salguero F.J.,. Uppadine L. H.,and Lehn J.-M., Angew. Chem. Int. Ed., **2004**, 43, 3644 – 3662.

44. Baxter P.N. W., Lehn J.-M., Fischer J. and Youinou M.-T., *Angew. Chem. Int. Ed. Engl.* , **1994**, *33*, 2284.

45. Sleiman H., Baxter P.N. W., Lehn J.-M. and Rissanen K., *J. Chem. Soc., Chem. Commun.*, **1995**, 715.

46. Heyke O., Wanmark K., Thomas J. and Lehn J.-M., *unpublished results.*

47. Kramer R., Lehn J.-M. and Marquis-Rigault A*., Proc. Natl. Acad. Sci.*, **1993**, *90*, 5394.

48. Newkome G. R., Cho T. J., Moorefield C. N., Baker G. R., Cush R., Russo P. S., *Angew. Chem. Int. Ed. Engl.*, **1999**, *38*, 3717.

49. Kadish K. M., Smith K. M., Guilard R., *The Porphyrin Handbook*; Ed., Sanders J. K. M., Academic Press, **2000**, *3*, 347-368.

50. Treibs A., Kreuzer F.-H., Justus Liebigs, *Ann. Chem*., **1968**, *718*, 208 – 223.

51. Ulrich G., Ziessel R., Harriman A., *Angew. Chem., Int. Ed.* **2008**, *47*, 1184–1201.

52. Loudet A., Burgess K., *Chem. Rev., 2007*, *107*, 4891–4932.

53. Coskun A., Akkaya E. U., *J. Am. Chem. Soc.* **2005**, *127*, 10464–10465.

54. Rurack K., Kollmannsberger M., Resch-Genger U., Daub J., *J. Am. Chem. Soc.* **2000**, *122*, 968–969.

55. Coskun A., Akkaya E. U., *J. Am. Chem. Soc.* **2006**, *128*, 14474–14475.

56. Zeng L., Miller E. W., Pralle A., Isacoff E. Y., Chang C. J., *J. Am. Chem. Soc.* **2006**, *128*, 10–11.

57. Coskun, A.; Deniz, E.; Akkaya, E. U. *Org. Lett.* **2005**, *7*, 5187–5189.

58. Saki N., Dinc T., Akkaya E. U., *Tetrahedron* **2006**, *62*, 2721–2725.

59. Coskun A., Turfan, B. T., Akkaya, E. U., *Tetrahedron Lett.* **2003**, *44*, 5649–5651.

60. Ekmekci Z., Yilmaz M. D., Akkaya E. U., *Org. Lett.,***2008**, *10*, 461–464.

61. Arbeloa T. L., Arbeloa F. L., Arbeloa I. L., Garcia-Moreno I., Costela A.,; Sastre, R., Amat-Guerri F., *Chem. Phys. Lett.* **1999**, *299*,315.

62. Haugland, R. P., *The Handbook-A guide to fluorescent probes and labeling technologies*, 10th ed.; Invitrogen Corp., **2005**.

63. Ziessel R., Goze C., Ulrich G., CQsario M., Retailleau P., Harriman A., Rostron J. P., *Chem. Eur. J.*, **2005**, *11*, 7366 – 7378.

64. Wan C.-W., Burghart A., Chen J., BergstrLm F., Johansson L. B.-A., Wolford M. F., Kim T. G., Topp M. R., Hochstrasser R. M., Burgess K., *Chem. Eur. J.*, **2003**, *9*, 4430 – 4431.

65. Li, F., Yang, S. I., Ciringh, Y. Z., Seth, J., Martin, C. H., Singh, D. L., Kim, D., Birge, R. R., Bocian, D. F., Holten, D., Lindsey, J. L., *J. Am. Chem. Soc.* **1998**, *120*, 10001–10017.

66. Atilgan, S., Ekmekci, Z., Dogan, A. L., Guc, D., Akkaya, E. U., *Chem. Commun.* **2006**, 4398–4400.

67. Erten-Ela, S., Yilmaz, M. D., Icli, B., Dede, Y., Icli, S., Akkaya, E. U., *Org. Lett.*; **2008,** ASAP article.

68. Boyer J. H., Haag A. M., Sathyamoorthi G., Soong M. L., Thangaraj K., *Heteroat. Chem.*, **1993**, *4*, 39 – 49.

69. Yogo T., Urano Y., Ishitsuka Y., Maniwa F., Nagano T., *J. Am.Chem. Soc.*, **2005**, 127, 12162 – 12163.

70. Baruah, M., Qin, W., Vallee, R. A. L., Beljonne, D., Rohand, T., Dehaen, W., Boens, N., *Org. Lett*,. **2005**, *7*, 4377.

71. Qin W., Rohand T., Baruah M., Stefan A., van der Auweraer M., Dehaen W., Boens N., *Chem. Phys. Lett.*, **2006**, *420*, 562 –568.

72. Dost, Z., Atilgan, S., Akkaya, E. U., *Tetrahedron*, **2006**, *62*, 8484–8488.

73. Deniz, E.; Isbasar, G. C.; Bozdemir, O. A.; Yildirim, L. T.; Siemiarczuk, A.; Akkaya, E. U., *Org. Lett.*, **2008**; ASAP Article.

74. Goze C., Ulrich G., Ziessel R., *Org. Lett.*, **2006**, *8*, 4445 – 4448.

75. Goze C., Ulrich G., Ziessel R., *J. Org. Chem.*, **2007**, *72*, 313 – 322.

76. Goze C., Ulrich G., Mallon L. J., Allen B. D., Harriman A., Ziessel R., *J. Am. Chem. Soc.*, **2006**, *128*, 10231 – 10239.

77. Sonogashira K., Tohda Y., Hagihara N., *Tetrahedron Lett.*, **1975**, *16*,4467.

78. Kollmannsberger M., Gareis T., Heinl S., Breu J., Daub J., *Angew. Chem.*, **1997**, *109*, 1391 – 1393; *Angew. Chem. Int. Ed.Engl.*, **1997**, *36*, 1333 – 1335.

79. Rurack K., Kollmannsberger M., Daub J., *New J. Chem.*, **2001**, *25*, 289 – 292.

80. Koutaka H., Kosuge J., Fukasaku N., Hirano T., Kikuchi K., Urano Y., Kojima H., Nagano T., *Chem. Pharm. Bull.*, **2004**, *52*,700 – 703.

81. Peng X., Du J., Fan J., Wang J., Wu Y., Zhao J., Sun S., Xu T., *J. Am. Chem. Soc.*, **2007**, *129*, 1500 – 1501.

82. Coskun A., Baytekin B. T., Akkaya E. U., *Org. Lett.*, **2002**, *4*, 2857 – 2859.

83. Goze C., Ulrich G., CharbonniRre L., Cesario M., PrangQ T., *Chem. Eur. J.*, **2003**, 9, 3748 – 3755.

84. Gorman, A.; Killoran, J.; O'Shea, C.; Kenna, T.; Gallagher, W. M.; O'Shea, D. F. *J. Am. Chem. Soc.*, **2004**, *126*, 10619.

85. Yogo T., Urano Y., Ishitsuka Y., Maniwa F., Nagano T., *J. Am. Chem. Soc.*, **2005**, *127*, 12162 – 12163.

86. Yilmaz, M. D.; Bozdemir, O. A.; Akkaya, E. U. *Org. Lett.*, **2006**, *8*, 2871.

87. D'Souza, F., Smith P. M., Zandler M. E.; McCarty A. L., Itou, M., Araki Y., Ito O., *J. Am. Chem. Soc.* **2004**, *126*, 7898.

88. Li, F., Yang S. I., Ciringh Y., Seth J., Martin C. H., Singh D. L., Kim, D., Birge R. R., Bocian D. F., Holten D., Lindsey J. S., *J.Am. Chem. Soc.* **1998**, *120*, 10001.

89. Grosshenny V., Romero F. M., Ziessel R., *J. Org. Chem.*, **1997**, *62*, 1491-1500.

APPENDIX

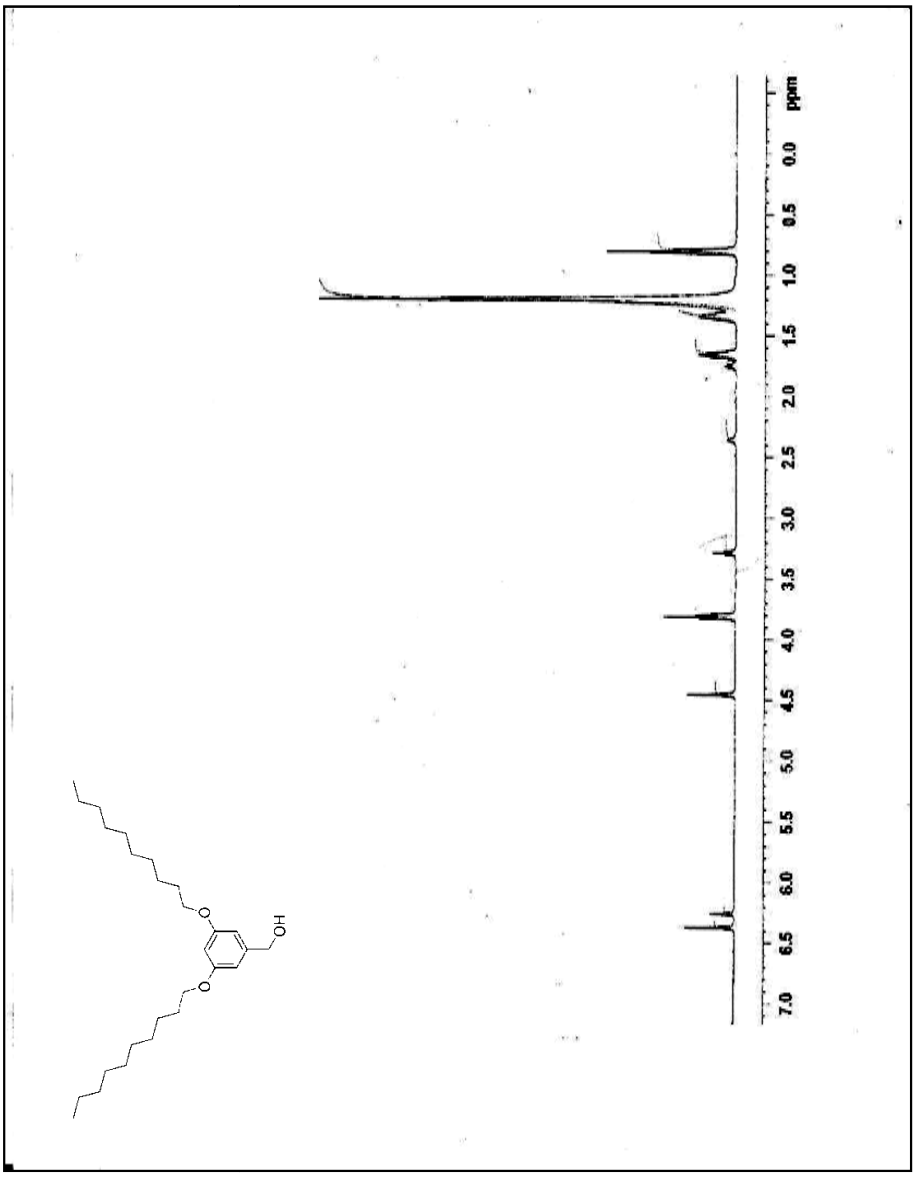

Figure 61. ^{1}H NMR spectrum (400 MHz, $CDCl_3$) of (**70**)

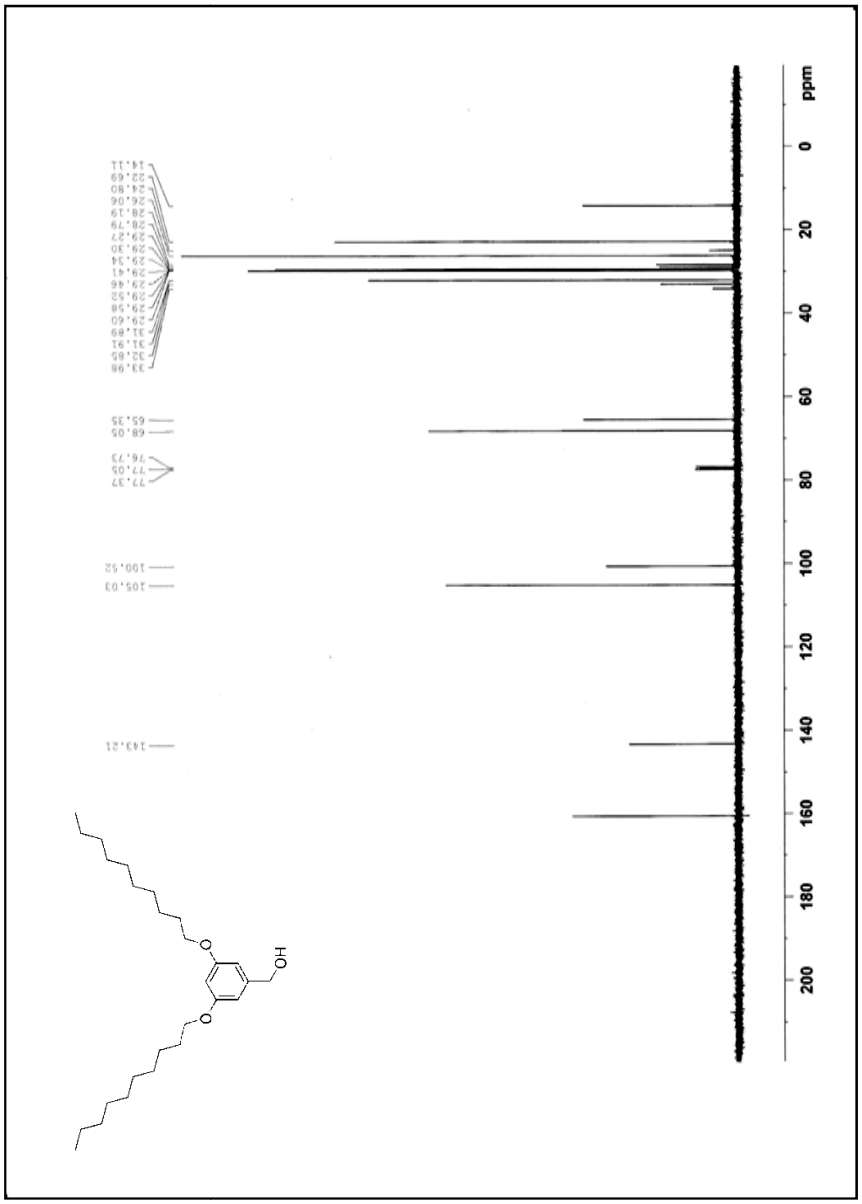

Figure 62. ^{13}C NMR spectrum (100 MHz, $CDCl_3$) of (**70**)

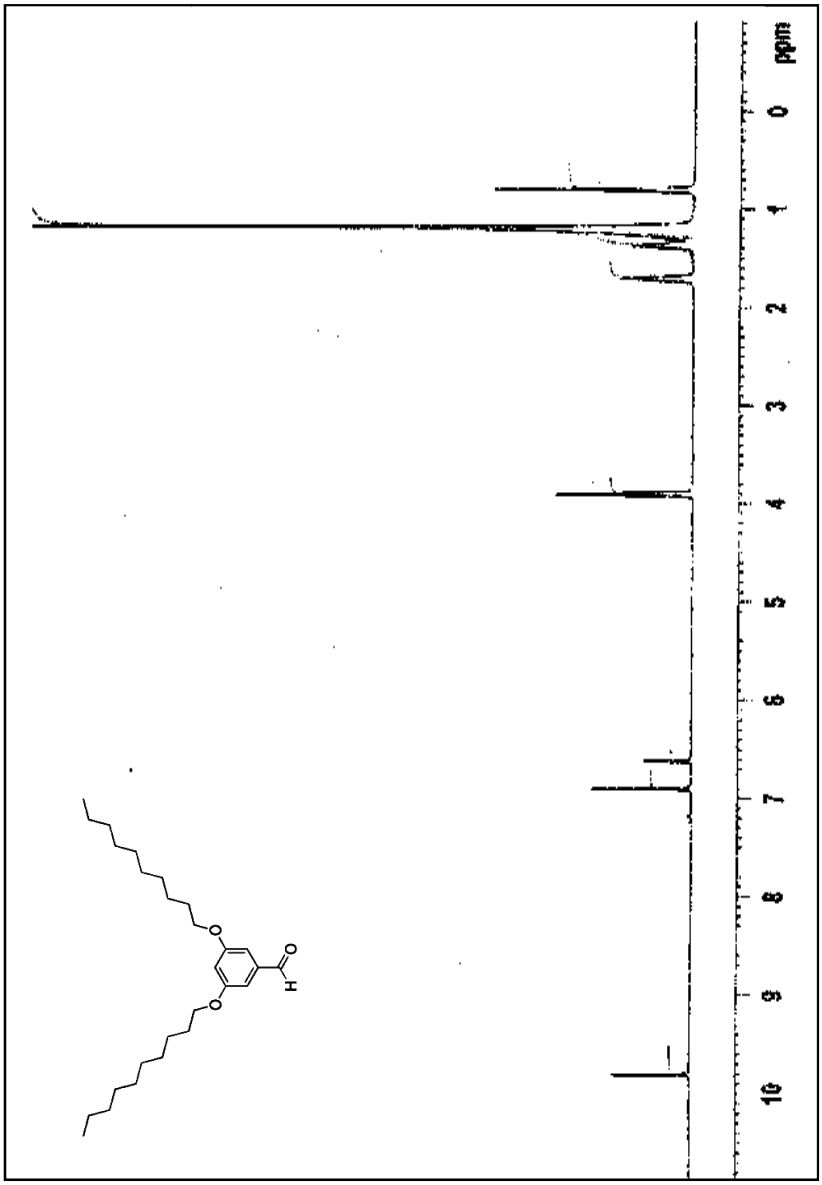

Figure 63. ^{1}H NMR spectrum (400 MHz, $CDCl_3$) of (**71**)

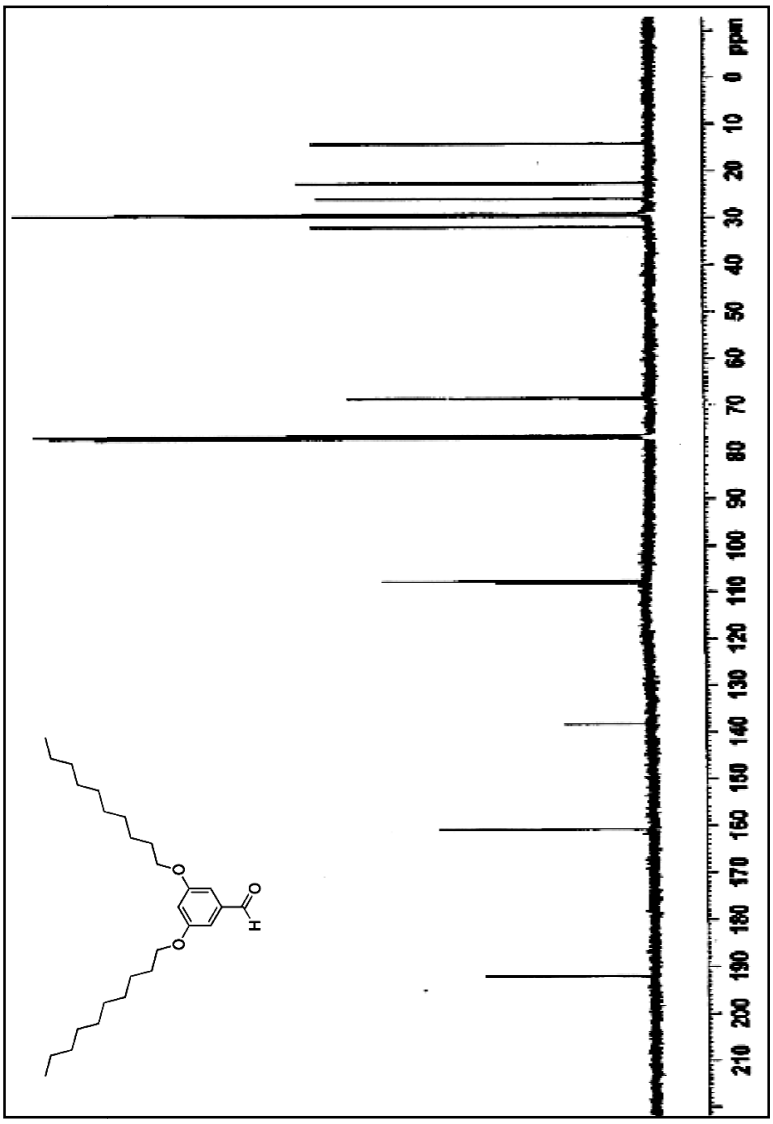

Figure 64. ^{13}C NMR spectrum (100 MHz, $CDCl_3$) of (71)

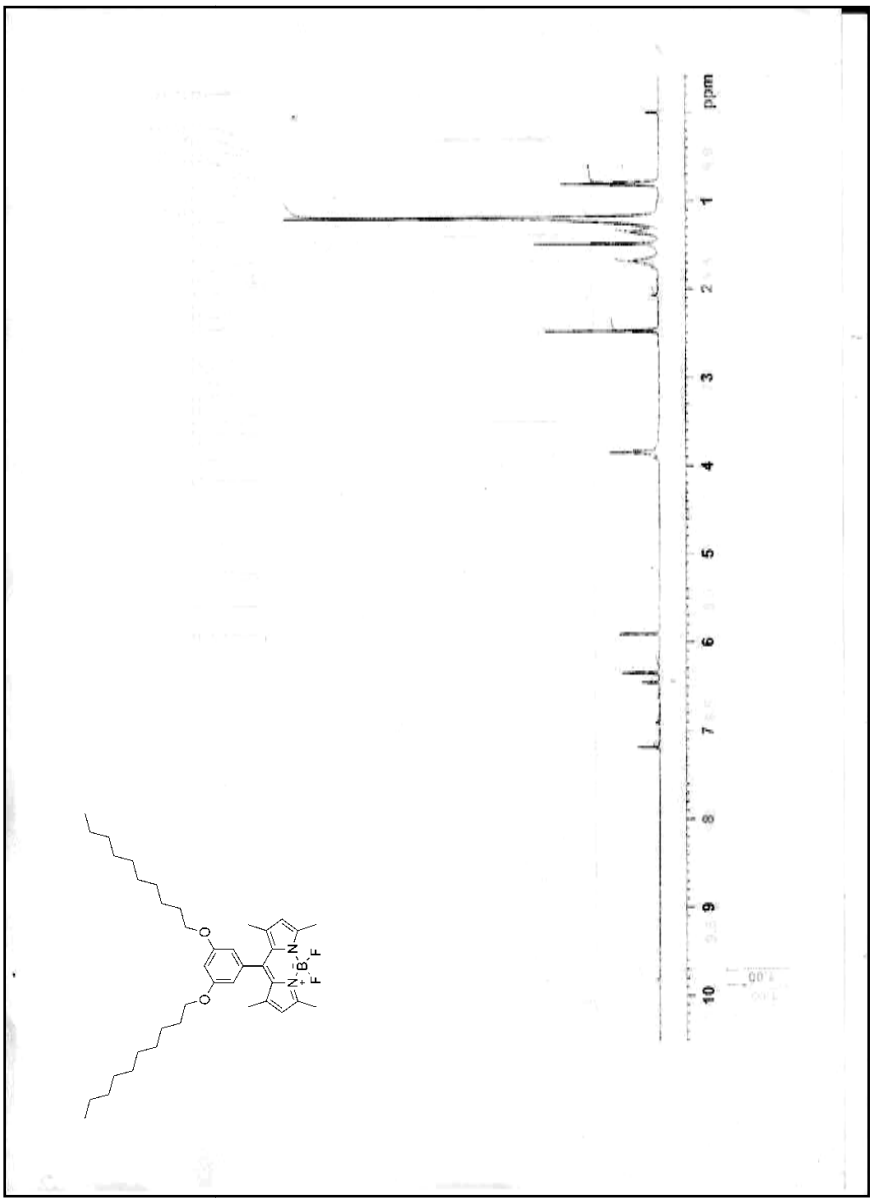

Figure 65. ^{1}H NMR spectrum (400 MHz, $CDCl_3$) of (**72**)

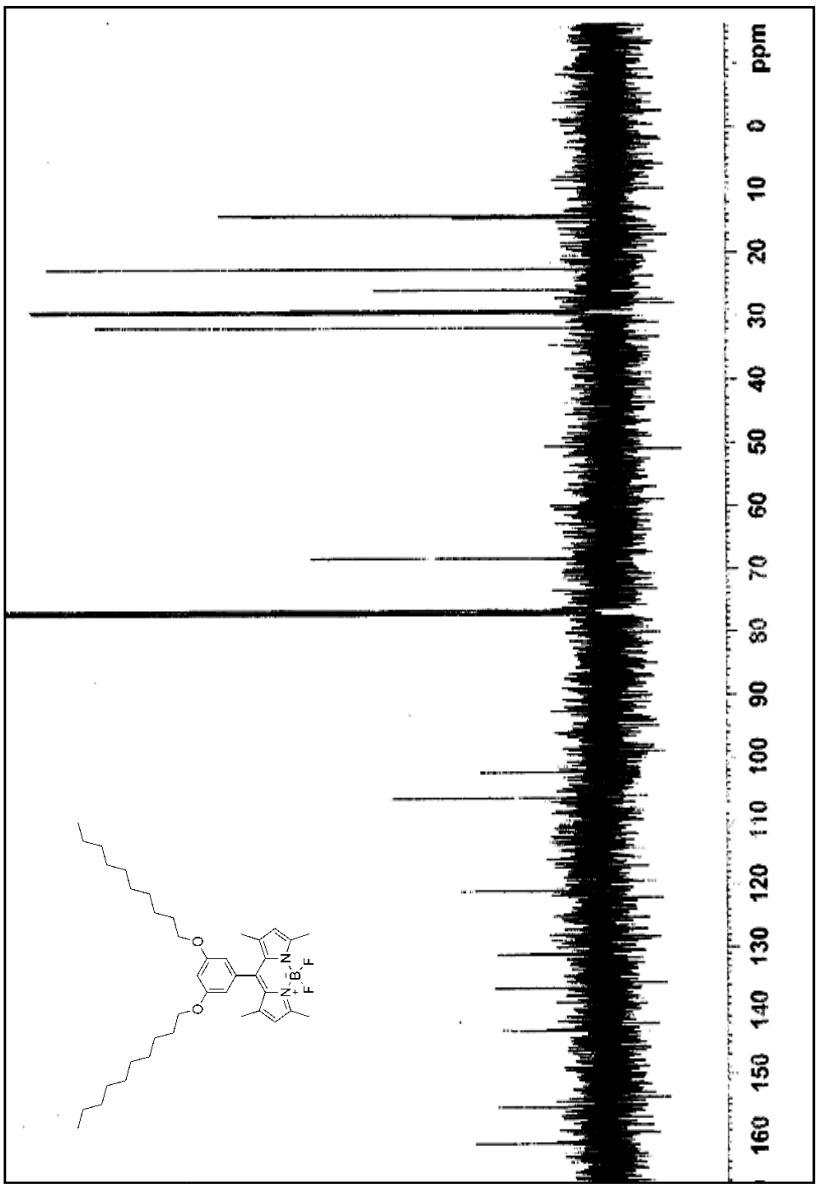

Figure 66. ^{13}C NMR spectrum (100 MHz, $CDCl_3$) of (**72**)

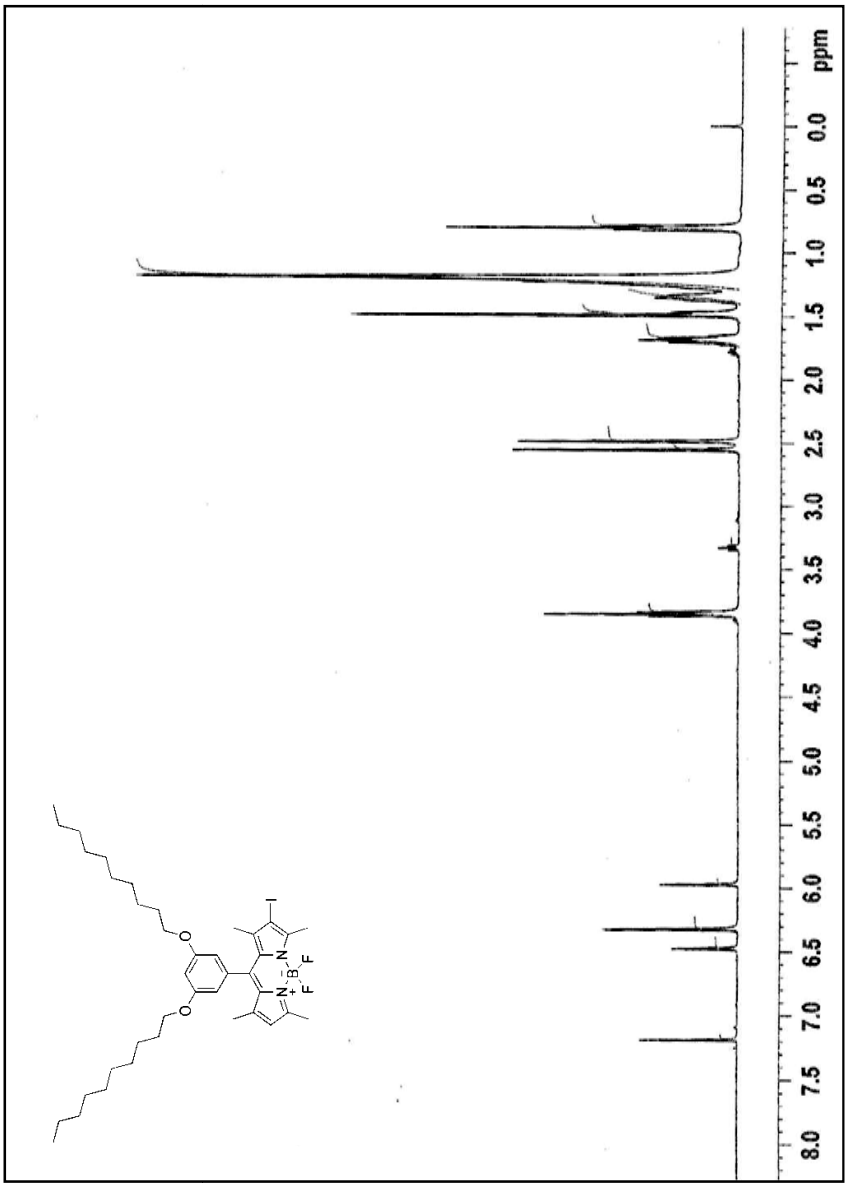

Figure 67. ^{1}H NMR spectrum (400 MHz, $CDCl_3$) of (**73**)

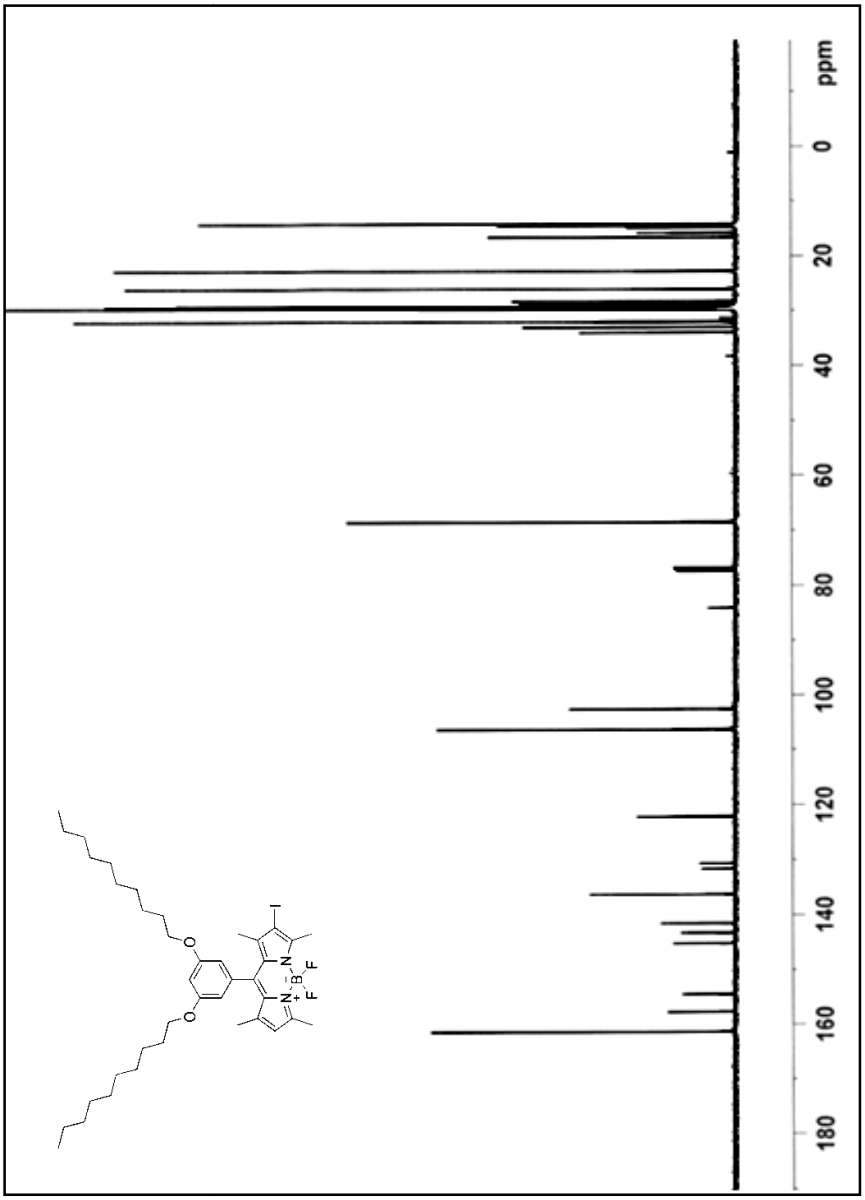

Figure 68. ^{13}C NMR spectrum (100 MHz, $CDCl_3$) of (**73**)

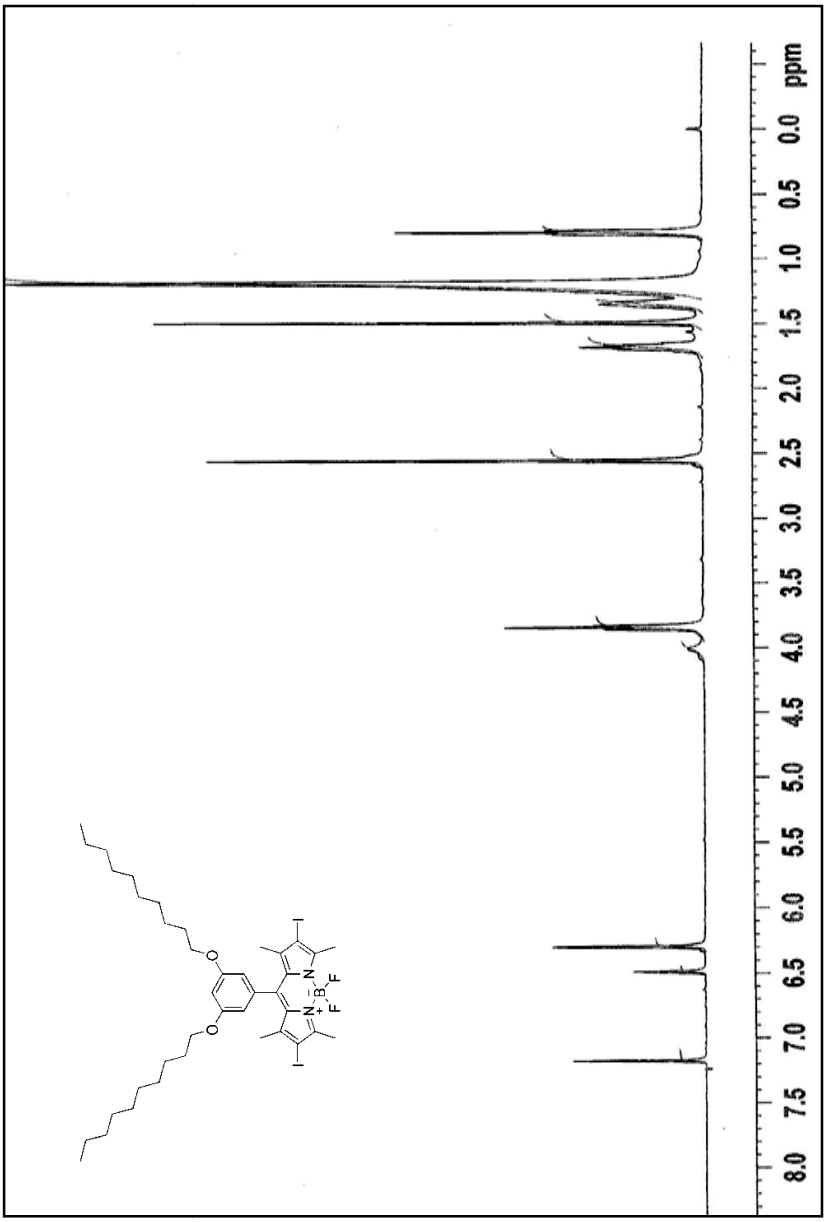

Figure 69. ^{1}H NMR spectrum (400 MHz, $CDCl_3$) of (**74**)

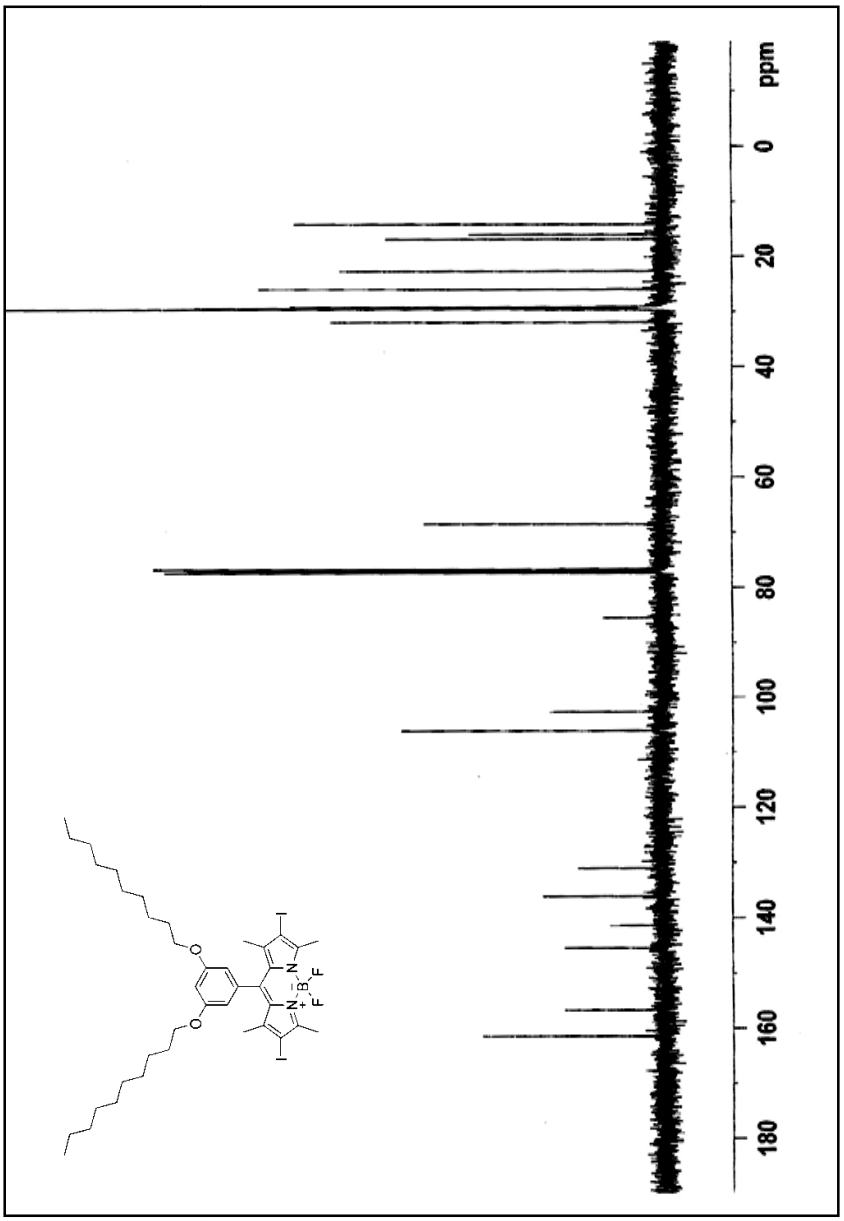

Figure 70. ^{13}C NMR spectrum (100 MHz, $CDCl_3$) of **(74)**

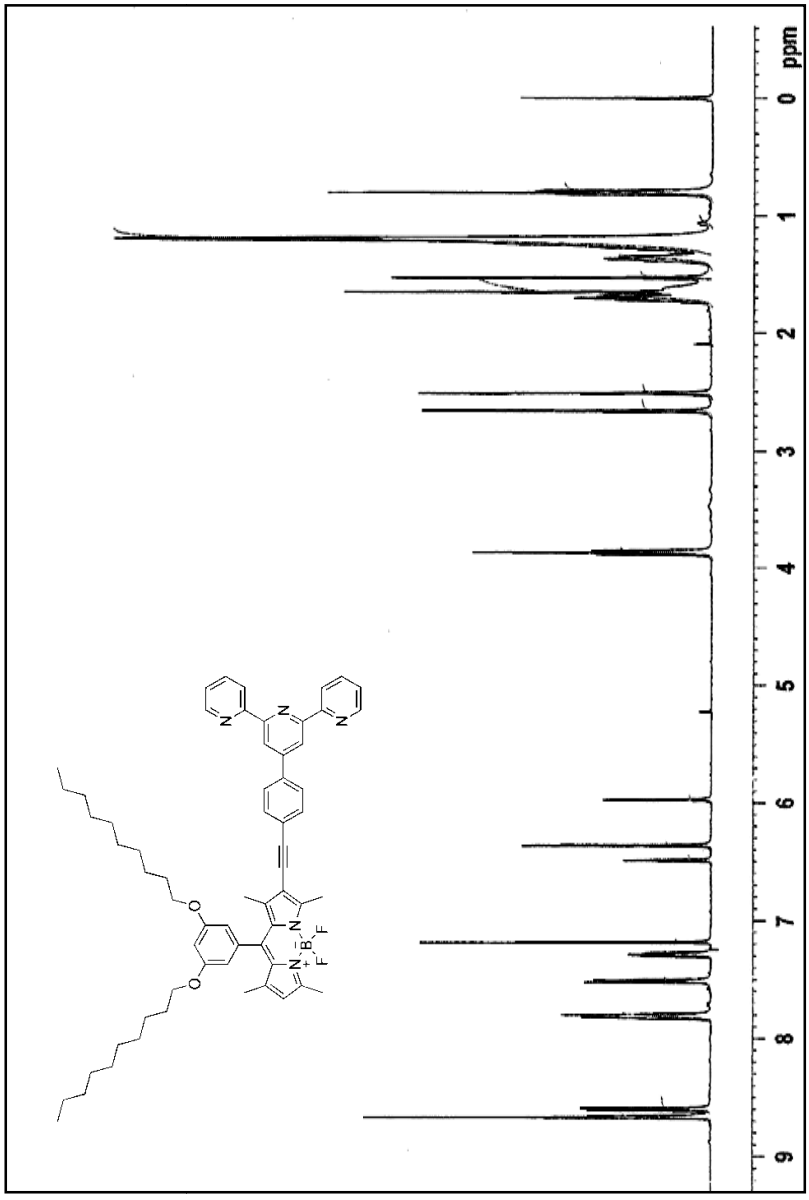

Figure 71. ^{1}H NMR spectrum (400 MHz, $CDCl_3$) of (**75**)

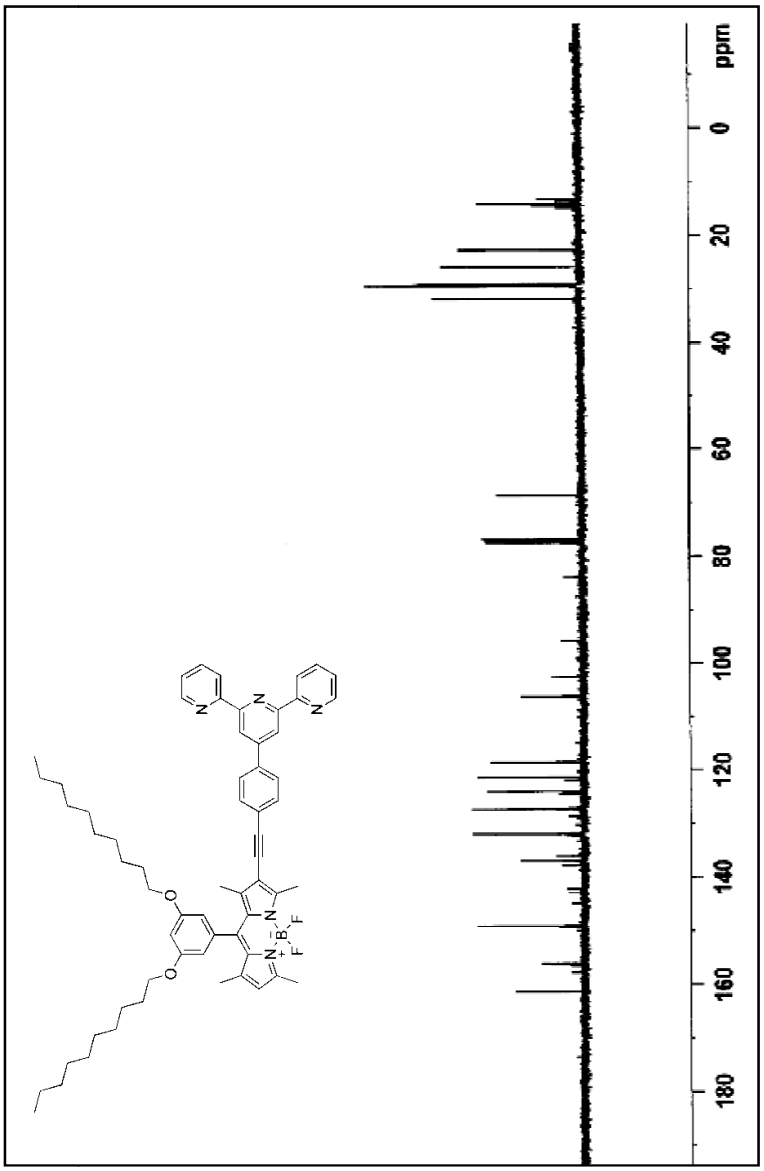

Figure 72. ^{13}C NMR spectrum (100 MHz, $CDCl_3$) of (**75**)

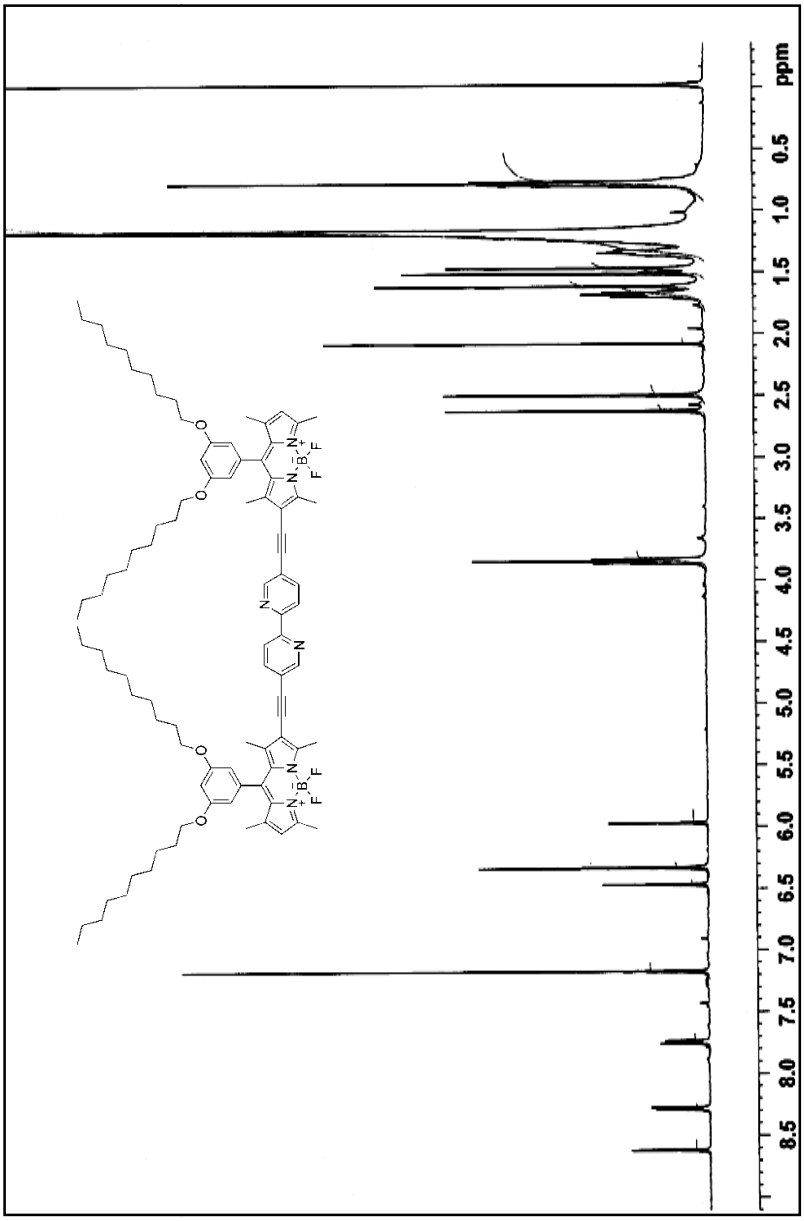

Figure 73. ^{1}H NMR spectrum (400 MHz, $CDCl_3$) of (**76**)

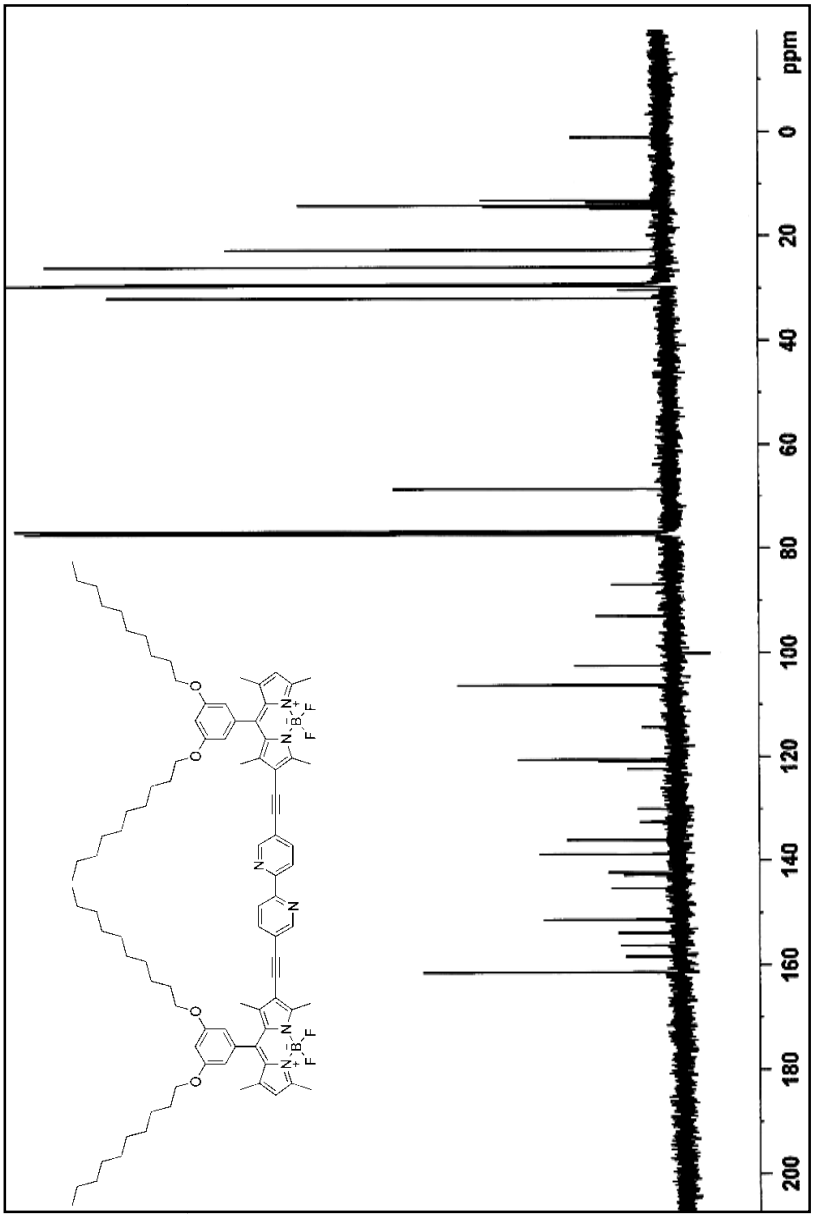

Figure 74. ^{13}C NMR spectrum (100 MHz, $CDCl_3$) of (**76**)

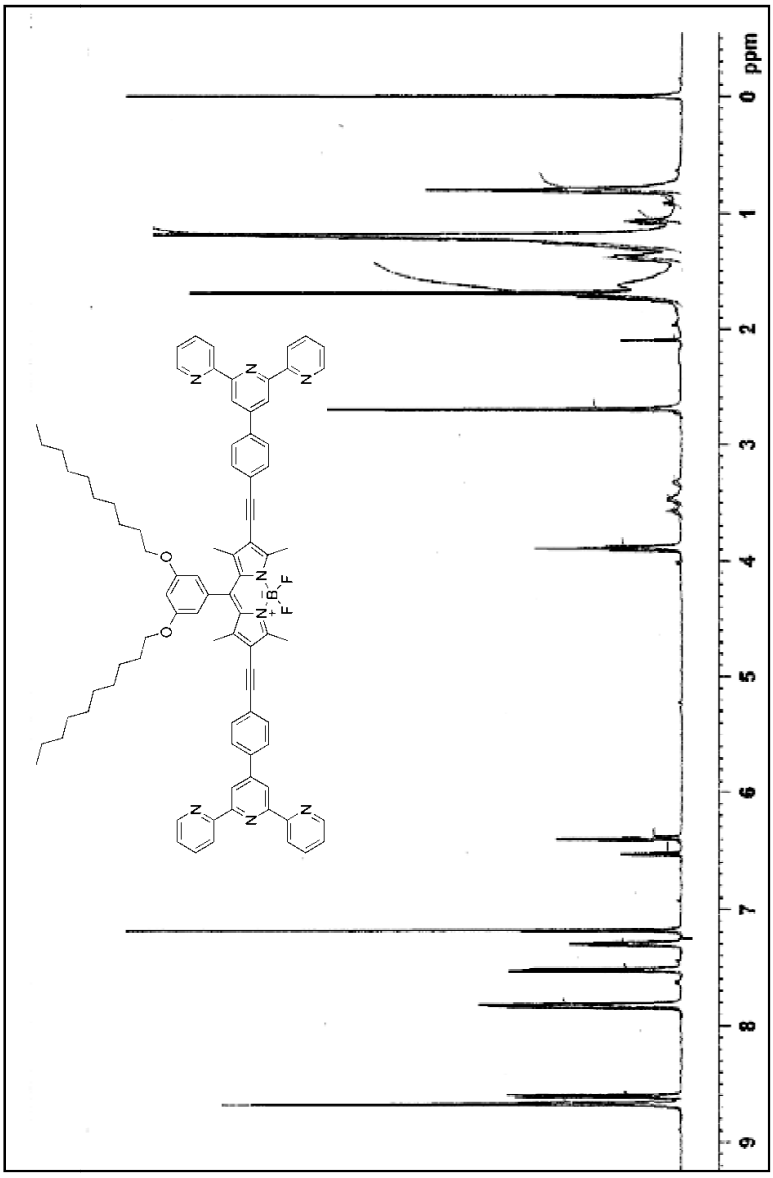

Figure 75. ^{1}H NMR spectrum (400 MHz, $CDCl_3$) of (**77**)

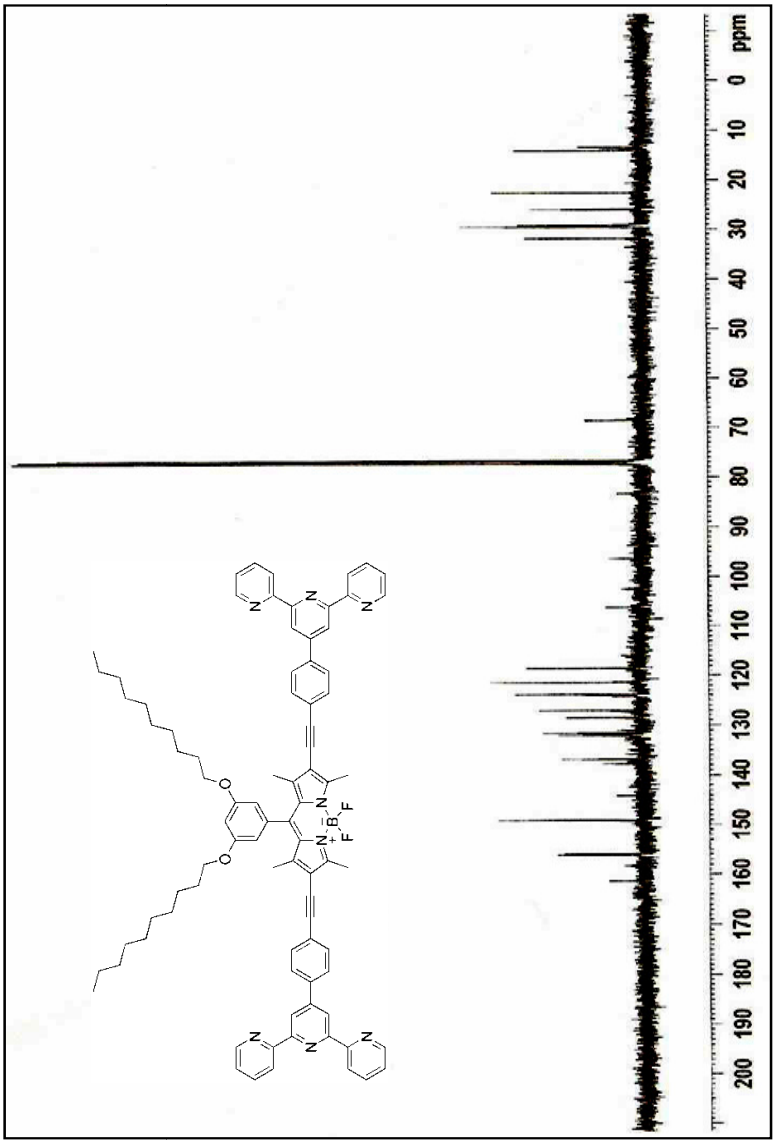

Figure 76. ^{13}C NMR spectrum (100 MHz, $CDCl_3$) of (**77**)

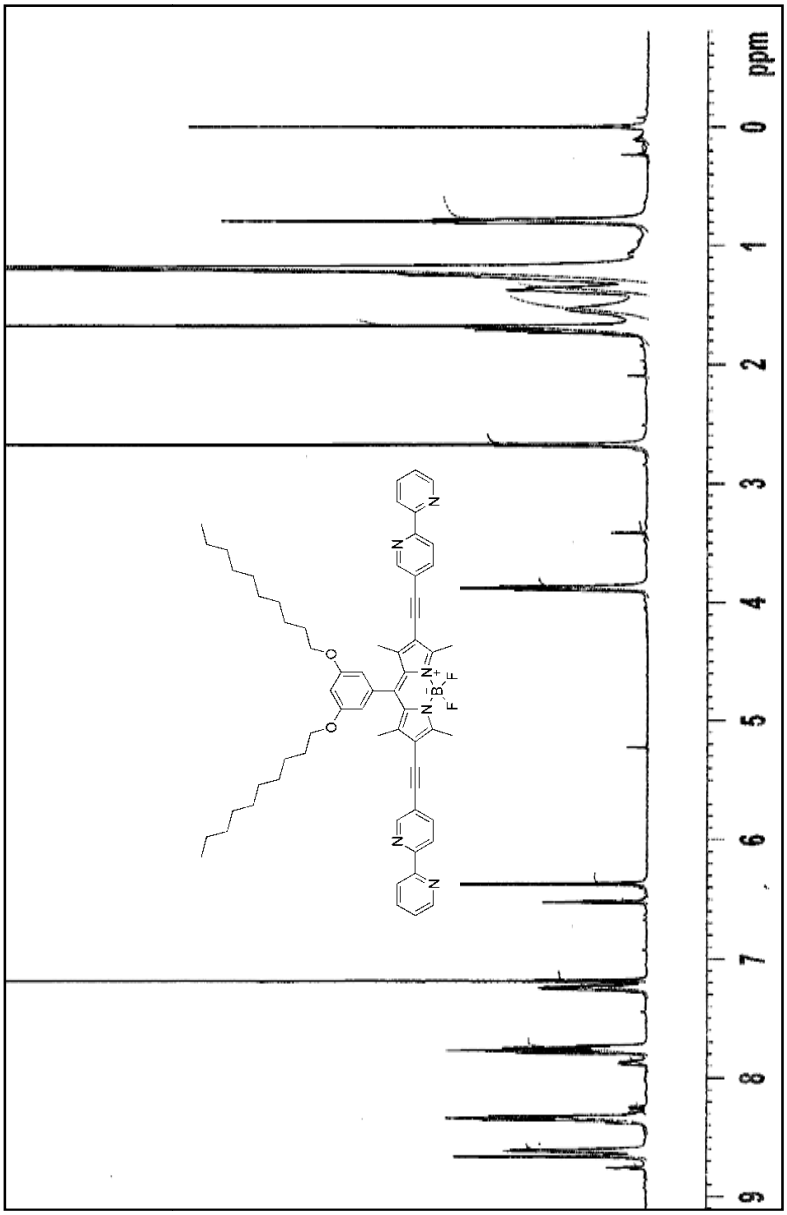

Figure 77. ^{1}H NMR spectrum (400 MHz, $CDCl_3$) of (**78**)

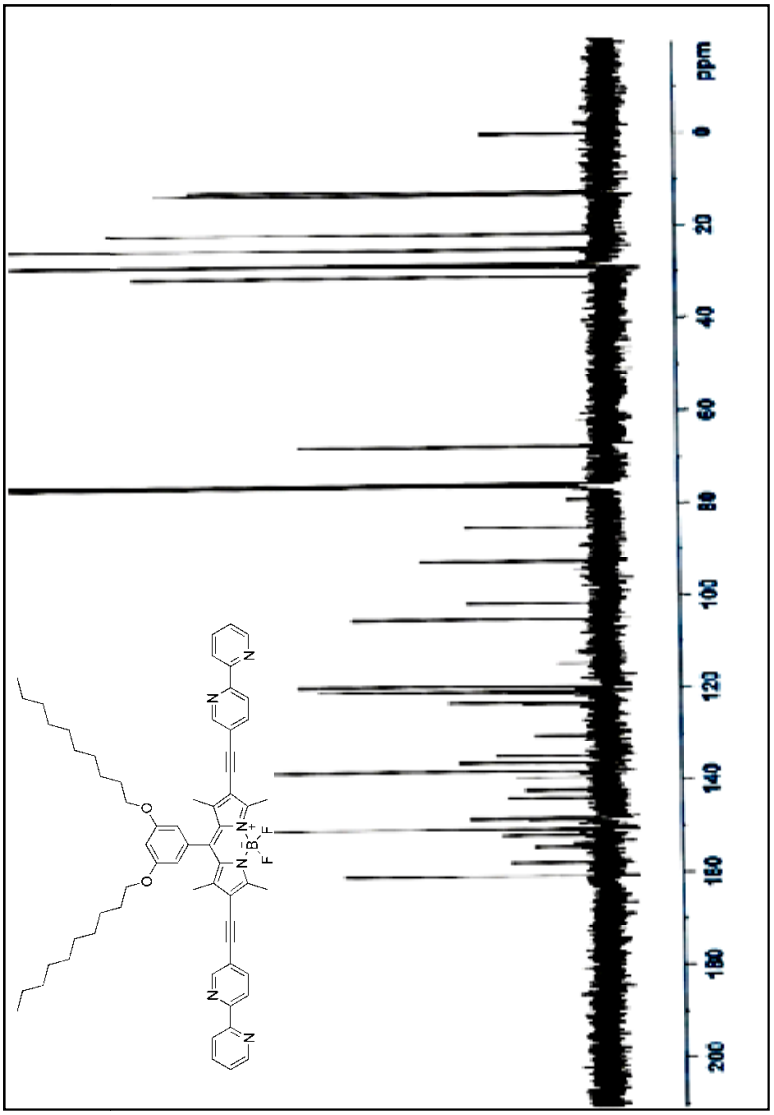

Figure 78. ^{13}C NMR spectrum (100 MHz, $CDCl_3$) of (**78**)

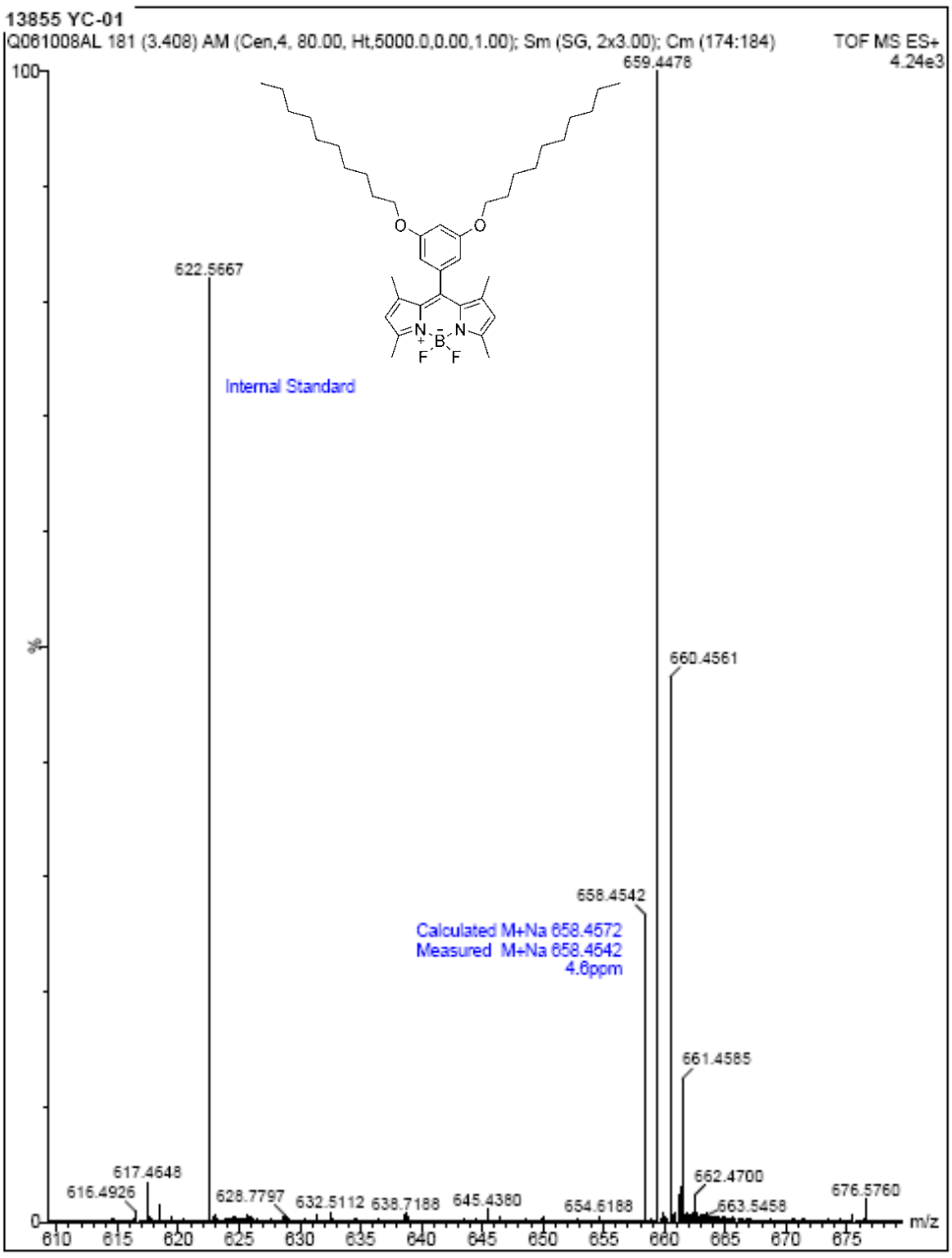

Figure 79. Mass Spectrum of (**72**)

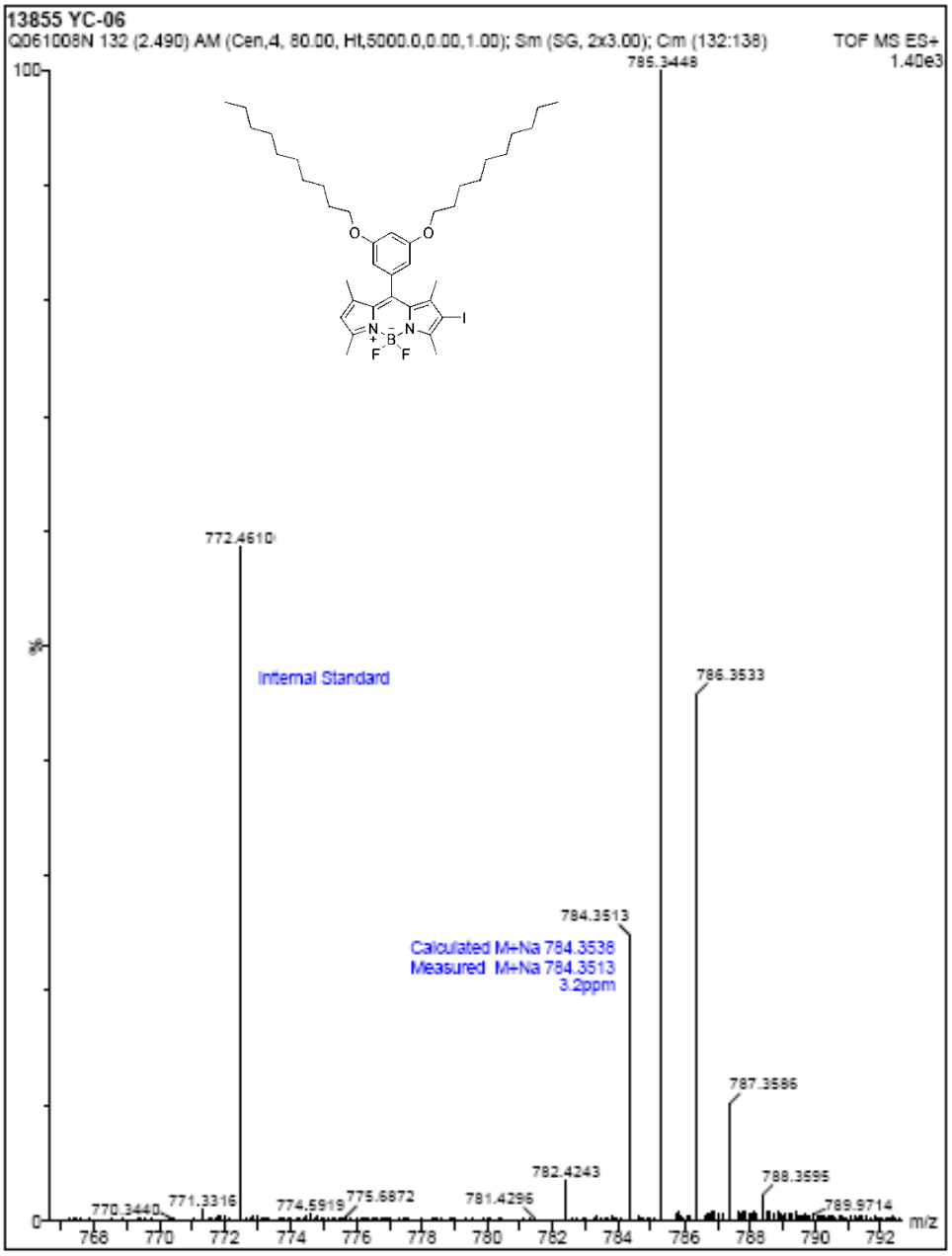

Figure 80. Mass Spectrum of (**73**)

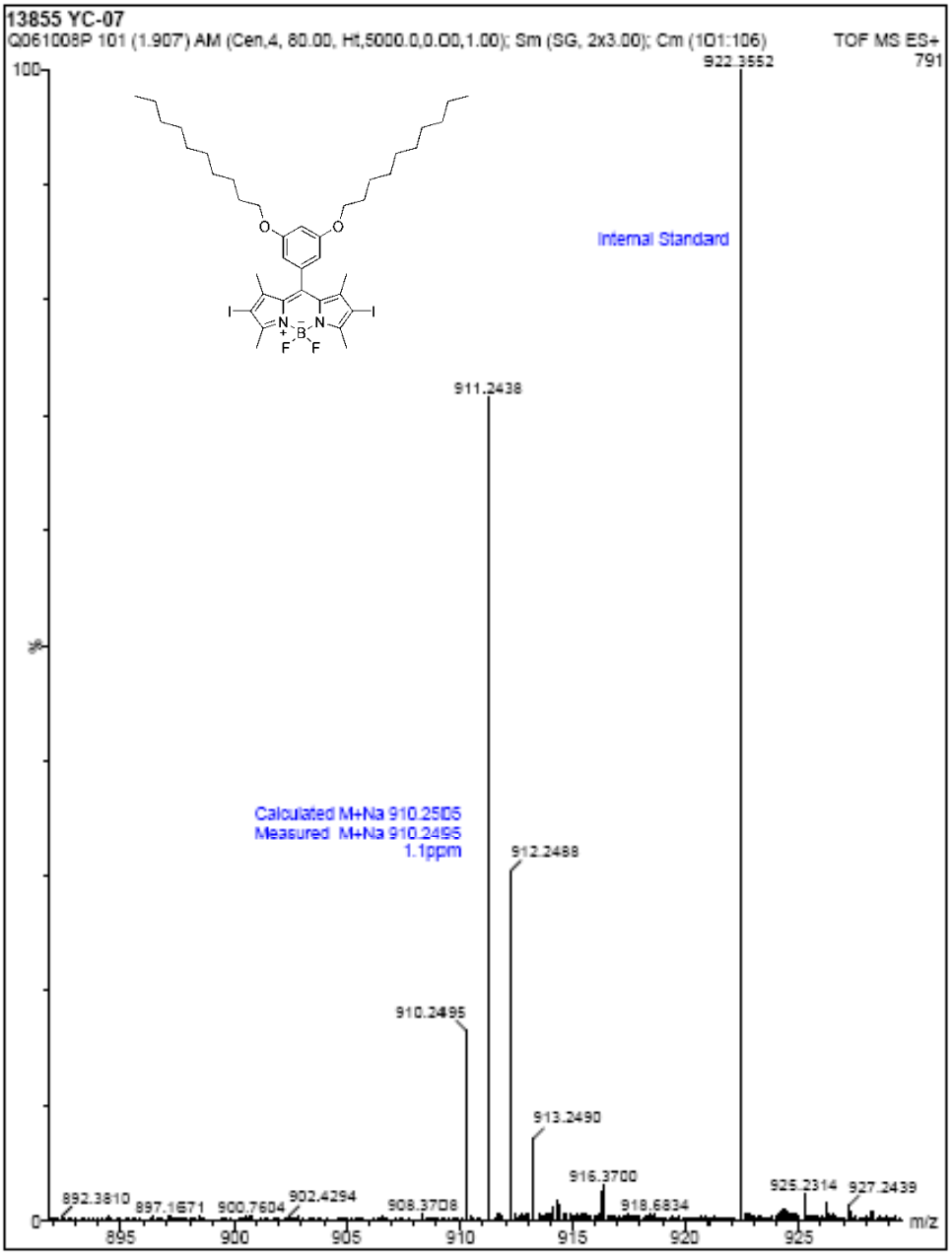

Figure 81. Mass Spectrum of (**74**)

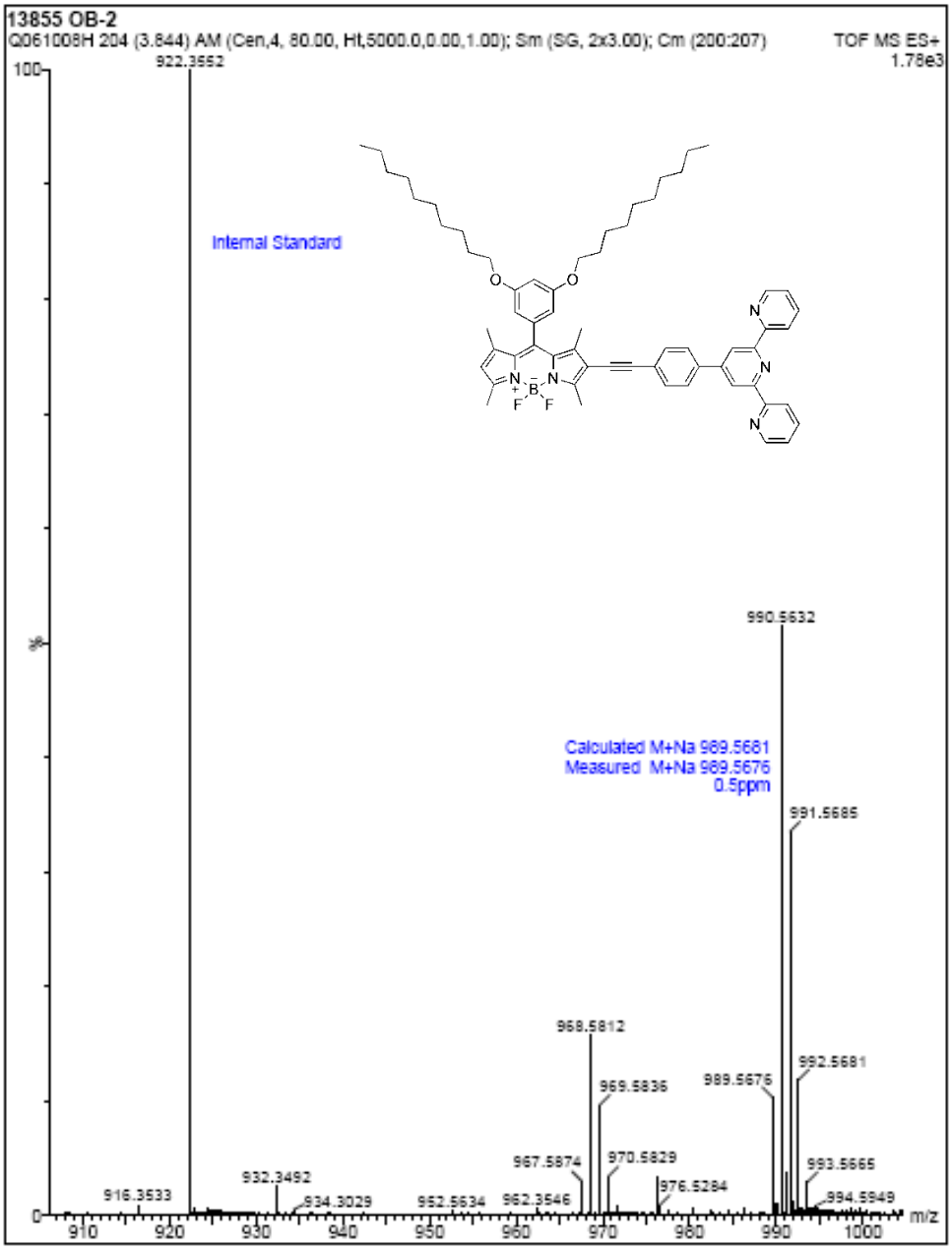

Figure 82. Mass Spectrum of (**75**)

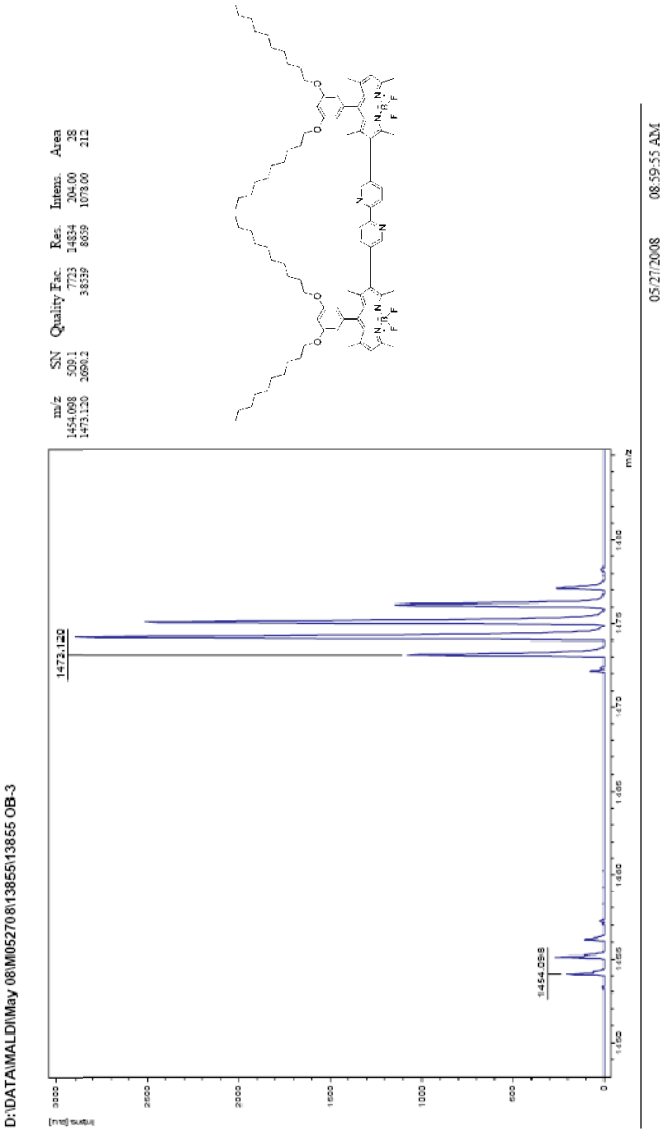

Figure 83. Mass Spectrum of (**76**)

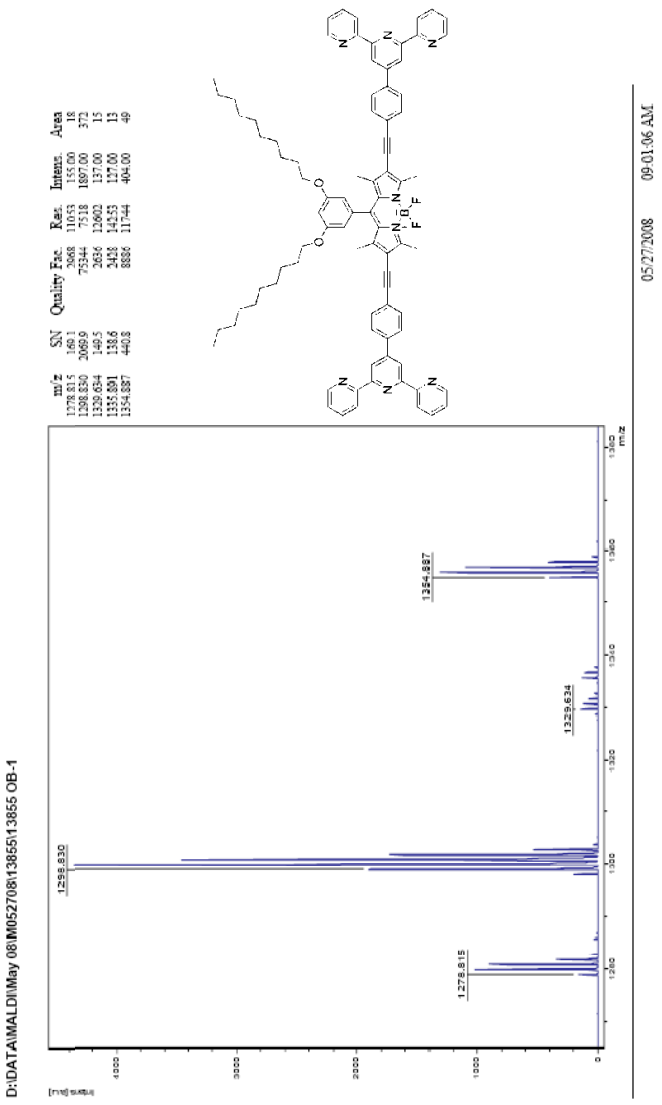

Figure 84. Mass Spectrum of (**77**)

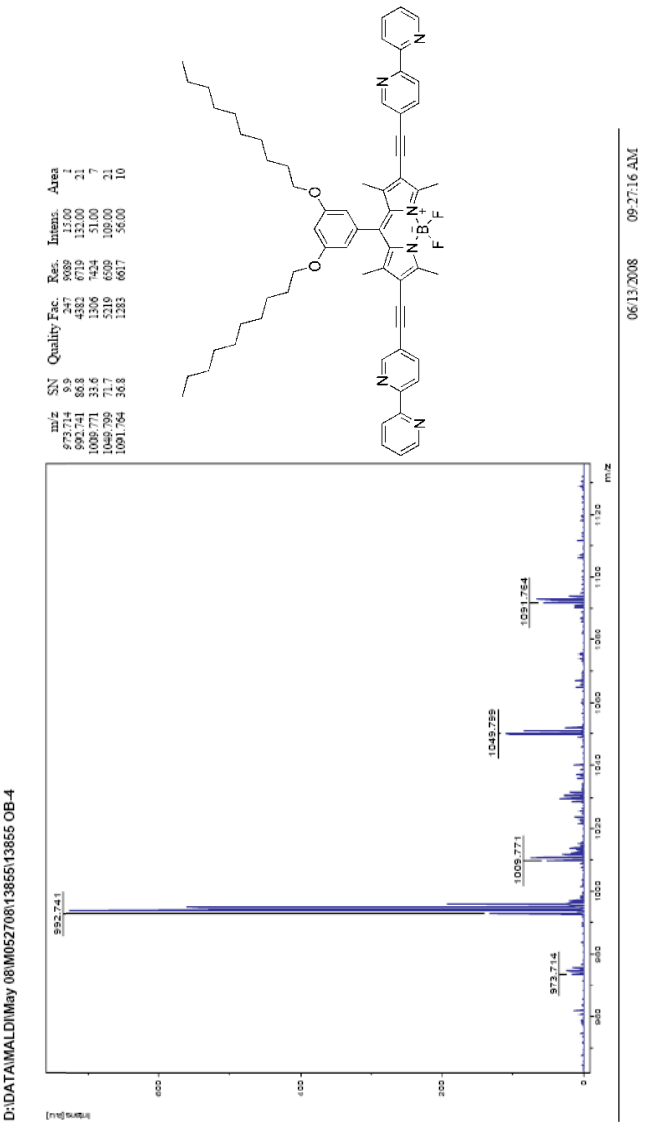

Figure 85. Mass Spectrum of (**78**)

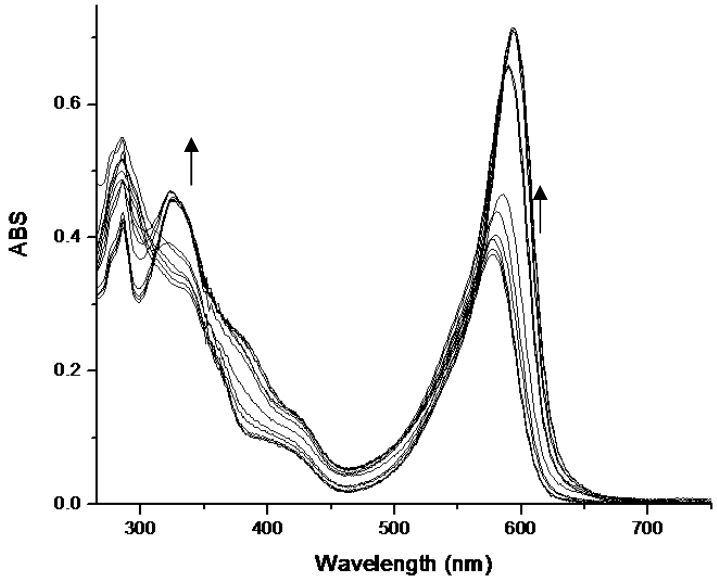

Figure 86. UV-Vis spectra obtained by the titration of **77** in 80:20 $CHCl_3$: MeOH ($5x10^{-6}$ M) with $Fe(ClO_4)_2$. Fe^{2+}: **77** ratio varies from bottom to top as : 0:1, 0.125:1, 0.25:1, 0.375:1, 0.5:1, 0.625:1, 0.75:1, 0.875:1, 1:1, 1.125:1, 1.250:1, 1.375:1, 1.5:1, 1.625:1, 1.750:1, 1.875:1, 2:1.

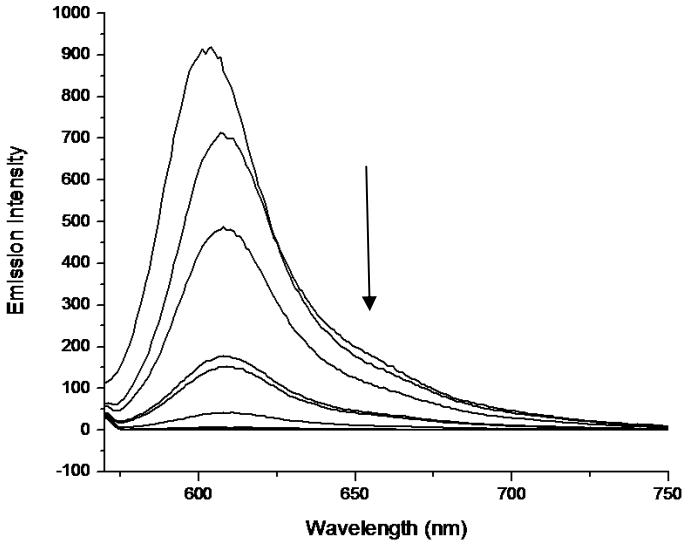

Figure 87. Fluorescence spectra obtained by the titration of **77** in 80:20 $CHCl_3$:MeOH ($5x10^{-6}$ M) with $Fe(ClO_4)_2$. Fe^{2+}: **77** ratio varies from top to bottom as : 0:1, 0.125:1, 0.25:1, 0.375:1, 0.5:1, 0.625:1, 0.75:1, 0.875:1, 1:1, 1.125:1, 1.250:1, 1.375:1, 1.5:1, 1.625:1, 1.750:1, 1.875:1, 2:1.